

2013-02-07

Responses of Stress-Tolerant Corals to Ocean Acidification

Remy R. Okazaki

University of Miami, rokazaki@rsmas.miami.edu

Follow this and additional works at: https://scholarlyrepository.miami.edu/oa_dissertations

Recommended Citation

Okazaki, Remy R., "Responses of Stress-Tolerant Corals to Ocean Acidification" (2013). *Open Access Dissertations*. 967.
https://scholarlyrepository.miami.edu/oa_dissertations/967

This Embargoed is brought to you for free and open access by the Electronic Theses and Dissertations at Scholarly Repository. It has been accepted for inclusion in Open Access Dissertations by an authorized administrator of Scholarly Repository. For more information, please contact repository.library@miami.edu.

UNIVERSITY OF MIAMI

RESPONSES OF STRESS-TOLERANT CORALS TO OCEAN ACIDIFICATION

By

Remy R. Okazaki

A DISSERTATION

Submitted to the Faculty
of the University of Miami
in partial fulfillment of the requirements for
the degree of Doctor of Philosophy

Coral Gables, Florida

May 2013

©2013
Remy R. Okazaki
All Rights Reserved

UNIVERSITY OF MIAMI

A dissertation submitted in partial fulfillment of
the requirements for the degree of
Doctor of Philosophy

RESPONSES OF STRESS-TOLERANT CORALS TO OCEAN ACIDIFICATION

Remy R. Okazaki

Approved:

Chris Langdon, Ph.D.
Professor of Marine Biology and Fisheries

M. Brian Blake, Ph.D.
Dean of the Graduate School

Peter K. Swart, Ph.D.
Professor of Marine Geology and Geophysics

Frank J. Millero, Ph.D.
Professor of Marine and
Atmospheric Chemistry

Diego Lirman, Ph.D.
Research Assistant Professor of
Marine Biology and Fisheries

Robert van Woesik, Ph.D.
Professor of Biological Sciences
Florida Institute of Technology

OKAZAKI, REMY R.

(Ph.D., Marine Biology and Fisheries)

Responses of Stress-Tolerant Corals to Ocean Acidification

(May 2013)

Abstract of a dissertation at the University of Miami.

Dissertation supervised by Professors Peter Swart and Chris Langdon.

No. of pages in text: (129)

Increased atmospheric $p\text{CO}_2$ is expected to reduce coral calcification through increased temperatures (global warming) and decreased pH (ocean acidification). Two species of corals found in Florida Bay, *Solenastrea hyades* and *Siderastrea radians*, exhibit high stress tolerance, persisting in an environment where seasonal swings in temperature and salinity often exceed tolerance limits for most other species of coral. The persistence of these two species in this marginal environment may provide insights into mechanisms of resilience to climate change stress. In other words, does tolerance to broad swings in physical environmental parameters also convey a tolerance to swings in the carbonate chemistry of Florida Bay water, which is also much broader than encountered in most coral reef environments? This dissertation combines laboratory and field studies to characterize the growth responses of stress tolerant corals to increased $p\text{CO}_2$ across a range of temperatures. Several Caribbean species were incorporated into the laboratory studies to provide comparisons across species. The role of the environment in determining coral responses to ocean acidification was investigated, as well as the utility of determining historical conditions from coral skeletal proxies. This dissertation demonstrates 1) the potential of a coral in Florida Bay to preserve signals of

water quality conditions including anomalous events in its skeleton, 2) stress-tolerant corals are still vulnerable to ocean acidification, 3) corals may face a trade-offs between calcification and stress tolerance, and 4) species-specific responses to simulated climate change (increased temperature and $p\text{CO}_2$).

ACKNOWLEDGEMENTS

I am and always will be grateful for Chris and Peter's support and expertise. Their commitment to science, broad interdisciplinary experience, leadership through example, and ability to build and fix any machine have all helped me develop as a scientist. Plus, they even found the time to help in the field.

I appreciate the insight and feedback from my committee, Peter Swart, Chris Langdon, Frank Millero, Diego Lirman, Robert van Woesik. Their help over the years has improved my experiments, analyses, and writing.

My gratitude and appreciation go to Jenn Grimm, for making graduate school a grand experience and whose support helped me finish this dissertation with a slightly lower blood pressure. I also thank my family for instilling a respect for science and education that got me here in the first place.

The most exciting times of my graduate experience have come from the opportunities to travel and do science. I thank Chris, Frank, and Katharina Fabricius for providing these opportunities to see the world and participate in new projects. I also thank Peter and Chris for winning National Science Foundation Grant 0550588 that made my education possible and included field-based activities that allowed me to dive.

In addition to the NSF grant, I have received financial support from a University of Miami fellowship and UM teaching assistantship, the Herbert W. Hoover Foundation, the Rosenstiel Alumni Association, the Stable Isotope Lab, the Marine Science Graduate School Organization (MSGSO) Student Travel Fund, and a Rowlands Research Support award.

Research was conducted under the following permits from Everglades National Park under the National Park Service (EVER), the Florida Keys National Marine Sanctuary (FKNMS), and the Florida Fish and Wildlife Conservation Commission through a Special Activity License (SAL):

EVER-2006-SCI-0045
EVER-2009-SCI-0043
FKNMS-2008-078
FKNMS-2009-117, FKNMS-2009-117-A1
FKNMS-2011-064
SAL-11-1182A-SRP

I have been blessed with amazing labmates (friends/collaborators/helpers/co-conspirators) in both the Langdon and Swart labs. In particular, I thank Rebecca Albright for paving the way, Nancy Muehllehner for bouncing ideas, help in the field/lab, and so much more, Erica Towle (without whose help I'd probably still be buoyant weighing corals right now), Jay Fisch for lab/field support, and Aly Venti for field support. I thank Quinn Devlin for her expertise and advice, Amanda Oehlert for help all-around, and Amanda Waite, Angela Rosenberg, and Amel Saied for assistance in the Stable Isotope Lab.

I have also benefited from the help of people in the field and lab, including but not limited to Carolina Mor, Renee Carlton, Kim Yates, Ben Mason, Kim Yates, Nate Smiley, Megan Morris, Dominic Vita, Sam Guffey, Natalie Kraft, Kasey Cantwell, Caitlin Hill, Eric Buck, Jennifer Lawrence, Marion Durand, Tauna Rankin, Nitzan Soffer, Ryan McMinds, Jenn Grimm, Erica Staaterman, Sean Bignami, Evan D'Alessandro, Brian Teare, Tobias Bornstein, Rivah Winter, Al Piggot, Ross Cunning, Jillian Schacher, Jesse Alpert, Carlos Gallo, Julie Cossavella, Christine Beggs, Magali Guichardot, Jonathan Diaz, MAST Academy high school helpers (Sarvesh Khemlani, Camille

Gladieux, Kelsey DeLisser, Fabiana Rodriguez, Bianca Guerrero, Enmanuel Espinales, Alejandro Fuste, Gianfranco Chacon).

Tom Capo has lent his knowledge, time, and lab space at the Rosenstiel School of Marine and Atmospheric Science (RSMAS) Experimental Fish Hatchery. My neighbors at the facility, Ron Hoenig, John Stieglitz, and others in the Aquaculture Program, shared resources and were helpful in troubleshooting. Others who have shared their time, resources, and equipment to improve my data and analyses include Mandy Karnauskas, Mark Fitchett, Wilson Mendoza, Andrew Baker, Paul Jones, Fen Huang, Stephanie Schopmeyer, Valerie Paul, Bill Hoffman, Wade Cooper, Dave McClellan, and Jack Javech. Cindy Lewis, Mike McCallister, and Andrew Crowder at Keys Marine Lab provided boat support for many years. Lauri McLaughlin and Joanne Delaney from the National Oceanic and Atmospheric Administration were helpful in coral collections.

The RSMAS community has been a rich source of collaborators, friends, helpers, and opportunities. I have never had the pleasure of working with such a diverse, knowledgeable, and laid-back crowd. I can only hope future work environments are as positive as this one.

TABLE OF CONTENTS

| | | Page |
|-----------------------|--|------|
| LIST OF FIGURES | | ix |
| LIST OF TABLES | | xiii |
| CHAPTER | | |
| 1 | INTRODUCTION | 1 |
| | Study aims..... | 6 |
| 2 | EFFECTS OF CLIMATE CHANGE ON TWELVE CARIBBEAN CORAL SPECIES | 8 |
| | Summary | 8 |
| | Background | 9 |
| | Methods..... | 10 |
| | Corals..... | 10 |
| | Treatments | 11 |
| | Experimental system | 11 |
| | Measurements and analyses | 13 |
| | Model projections..... | 15 |
| | Results..... | 17 |
| | Treatment conditions..... | 17 |
| | Calcification | 17 |
| | CO ₂ responses..... | 18 |
| | Growth projections | 21 |
| | Discussion | 25 |
| | Calcification responses..... | 25 |
| | Growth projections | 28 |
| 3 | STRESS-TOLERANT CORALS OF FLORIDA BAY ARE VULNERABLE TO OCEAN ACIDIFICATION..... | 31 |
| | Summary | 31 |
| | Background..... | 32 |

| | | |
|---|---|----|
| | Florida Bay as a natural laboratory | 33 |
| | Stress tolerant corals..... | 36 |
| | Methods..... | 36 |
| | Field site | 36 |
| | Chemical measurements..... | 39 |
| | Incubations | 39 |
| | CO ₂ treatments | 40 |
| | Biological variables..... | 43 |
| | Chemical environment | 44 |
| | Statistical analyses..... | 44 |
| | Results..... | 46 |
| | Field conditions | 46 |
| | Calcification and photosynthesis..... | 46 |
| | Calcification and net photosynthesis responses | 49 |
| | Discussion..... | 50 |
| | Calcification and net photosynthesis..... | 50 |
| | Role of the environment..... | 53 |
| 4 | CORALS MAY FACE A TRADEOFF BETWEEN STRESS TOLERANCE AND CALCIFICATION | 57 |
| | Summary | 57 |
| | Background..... | 57 |
| | Methods..... | 60 |
| | Collections and transplantation | 60 |
| | Incubations | 61 |
| | Statistics..... | 62 |
| | Results..... | 64 |
| | Biological rates..... | 64 |
| | Mortality..... | 64 |
| | Discussion..... | 67 |
| 5 | INSIGHTS INTO PAST FLORIDA BAY CONDITIONS FROM A 190- YEAR OLD <i>SOLENASTREA BOURNONI</i> CORAL | 70 |
| | Summary | 70 |
| | Background..... | 71 |

| | |
|---|-----|
| Florida Bay | 71 |
| Coral | 73 |
| Skeletal proxies for environmental conditions | 74 |
| Previous calibrations of geochemical proxies for environmental conditions | 76 |
| Chronology resolution and hurricanes | 77 |
| Methods..... | 78 |
| Environmental data..... | 78 |
| SERC data | 79 |
| Coral data | 80 |
| Chronology..... | 82 |
| Carbon isotopes | 83 |
| Hurricane data | 84 |
| Skeletal data and proxy relationships..... | 86 |
| Results..... | 87 |
| Water quality data comparisons | 87 |
| Chronology and coral growth rates | 88 |
| Coral skeleton..... | 88 |
| Coral $\delta^{13}\text{C}$ isotopes and hurricane frequency | 90 |
| Paleoreconstructions of temperature, salinity, and saturation state..... | 95 |
| Discussion..... | 99 |
| Chronology..... | 99 |
| Proxies for past temperature and salinity | 101 |
| | |
| 6 CONCLUSIONS..... | 107 |
| Intra-species results..... | 107 |
| Potential mechanisms for calcification resistance to pCO_2 | 108 |
| Tradeoffs in coral calcification | 111 |
| Coral growth records and proxies | 111 |
| Significance and applications | 112 |
| | |
| WORKS CITED | 114 |

List of Figures

- Figure 1.1. Three separate time series datasets have documented ocean acidification, i.e. pCO₂ increases and pH declines, since 1985: European Station for Time-series in the Ocean (ESTOC) 29°N, 15°W (blue); Hawaii Ocean Time-Series (HOT), 23°N, 158°W (green); Bermuda Atlantic Time-series Study (BATS), 31/32°N, 64°W (red) (IPCC 2007).3
- Figure 1.2. A compilation of several ocean acidification studies up to 2005 show a consistent pattern of a 28% decrease in coral calcification per unit decrease in aragonite saturation state (Ω_{arag}). A later review (Kleypas and Langdon 2006) adjusted this figure to $\Delta 22\% \Omega_{\text{arag}}^{-1}$. (Adapted from (Langdon and Atkinson 2005)).4
- Figure 2.1. Schematic of the experimental tank system. Elevated pCO₂ is achieved by mixing pure CO₂ with ambient air, then passing the gas through a Venturi injector into the 200 L sump tank. Water temperature is regulated with a sensor than turns on heating or countercurrent cooling as needed. Seawater from the sump tank circulates to the top holding tank and gravity feeds back into the sump.....13
- Figure 2.2. Projected future temperature and Ω_{arag} under the Representative Concentration Pathway (RCP) 8.5 emissions scenario based on the Geophysical Fluid Dynamics Laboratory’s baseline earth system model for the rectangular grid bounded by 24.1°N, 82.0°W at the southwest vertex and 25.1°N, 81.0°W at the northeast vertex.16
- Figure 2.3. Coral growth rates across treatments. Carbon dioxide treatments are graphed on the x-axis and control and elevated temperatures are blue and red colors, respectively. Circles represent mean, and error bars are 95% confidence intervals. Total sample size for each species is listed in the bottom corner. Note: X-axis is not proportional.21
- Figure 2.4. Projected relative coral growth to the year 2100 based annual average temperature and Ω_{arag} from the RCP 8.5 emissions scenario. Growth is normalized to the year 2006. Shaded area represents 95% confidence limit. These confidence bounds reflect only the error in the coral growth models and do not include uncertainty in the climate models. They narrow with time because projected annual average temperatures increase from 24.5°C to 26.5°C in 2100 while this experiment tested coral growth at 27°C and 30.5°C. These treatment temperatures reflect the average projected summer temperature increases. *D. strigosa* and *P. divaricata* models reflect variable calcification rates. *M. faveolata* projections should be considered with caution given the observed interaction between temperature and pCO₂.23
- Figure 3.1. The field site, denoted by a star, is just north of Peterson Keys in Florida Bay.33
- Figure 3.2. Water quality parameters over the course of the study period. This area of Florida Bay regularly experiences hypersalinity, summer temperatures in excess of 30°C, and winter cold spell temperatures below 15°C. The pH

| | |
|--|----|
| rarely fell below 8.0. Gaps in the pH record were due to sensor malfunctions..... | 35 |
| Figure 3.3. Corals were placed in incubation chambers to measure calcification and net photosynthesis. Carbon dioxide levels were elevated above ambient conditions by equimolar additions of NaHCO ₃ and HCl through a sampling port at the top. Water samples were drawn from the same port. Photo credit: Evan D’Alessandro..... | 42 |
| Figure 3.4. Boxplots of pooled calcification and net photosynthesis data..... | 48 |
| Figure 3.5. Calcification (G) correlated with net photosynthesis (NP) for a) <i>Siderastrea radians</i> and b) <i>Solenastrea hyades</i> . Lines represent best fit models while shaded regions represent 95% confidence intervals. <i>Siderastrea radians</i> is fitted to the hyperbolic tangent function: $G = 14.59 \tanh(NP/46.34)$. <i>Solenastrea hyades</i> is fitted to the linear regression: $G = 0.31 NP + 0.29$ | 49 |
| Figure 3.6. Composite monthly saturation state based on pH recorded at the field site and discrete monthly total alkalinity (TA) samples over approximately three years from 2007-2010. CO2Sys was used to calculate saturation state as discussed in the methods section. Black line represents median aragonite saturation state (Ω_{arag}), dark shaded region represents middle 50% of composite values, light shaded region represents full range of composite estimates of Ω_{arag} . Dotted horizontal line represents modern-day oceanic average saturation state of 3.6. Saturation states in Florida Bay are generally closer to pre-industrial levels of 4.6 for most of the year. As a result, Florida Bay is chemically favorable for calcification. | 54 |
| Figure 4.1. Reciprocal transplant field sites. The star denotes Peterson Keys and the triangle denotes Triangles patch reef. The sites are approximately 30 km apart..... | 58 |
| Figure 4.2. Calcification (a), calcification response (b), net photosynthesis (c), and calcification:net photosynthesis ratios (d) for control Florida Bay corals (FB in FB, dark green circles, n=28), Florida Bay corals transplanted to Triangles (FB in Tri, light green circles, n=12), control Triangles corals (Tri in Tri, dark blue triangles, n=17), and Triangles corals transplanted to Florida Bay (Tri in FB, light blue triangles, n=25). Rates and responses were natural log-transformed to meet assumptions of ANOVA. R_{calcif} included negative numbers, hence 4.3 was added to shift numbers so they could be ln-transformed. Points are means \pm 95% confidence interval bars. | 66 |
| Figure 5.1. The field site, denoted by a star, is just north of Peterson Keys in Florida Bay. | 73 |
| Figure 5.2. Temperature and salinity data from the SERC monthly water sample data for Peterson Keys (Station 20)..... | 79 |
| Figure 5.3. Chronology established by matching actual and expected $\delta^{18}O_C$. First, the $\delta^{18}O_W$ and a 3-point moving average of water temperatures were used to calculate expected $\delta^{18}O_C$ following (Leder et al. 1996). Second, actual $\delta^{18}O_C$ | |

was assigned dates so that the peaks, troughs, and interannual variability matched as closely as possible the dates associated with the expected $\delta^{18}\text{O}_C$83

Figure 5.4. Positive x-radiograph of the *S. bournoni* skeleton from Peterson Keys, cored April 2008. The green line signifies the approximate location and lengths of the drilling transects, with sample number (#) and distance in mm annotated in green. The smaller green line represents Transect 2B. The larger line represents Transect 1A and 2B combined. Transect 1B (not shown) was drilled above Transect 2B. Several chronologies are shown based on different methodologies: (black) visual assessment of density bands, (orange) derivatives of density splines calculated in CoralXDS+, (purple) $\delta^{18}\text{O}_C$ minima correspond to annual maximum temperatures on September 1, (yellow) actual $\delta^{18}\text{O}_C$ are aligned with expected $\delta^{18}\text{O}_C$ calculated from temperature and $\delta^{18}\text{O}_W$ records. Purple and yellow dates are annotated based on measured distances (green line). The chronology based on actual/expected $\delta^{18}\text{O}_C$ (yellow) was used for all analyses. The double-band marked 1982 in the black, visual-based chronology was also demarked as 1982 in Healy (1996). This figure illustrates the complexities of deriving the exact chronology.85

Figure 5.5. Comparisons of high frequency environmental logger data to SERC data for (a) temperature and (b) salinity, with coefficients of determination and residual mean square error (RMSE).87

Figure 5.6. Annual extension, density, and growth for the coral core. Extension and calcification decreased slightly from 1950 to 2000 while density increased. (Courtesy of K. Helmle)89

Figure 5.7. Coral oxygen and carbon isotopic data from the coral core extending from 1985 to 2008. Transect 1A transitions to Transect 2B in 1994. Overlapping isotopic values were similar, indicating carbon and oxygen isotopes are spatially consistent and movements in signals represent true conditions rather than sampling artifact.91

Figure 5.8. Boxplots of annual coral oxygen and carbon isotopic data. Carbon isotopes exhibit a large increase from 1990 to 1993 before settling back into a regular long-term average pattern. In comparison, oxygen has less interannual variation.92

Figure 5.9. Trace metal ratios for the coral. Transect 2B extends from 1985-1994 and Transect 1B extends from 1996-2008. The values bridging the gap between the two sections in 1995 are from Transect 1A (shaded gray).93

Figure 5.10. Carbon isotopic anomalies spanning 1860-2008, adjusted for the Flagler railroad construction and background anthropogenic signal. The lines represent hurricanes that passed <30 km from the coral (red), through Florida Bay >30 km from the coral (orange), across the Everglades (blue), across the bay and Everglades (purple), far from the coral (grey). Skeletal $\delta^{13}\text{C}$ is expected to increase after red and orange lines, and decrease after blue lines. Purple and grey lines were ignored because carbon isotopes could shift in either direction or have no effect following those storms.94

| | |
|---|-----|
| Figure 5.11. Proxies used in salinity reconstructions reconstructions: (a) salinity from $\delta^{18}\text{O}_w$, (b) temperature from the difference between coral and water $\delta^{18}\text{O}$, and (c) temperature from Sr/Ca ratios. Salinity reconstructions were fairly accurate from (a) and (b), but not when (a)-(c) were combined. Plots are annotated with coefficients of determination and residual mean square error (RMSE)..... | 97 |
| Figure 5.12. Reconstructed salinity (red) compared to actual salinity (black) from SERC records (a) before and (b) after the Sr/Ca paleothermometer is added, as well as from the (c) temperature composite substituting for the Sr/Ca paleothermometer. | 98 |
| Figure 5.13. Monthly composite temperature from SERC data for Peterson Keys (Station 20) for 1991-2008 where January is Month 01..... | 98 |
| Figure 5.14. Reconstructed Ω_{arag} using $\delta^{18}\text{O}_C$ and composite temperature. Shaded light blue area represents the 95% confidence interval for the local regression smoothed curve (blue line, span = 0.05)..... | 99 |
| Figure 5.15. Seawater Sr/Ca values in Florida Bay. Gray dots represent values for all 28 subbasins for all available dates, and red dots represent Peterson Keys. The blue line is the modeled Sr/Ca due to 5 ppm increase in [Ca] from groundwater. | 103 |

List of Tables

| | |
|--|----|
| Table 2.1. Experimental conditions (mean \pm SEM) for each treatment include two replicate tanks. | 17 |
| Table 2.2. Growth rates of corals (mg d ⁻¹), reported as mean \pm SD (n). “nd” signifies no data. | 19 |
| Table 2.3. Results of Scheirer-Ray-Hare (<i>A. cervicornis</i> , <i>M. faveolata</i>) and two-way ANOVA tests (all other species). Significant results ($\alpha = 0.05$) are noted with an asterisk. | 20 |
| Table 2.4. Constants for calcification response variables. Slopes (m) represent change in calcification per unit increase in Ω_{arag} for each treatment temperature (T). <i>A. cervicornis</i> only had two data points for the regression at 30°C, hence residual mean square error (RMSE) is not applicable (NA). The other variables are regression intercepts (b) and coefficients of determination (r^2). ... | 22 |
| Table 2.5. Projected changes in coral growth by the year 2100 relative to rates in 2010 (%). Multiple linear regression constants for aragonite saturation state (Ω_{arag}), temperature, and intercepts are listed. | 23 |
| Table 3.1: Physical parameters measured during field trips. Sample sizes refer to the total number of corals measured on a particular date. | 37 |
| Table 3.2. Pooled calcification (G) and net photosynthesis (NP) measurements for <i>Siderastrea radians</i> and <i>Solenastrea hyades</i> . Subscripts ‘ambient’ and ‘CO ₂ ’ indicate control and elevated pCO ₂ conditions, respectively. Values are reported as mean \pm standard deviation (sample size). | 47 |
| Table 3.3: Multilevel model comparisons of the only observed significant calcification response variable, change in saturation state, against a null model accounting only for coral. | 50 |
| Table 4.1. Environmental conditions at the Florida Bay and Triangles patch reef field sites. The parameters pH _t , Ω_{arag} , and pCO ₂ are reported at ambient temperature. Light is converted from a Lux sensor into PAR using an assumed conversion of PAR = Lux/50. | 59 |
| Table 4.2. Biological variables (mean \pm SD) measured for the four treatments with sample size (n) in the adjacent column. | 63 |
| Table 4.3. Two-way analysis of variance (ANOVA) results tables for calcification, calcification responses, net photosynthesis and calcification:net photosynthesis ratios for the reciprocal transplant experiment. | 65 |
| Table 5.1. Relationships between interpolated monthly coral skeletal values and SERC environmental data. The Leder et al. (1996) calibration is derived from <i>Montastraea annularis</i> while the calibrations from this study are based only on <i>Solenastrea bournoni</i> . T = Temperature (°C), S = Salinity, $\delta^{18}\text{O}_\text{C}$ = coral oxygen isotopes (‰), $\delta^{18}\text{O}_\text{W}$ = water oxygen isotopes (‰), Sr/Ca = Strontium/Calcium (mM/M). RMSE = residual mean square error. | 96 |

Chapter 1: Introduction

Corals reefs are one the world's most diverse ecosystems, yet they cover only 0.05% of the Earth's surface (Spalding and Grenfell 1997). These oases of biodiversity support large amounts of biomass (Reaka-Kudla 1997; Roberts et al. 2002) in oligotrophic waters, providing food and shelter for many taxa. They provide approximately \$375B y^{-1} in food, tourism, and ecosystem services to coastal human populations (Costanza et al. 1997). Reefs also contribute substantially to the global carbonate budget, producing approximately 0.75 Gt of carbonate per year (Vecsei 2004).

Despite their importance, reefs worldwide have experienced persistent and widespread decline from warming, over-fishing, eutrophication, disease and other stressors (Bohnsack 1993; Glynn 1993; Hoegh-Guldberg 1999; Kleypas et al. 1999b; Jackson et al. 2001; Gardner et al. 2003; Pandolfi et al. 2003; Birkeland 2004; Hoegh-Guldberg et al. 2007). These declines have degraded structural complexity (Alvarez-Filip et al. 2009) with consequent habitat losses for reef fishes (Paddack et al. 2009). Many studies have concluded that climate change threatens reefs due to the negative effects of increased temperature and pCO_2 on corals and their symbiotic algae (Gates et al. 1992; Iglesias-Prieto et al. 1992; Jones et al. 1998; Hoegh-Guldberg 1999; Fitt et al. 2001). Temperature stress has resulted in worldwide coral bleaching events (Glynn 1993,1996), a phenomenon where corals expel their symbiotic algae and thus lose a significant source of energy. Prolonged bleaching often results in large-scale mortality, with much of the world's coral cover lost in the abnormally warm 1998 El Niño (Baker et al. 2008). Few global mass coral bleaching events were recorded before 1979 (Glynn

1993), but now they are expected to increase in frequency and severity with global warming (Hughes et al. 2003). Furthermore, the burning of fossil fuels since the start of the Industrial Revolution has increased atmospheric CO₂ by over 100 ppm. The world's oceans have absorbed ~33-50% of this CO₂ (Sabine et al. 2004), which has in turn caused well-documented reductions in pH and concomitant decreases in carbonate ion (Dore et al. 2009; González-Dávila et al. 2010). This decrease in pH, termed ocean acidification, is changing ocean chemistry (Caldeira and Wickett 2003; Feely et al. 2004; Caldeira and Wickett 2005; Orr et al. 2005; Cao et al. 2007; Doney et al. 2009) at unprecedented rates (Ridgwell and Schmidt 2010; Hönlisch et al. 2012) towards conditions unfavorable for reef growth (Kleypas et al. 1999a; Langdon et al. 2000; Leclercq et al. 2000; Orr et al. 2005; Marubini et al. 2008). Field studies of naturally bubbled CO₂ areas reveal losses of marine calcifiers and biodiversity relative to nearby control sites (Hall-Spencer et al. 2008; Fabricius et al. 2011).

Additional studies and meta-analyses (Langdon and Atkinson 2005; Ries et al. 2009; Hendriks et al. 2010; Kroeker et al. 2010) have documented calcification declines across many species. Aragonite saturation levels, measures of how favorable ocean conditions are for calcification, are expected to compress the zone favorable to calcifying organisms towards lower latitudes and shallower depths (Feely et al. 2004; Orr et al. 2005). However, warming temperatures have pushed coral distributions polewards (Yamano et al. 2011). Consequently corals are caught between declining saturation states and increasing water temperatures.

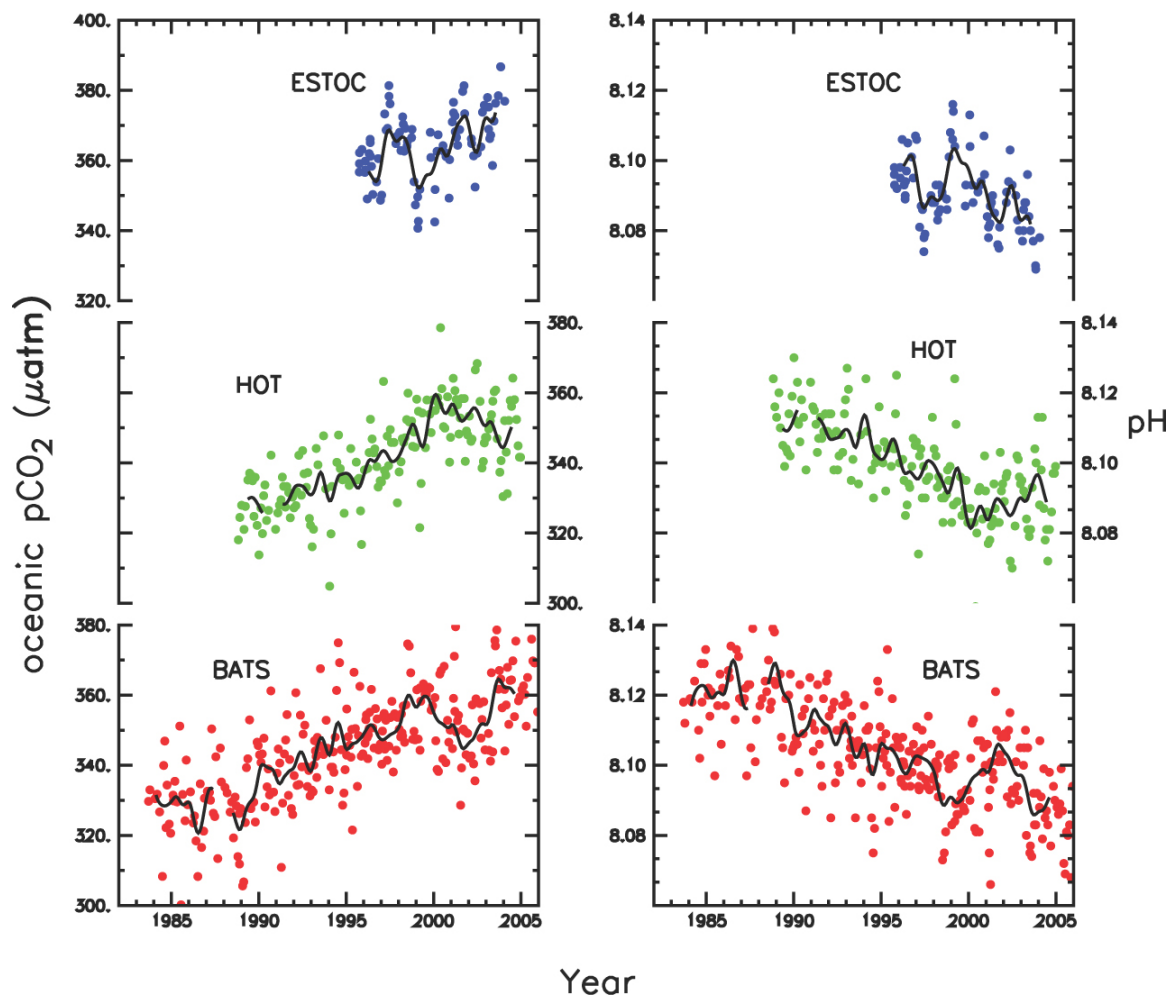


Figure 1.1. Three separate time series datasets have documented ocean acidification, i.e. pCO₂ increases and pH declines, since 1985: European Station for Time-series in the Ocean (ESTOC) 29°N, 15°W (blue); Hawaii Ocean Time-Series (HOT), 23°N, 158°W (green); Bermuda Atlantic Time-series Study (BATS), 31/32°N, 64°W (red) (IPCC 2007).

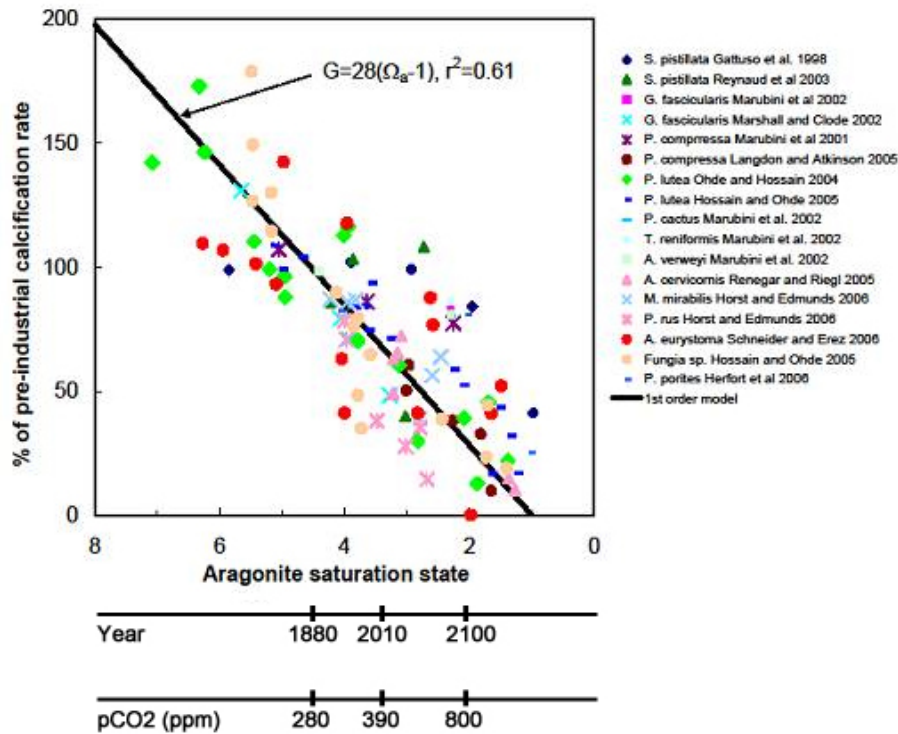


Figure 1.2. A compilation of several ocean acidification studies up to 2005 show a consistent pattern of a 28% decrease in coral calcification per unit decrease in aragonite saturation state (Ω_{arag}). A later review (Kleypas and Langdon 2006) adjusted this figure to $\Delta 22\% \Omega_{\text{arag}}^{-1}$. (Adapted from (Langdon and Atkinson 2005)).

Adaptation to climate changes occurring 10- to 100-times faster than the previous 55 million years require reproductive success (van Woesik and Jordan-Garza 2011), yet several studies document negative effects of ocean acidification across multiple reproductive stages (Albright et al. 2008; Kurihara 2008; Albright et al. 2010; Morita et al. 2010; Albright and Langdon 2011; Doropoulos et al. 2012). Another genetic means for corals to cope with climate change is hybridization, but this phenomenon is rare (van Oppen and Gates 2006). Corals that are currently better adapted to tolerate stress or corals that host thermally-tolerant symbiotic algae are more likely to persist under future climate change. Though studies have shown corals can rely on their symbiotic

zooxanthellae to impart some thermal tolerance (Baker et al. 2004; Berkelmans and van Oppen 2006), this may come with an energetic cost (Little et al. 2004; Jones and Berkelmans 2010). Furthermore, this thermal tolerance may be limited to 1.5°C (Berkelmans and van Oppen 2006), below the $\geq 2^\circ\text{C}$ warming predicted for the Caribbean by the end of the century (Sheppard and Rioja-Nieto 2005; Carricart-Ganivet et al. 2012) and below the estimated 0.2-1.0°C decadal increase in thermal tolerance required by corals to cope with increased warming (Donner et al. 2005). Consequently, studying corals that already are resistant to stress, including extremes in temperature, salinity, burial, eutrophication, and aerial exposure, may provide insights into how these organisms will fare under future climate change as well as what mechanisms they use to cope with those climate change stressors of increased temperature and pCO₂. Corals from Florida Bay provide model organisms for such studies due to their stress-tolerance abilities (Vaughan 1913; Yonge 1936; Macintyre and Pilkey 1969; Lewis 1989; Rice and Hunter 1992; Lirman et al. 2002; Lirman et al. 2003; Macintyre 2003; Chartrand et al. 2009; Lirman and Manzello 2009; Crook et al. 2012). Throughout this dissertation, the term “stress-tolerant” refers to corals that generally persist where the aforementioned physical stressors limit most other coral species. Florida Bay’s shallow environment amplifies extremes in temperature, salinity, and light, while oxidized organic matter and algal blooms subject corals to large seasonal swings in pCO₂ of several hundred ppm (Millero et al. 2001). Thus Florida Bay mimics potential future conditions and is an ideal location to study coral responses to climate change.

STUDY AIMS

The goals of this dissertation were to determine stress tolerant coral responses to experimentally manipulated climate change factors. The first study examined the growth of three common Florida Bay corals, *Solenastrea hyades*, *Siderastrea radians*, and *Porites divaricata*, along with nine other common Caribbean species in a laboratory study. The goal of this study was to evaluate coral responses to both warming temperatures and increased pCO₂, and assess relative susceptibility to these stressors.

The second study focused on *S. hyades*'s and *S. radians*'s seasonal *in situ* growth under a range of naturally-mediated ambient pCO₂ conditions, where corals have ample feeding opportunities, while light, water flow, and other parameters are naturally-mediated. On top of this natural variability, increased pCO₂ manipulations assessed their growth responses to ocean acidification.

The third objective was to determine the role of environment in the responses of *S. hyades* to increased pCO₂. Corals from Florida Bay were reciprocally-transplanted with conspecifics from a more stable, oceanic patch reef. Like the previous experiment, pCO₂ was elevated above natural, ambient conditions. The goal of this field-based study was to determine if stress-tolerant corals, freed from their stressful conditions, were better able to calcify and/or resist ocean acidification.

The fourth study examined the coral growth record from a 190-year old *Solenastrea bournoni* colony growing at the field site in Peterson Keys, Florida Bay, in relation to a 19-year record of water chemistry for the area. This study explored proxies of environmental conditions based on stable isotopes and trace metal ratios from the coral skeleton, using the long-term water quality record for calibration.

Altogether, this dissertation characterizes the responses of stress tolerant corals to climate change, with special emphasis on ocean acidification. Coral growth is examined under past, present, and future conditions in lab and field experiments. These studies provide data on understudied species and highlight the importance of environmental history in defining coral responses to stress.

Chapter 2: Effects of Climate Change on Twelve Caribbean Coral Species

SUMMARY

As reefs continue to decline with increasing temperatures and ocean acidification, their trajectories are likely to differ depending on their species composition and diversity, with subsequent effects on the fauna those reefs support. Determining which corals are most vulnerable to climate change stressors can improve predictive capabilities for reef changes through time and improve the allocation of conservation efforts. Growth of twelve Caribbean species was measured under increased temperature and pCO₂ for eight weeks. Corals exhibited species-specific responses, but in general responded more negatively and rapidly to temperature than pCO₂. In terms of relative growth responses, *Porites astreoides* was the most sensitive with no net growth predicted by the end of the century. Some species had high variability among individuals, which may be a source of resilience to climate stressors over time. The weedy, stress-tolerant corals *Siderastrea radians* and *Solenastrea hyades* responded positively to increasing temperature, for which the elevated temperature treatment was likely closer to their thermal optimum. *Siderastrea siderea*, a reef-building coral, maintained constant growth across all treatments, indicating this species may also be resistant to climate change.

BACKGROUND

Coral reefs are diverse ecosystems that vary in their coral species composition, which in turn shapes the underlying habitat and the species those reefs can support (Hixon and Beets 1993; Cheal et al. 2008). While much research indicates corals will decline due to the climate change effects of ocean acidification and global warming (IPCC 2007), recent research has shown that some coral species may be able to resist climate change by shifting the types of symbiotic dinoflagellates they host (Baker et al. 2004; Berkelmans and van Oppen 2006) or by relying on heterotrophy to meet their nutritional needs until conditions permit their symbionts to recover (Grottoli et al. 2006). Consequently, as atmospheric pCO₂ continues to increase, reefs worldwide are likely to experience non-uniform impacts due to differences in climate sensitivity of the coral species that comprise different reefs. The relative sensitivity of corals to climate change will influence which reefs persist into the future and thereby what diversity these reefs can host (Gratwicke and Speight 2005b,a; Wilson et al. 2006).

However, comparing across species is challenging because experiments differ in their treatments, conditions, seasonality, and duration. Consequently, different methodologies can confound decision-making for reef managers and introduce variability for modelers seeking to predict species change over time. This experiment tested growth of twelve common Caribbean species to both elevated temperature and pCO₂ under the same conditions for eight weeks to provide a broad species comparison. This study included the endangered *Acropora cervicornis*, as well as two species considered for endangered species listing, *Dichocoenia stokesii* and *Montastraea faveolata*. The other species included *Agaricia agaricites*, *Diploria clivosa*, *Diploria strigosa*, *Montastraea cavernosa*, *Porites astreoides*, and *Siderastrea siderea*. Three stress-tolerant, non-reef

building species included *Porites divaricata*, *Siderastrea radians*, and *Solenastrea hyades*. Little to no data exist on responses to warming and ocean acidification for many of these species.

METHODS

Corals

Corals were collected from the Florida Keys (Key West, Florida Bay, and Key Biscayne) in the summer of 2011 and brought to the University of Miami's Climate Change facility where they were cored into 2.5 cm diameter fragments and glued to labeled ceramic plugs. Branching corals were clipped to approximately 5 cm long fragments. Coral fragments (hereafter referred to as corals) were allowed to recover for at least one month and showed polyp extension as well as tissue growth over cut scars. Corals were randomly assigned across treatments, stratifying by parent colony where the total number of corals per colony was greater than or equal to the total number of treatments. The total number of colonies per species ranged from 5 to 72, with smaller species like *P. divaricata* and *S. radians* requiring more colonies for a given sample size than *Montastrea* spp or other larger mounding corals. Total number of corals per species ranged from 17-151, depending on availability at the time of the study as well as mortality. Although rates were not normalized to exact surface area, fragments were all approximately the same size; hence fragment size should not confound treatment effects. One-way analysis of variance (ANOVA) for each species of baseline, pre-experiment growth over a month determined no differences, indicating corals started the experiment

with the same growth rates across treatments and any subsequent observed differences were due to the treatments.

Treatments

Treatments consisted of three pCO₂ treatments crossed with two temperatures. The pCO₂ levels were 390 (control), 1200, and 1600 ppm. The temperature treatments were 27°C (control) and 30.5°C (sub-lethal stress), which represents the bleaching threshold for corals in the Florida Keys (Manzello et al. 2007). Treatments were duplicated across tanks, with twelve tanks total. Corals were randomly reassigned within treatments twice during the experiment to account for any possible cohort effects, and tanks were randomly reassigned treatment conditions three times during the experiment to account for any potential tank effects. The experiment ran for eight weeks from October to December 2011.

Experimental system

A schematic of the experimental system is shown in Fig. 2.1. Mass flow controllers (Sierra Instruments Model 810C) set the treatment gas concentrations by controlling the mixing rate of ambient air and pure CO₂. Tanks were bubbled with the gas mixtures through Venturi injectors. Tank pCO₂ levels varied by ± 50 , ± 300 , ± 400 ppm in control, medium, and high pCO₂ treatments respectively. This variation followed a diurnal pattern consistent with natural reefs where pCO₂ declines through the day and increases through the night. Omega Engineering temperature controllers (Model CN9000) regulated temperature within $\pm 0.1^\circ\text{C}$ using a heating element and counter-current cooling coils. A HOBO U30 data logger (Onset Computer) recorded

temperatures for each tank every 5 minutes along with light through a centrally-located PAR sensor. Treatments were ramped up from ambient to target levels at rate of $\sim 0.3^{\circ}\text{C d}^{-1}$ and $100\text{-}200\text{ ppm d}^{-1}$. Water samples were collected weekly from each tank to document chemical conditions while temperature and salinity were checked with a handheld meter (YSI Model 30). Tris synthetic seawater buffer (Nemzer and Dickson 2005) was used to calibrate the pH sensor (Orion) on the total scale. Total alkalinity (TA) was measured in duplicate on an automated Gran titrator, and dissolved inorganic carbon (DIC) was measured in duplicate on a coulometer (UIC, Inc). Salinity was measured on a Guildeline 8410A Salinometer. Total alkalinity and DIC along with the input temperatures and salinity were then used to estimate saturation state with the program CO2SYS (Lewis and Wallace 1998; Pierrot et al. 2006) using dissociation constants from Mehrbach et al. (1973) as refit by Dickson and Millero (1987) and Dickson (1990).

Corals occupy different niche spaces on reefs, with some corals like *Acropora* spp favoring shallow areas with more light and others like *Agaricia* spp occupying deeper, more shaded areas (Bak and Engel 1979; Chappell 1980). Testing corals under all possible conditions was not feasible, and this experiment attempted to replicate the average reef habitat. Tanks were supplied with $10\text{ }\mu\text{m}$ -filtered seawater from Bear Cut, Virginia Key, and seawater was pumped through the tanks at $\sim 150\text{-}200\text{ mL min}^{-1}$. The approximate tank turnover time is 0.8 to 1.3 d. Corals were exposed to natural sunlight, and light levels were adjusted such that average peak sunlight was $327 \pm 14\text{ }\mu\text{mol quanta m}^{-2}\text{ s}^{-1}$ (mean \pm standard error, $n=66$) and total light exposure per day was $3.7 \pm 0.2\text{ mol quanta m}^{-2}$ ($n=66$). Corals were fed biweekly a diet of live rotifers ($\sim 10\text{ rotifers L}^{-1}$) and

larval feed (AP brand). The larval feed was composed of $\sim 6 \text{ mg L}^{-1}$ each of $<100 \mu\text{m}$ particles and $250\text{-}450 \mu\text{m}$ particles. Aquarium pumps with water diffusers kept food suspended in the tank during feeding. Corals were allowed to feed for four hours starting late afternoon to early night, after which the feeding water was discarded.

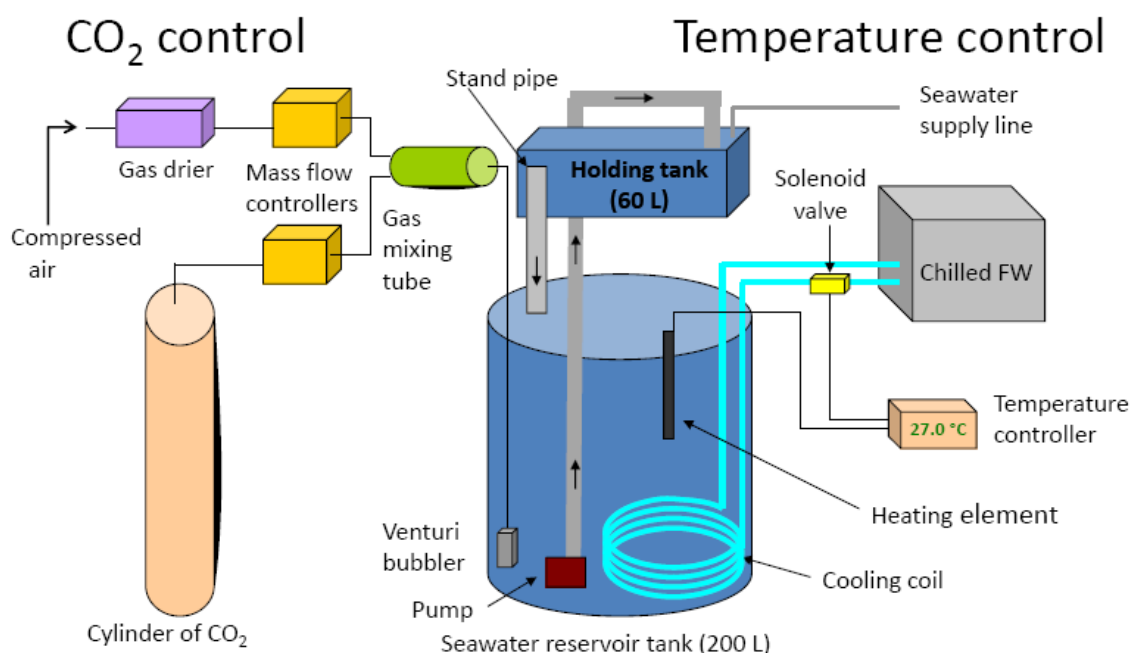


Figure 2.1. Schematic of the experimental tank system. Elevated pCO₂ is achieved by mixing pure CO₂ with ambient air, then passing the gas through a Venturi injector into the 200 L sump tank. Water temperature is regulated with a sensor that turns on heating or countercurrent cooling as needed. Seawater from the sump tank circulates to the top holding tank and gravity feeds back into the sump.

Measurements and analyses

The buoyant weight of corals was recorded every two weeks (Davies 1989). The slope of mass increase over time was used to determine growth rates. Corals with

buoyant weights that oscillated through time, ex. weights that increased, decreased, then increased again, were excluded from analyses.

During week 6, one tank (1600 ppm pCO₂, 30.5°C) experienced sudden mortality of all corals, algae, epiphytes, and resident amphipods. The cause of this mortality was unknown but likely was not a chronic problem because a temperature logger did not record any abnormalities, salinity was normal, and organisms placed in the same water later did not experience any mortality. Consequently, calcification data for these corals did not include a final time point.

Calcification was analyzed via two-way ANOVA with type II sums of squares and with temperature and pCO₂ as fixed, between-groups factors for all species except *M. faveolata* and *A. cervicornis* because these two species departed from normality/homoscedasticity assumptions. These two species were analyzed using Sheirer-Ray-Hare tests, non-parametric versions of ANOVA. For species where calcification was unchanged in one of the temperature treatments, a one-way ANOVA of growth by CO₂ was conducted on the other temperature treatment corals. The purpose of these tests was to examine the secondary effects of CO₂ that would have otherwise be undetected due to the larger temperature signal swamping the CO₂ signal. Normality was evaluated through graphical analysis of linear model residuals, and homoscedasticity was evaluated using Levene's tests. Linear regressions of mean calcification by saturation state for each temperature were also calculated to derive CO₂ reponse parameters. Linear regressions were chosen based on ease of comparison across species and previous studies indicating linear relationships between calcification and Ω_{arag} . These regressions are

based on ambient saturation states instead of treatment-averaged saturation states. All statistical analyses were performed in the computer program R (Team 2011).

Model projections

Calcification rates were fit to multiple linear regression models with temperature and aragonite saturation state as independent variables. Projected future sea surface temperatures (SSTs), salinity, total alkalinity, and $p\text{CO}_2$ were obtained from the Geophysical Fluid Dynamics Laboratory's (GFDL) baseline earth system model (ESM2M) (Taylor et al. 2012), assuming the Representative Concentration Pathway (RCP) 8.5 (van Vuuren et al. 2011). This is the most extreme emissions scenario in the upcoming Intergovernmental Panel on Climate Change (IPCC) Fifth Assessment Report but is still a relatively conservative business-as-usual scenario (Riahi et al. 2011). It assumes that by year 2100, radiative forcing is 8.5 W m^{-2} , population is 12B, energy sources are coal-intensive with high green house gas emissions, and there are few technological improvements in energy efficiency. RCP 8.5 was chosen because previous IPCC forecasts in the 1990s have underestimated actual emissions since 2000 (Raupach et al. 2007). Monthly data to year 2100 were obtained from the GFDL data portal (Last accessed June 2012 from <http://nomads.gfdl.noaa.gov/>) for the rectangular grid bounded by 24.1°N , 82.0°W at the southwest vertex and 25.1°N , 81.0°W at the northeast vertex. Aragonite saturation states were calculated from the data using CO2Sys using the aforementioned constants. The data on future projected SSTs and aragonite saturation state (Fig. 2.2) were inputted into the multiple linear regression models to obtain calcification rates. Calcification rates were normalized to the average annual rate in

2006, the earliest year available in the climate projection dataset, to facilitate comparisons of relative projected changes in growth over time.

The calcification models do not have biological inputs such as bleaching thresholds, upper thermal limits, or larval recruitment.

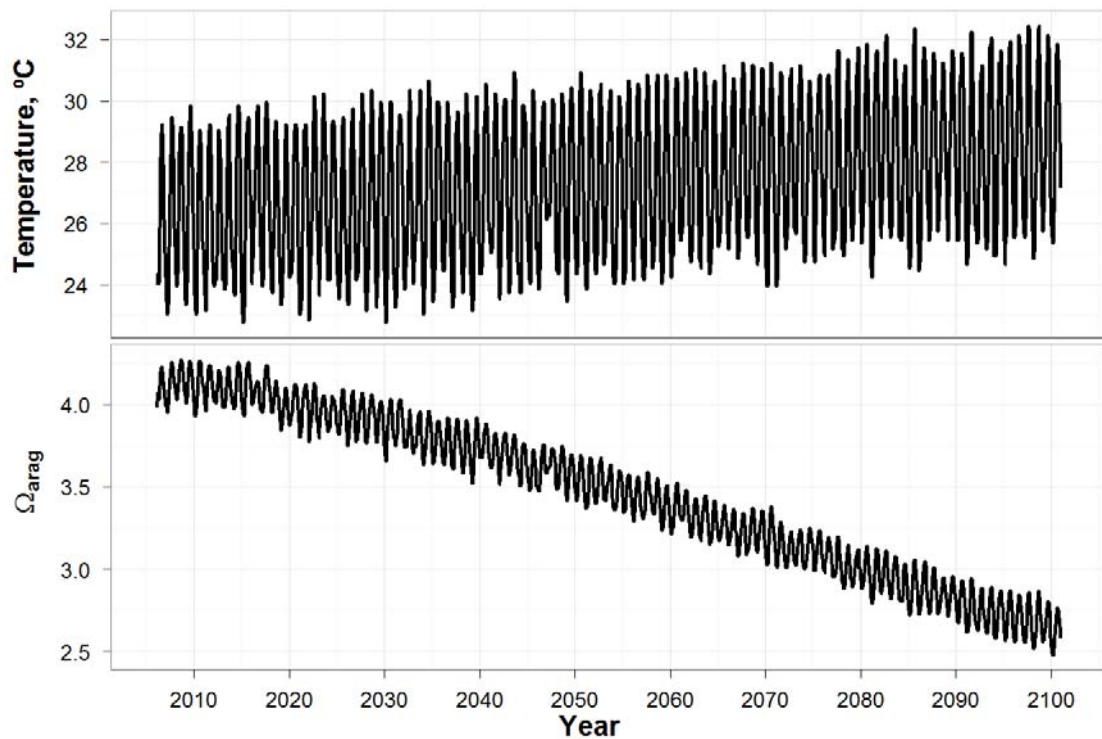


Figure 2.2. Projected future temperature and Ω_{arag} under the Representative Concentration Pathway (RCP) 8.5 emissions scenario based on the Geophysical Fluid Dynamics Laboratory's baseline earth system model for the rectangular grid bounded by 24.1°N, 82.0°W at the southwest vertex and 25.1°N, 81.0°W at the northeast vertex.

RESULTS

Treatment conditions

Carbon dioxide levels increased from ambient levels (395 ppm) to 1150 and 1600 ppm in medium and high pCO₂ treatments, respectively. Increasing pCO₂ yielded concomitant increases in DIC from 2040 to 2340 $\mu\text{mol kg}^{-1}$ seawater (SW) and declines in pH from 8.0 to 7.5. Total alkalinity levels ranged 2360 to 2460 $\mu\text{mol kg}^{-1}$ SW across treatments.

Table 2.1. Experimental conditions (mean \pm SEM) for each treatment include two replicate tanks.

| Treatment | Temp. (°C) | n | TA ($\mu\text{mol kg}^{-1}$ SW) | DIC ($\mu\text{mol kg}^{-1}$ SW) | pH _t | Ω_{arag} | pCO ₂ (ppm) |
|-----------|------------|----|----------------------------------|-----------------------------------|-----------------|------------------------|------------------------|
| 1 | 27 | 22 | 2363 \pm 41 | 2044 \pm 42 | 8.01 \pm 0.06 | 3.1 \pm 0.5 | 410 \pm 54 |
| 2 | 27 | 19 | 2414 \pm 39 | 2280 \pm 46 | 7.63 \pm 0.13 | 1.6 \pm 0.5 | 1176 \pm 294 |
| 3 | 27 | 21 | 2430 \pm 33 | 2347 \pm 46 | 7.49 \pm 0.07 | 1.1 \pm 0.2 | 1606 \pm 236 |
| 4 | 30.5 | 14 | 2406 \pm 45 | 2037 \pm 55 | 8.05 \pm 0.05 | 3.8 \pm 0.6 | 381 \pm 41 |
| 5 | 30.5 | 14 | 2460 \pm 51 | 2289 \pm 67 | 7.67 \pm 0.11 | 1.9 \pm 0.4 | 1100 \pm 272 |
| 6 | 30.5 | 13 | 2453 \pm 74 | 2339 \pm 85 | 7.54 \pm 0.16 | 1.6 \pm 0.8 | 1590 \pm 435 |

Calcification

Mean calcification in control treatments ranged from 0.3 ± 1.6 mg coral⁻¹ d⁻¹ (mean \pm standard deviation) for *P. divaricata* to 9.7 ± 4.4 mg coral⁻¹ d⁻¹ for *A. agaricites* (Table 2.2, Fig. 2.3). Corals showed species-specific responses to increased temperature and pCO₂, with six species (*A. cervicornis*, *D. stokesii*, *D. clivosa*, *P. astreoides*, *S. radians*, *S. hyades*) showing statistically significant responses to temperature (Table 2.3). Growth responded positively to temperature for two of these species, *S. radians* and *S. hyades*. *S. hyades* showed a pCO₂ effect at 30°C (one-way ANOVA F(1,66) = 5.2, p = 0.02), but not at 27 °C treatments while *P. astreoides* had a pCO₂ response at 27°C (one-

way ANOVA $F(1,74) = 9.6$, $p = 0.003$) but not 30°C. *A. cervicornis* had complete mortality in the high temperature, highest pCO₂ treatment. *A. agaricities* responded only to pCO₂. *M. cavernosa* calcification declined significantly with both increased temperature and pCO₂. *M. faveolata* exhibited an interaction whereby calcification ceased at the intermediate CO₂ and elevated temperature. *D. strigosa*, *P. divaricata*, and *S. siderea* did not respond significantly to either treatment variable.

CO₂ responses

Coral calcification regressions of mean calcification to pCO₂ at each temperature showed a range of responses, with most corals exhibiting 10-70% relative declines in calcification per unit change Ω_{arag} (Table 2.4). Slopes were greater at the elevated temperatures, indicating larger declines in calcification as temperature increases. No changes (slope = 0) were observed in a few species and treatments, which was due to either low to zero calcification rates in a particular temperature treatment (*P. astreoides* 30.5°C) or no measurable response to increasing pCO₂ (*A. cervicornis* 27°C, *D. stokesii* 27°C and 30°C, *D. strigosa*, 30°C, *S. siderea* 27°C and 30°C).

Table 2.2. Growth rates of corals (mg d^{-1}), reported as mean \pm SD (n). “nd” signifies no data.

| Species | Temp. (°C) | pCO ₂ (ppm) | | |
|------------------------------|---------------|------------------------|---------------------|---------------------|
| | | 400 | 1200 | 1600 |
| <i>Acropora cervicornis</i> | 27 | 6.4 \pm 2.9 (4) | 5.3 \pm 3.5 (4) | 6.8 \pm 4.4 (6) |
| | 30.5 | 1.3 (1) | -1.4 \pm 1 (2) | nd |
| <i>Agaricia agaricites</i> | 27 | 9.7 \pm 4.4 (9) | 7.4 \pm 4.8 (9) | 6.1 \pm 3.3 (9) |
| | 30.5 | 11 \pm 4.8 (9) | 6.8 \pm 2.8 (9) | 4.4 \pm 3.9 (9) |
| <i>Dichocoenia stokesii</i> | 27 | 3.1 \pm 2 (9) | 2.3 \pm 2.7 (9) | 3 \pm 2.1 (10) |
| | 30.5 | 1 \pm 2.4 (9) | 1.2 \pm 2.1 (9) | 0.7 \pm 2.1 (12) |
| <i>Diploria clivosa</i> | 27 | 3.7 \pm 4.9 (6) | 1.5 \pm 3.3 (6) | 1.6 \pm 2 (6) |
| | 30.5 | 1.5 \pm 4 (5) | -0.4 \pm 0.6 (6) | -0.8 \pm 1.2 (6) |
| <i>Diploria strigosa</i> | 27 | 2.2 \pm 2.2 (7) | 0.3 \pm 3.1 (7) | 0.1 \pm 4.1 (7) |
| | 30.5 | 1.4 \pm 3.4 (7) | 1.1 \pm 3.1 (7) | 1.9 \pm 2.5 (7) |
| <i>Montastraea cavernosa</i> | 27 | 2 \pm 1.2 (24) | 2 \pm 1.3 (24) | 1.3 \pm 0.8 (24) |
| | 30.5 | 1.1 \pm 1.1 (25) | 0.7 \pm 0.8 (23) | -0.4 \pm 1.2 (24) |
| <i>Montastraea faveolata</i> | 27 | 6.9 \pm 3.5 (23) | 5.8 \pm 4.6 (21) | 5.3 \pm 5.4 (21) |
| | 30.5 | 5.3 \pm 4.7 (21) | -0.1 \pm 1.2 (19) | 6.2 \pm 4.6 (21) |
| <i>Porites astreoides</i> | 27 | 1.1 \pm 1.4 (25) | 0.5 \pm 1.1 (26) | 0 \pm 1.2 (25) |
| | 30.5 | -0.3 \pm 1.5 (25) | -0.8 \pm 1.7 (26) | -0.1 \pm 1.5 (24) |
| <i>Porites divaricata</i> | 27 | 0.3 \pm 1.6 (22) | -0.5 \pm 3 (19) | -0.1 \pm 1.4 (19) |
| | 30.5 | 0.8 \pm 2.6 (19) | 0.4 \pm 1.3 (19) | -0.1 \pm 1.6 (19) |
| <i>Siderastrea radians</i> | 27 | 1.4 \pm 1.1 (25) | 1.4 \pm 1.5 (26) | 1 \pm 1.2 (23) |
| | 30.5 | 2.3 \pm 1.8 (24) | 2 \pm 1.6 (25) | 1.7 \pm 1.7 (22) |
| <i>Siderastrea siderea</i> | 27 | 5.8 \pm 3.7 (22) | 5.1 \pm 2.9 (22) | 5.1 \pm 2.8 (24) |
| | 30.5 | 5.2 \pm 3.4 (24) | 5.6 \pm 3 (23) | 4.9 \pm 3.2 (23) |
| <i>Solenastrea hyades</i> | 27 | 2.4 \pm 1.9 (26) | 2.1 \pm 1.9 (23) | 2.8 \pm 2.2 (23) |
| | 30.5 | 4.5 \pm 2.2 (23) | 3.1 \pm 1.6 (22) | 3.2 \pm 2.5 (23) |

Table 2.3. Results of Scheirer-Ray-Hare (*A. cervicornis*, *M. faveolata*) and two-way ANOVA tests (all other species). Significant results ($\alpha = 0.05$) are noted with an asterisk.

| Species | Effect | SS | df | H | p | Species | Effect | SS | df | H | p |
|-----------------------|--------------------------|-----|-----|------|---------|----------------------|--------------------------|------|-----|-----|---------|
| <i>A. cervicornis</i> | Temperature | 79 | 1 | 5 | 0.02* | <i>M. faveolata</i> | Temperature | 104 | 1 | 5 | 0.03* |
| | pCO ₂ | 9 | 2 | 1 | 0.74 | | pCO ₂ | 279 | 2 | 13 | 0.001* |
| | Temp. x pCO ₂ | 1 | 1 | 0.1 | 0.79 | | Temp. x pCO ₂ | 292 | 2 | 14 | 0.001* |
| | Residuals | 160 | 12 | | | | Residuals | 2295 | 136 | | |
| Species | Effect | SS | df | F | p | Species | Effect | SS | df | F | P |
| <i>A. agaricites</i> | Temperature | 2 | 1 | 0.1 | 0.74 | <i>P. astreoides</i> | Temperature | 31 | 1 | 15 | <0.001* |
| | pCO ₂ | 238 | 2 | 7.2 | 0.002* | | pCO ₂ | 9 | 2 | 2 | 0.11 |
| | Temp. x pCO ₂ | 21 | 2 | 0.6 | 0.53 | | Temp. x pCO ₂ | 12 | 2 | 3 | 0.05 |
| | Residuals | 795 | 48 | | | | Residuals | 291 | 145 | | |
| <i>D. stokesii</i> | Temperature | 51 | 1 | 10 | 0.003* | <i>P. divaricata</i> | Temperature | 7 | 1 | 1.8 | 0.19 |
| | pCO ₂ | 1 | 2 | 0.1 | 0.9 | | pCO ₂ | 11 | 2 | 1.3 | 0.27 |
| | Temp. x pCO ₂ | 4 | 2 | 0.4 | 0.7 | | Temp. x pCO ₂ | 4 | 2 | 0.5 | 0.64 |
| | Residuals | 263 | 52 | | | | Residuals | 450 | 111 | | |
| <i>D. clivosa</i> | Temperature | 40 | 1 | 4.3 | 0.047* | <i>S. radians</i> | Temperature | 18 | 1 | 8 | 0.01* |
| | pCO ₂ | 35 | 2 | 1.9 | 0.17 | | pCO ₂ | 8 | 2 | 1.7 | 0.19 |
| | Temp. x pCO ₂ | 0.3 | 2 | 0.01 | 0.99 | | Temp. x pCO ₂ | 1 | 2 | 0.1 | 0.88 |
| | Residuals | 265 | 29 | | | | Residuals | 312 | 139 | | |
| <i>D. strigosa</i> | Temperature | 4 | 1 | 0.4 | 0.54 | <i>S. siderea</i> | Temperature | 0.2 | 1 | 0 | 0.88 |
| | pCO ₂ | 9 | 2 | 0.5 | 0.62 | | pCO ₂ | 6 | 2 | 0.3 | 0.73 |
| | Temp. x pCO ₂ | 12 | 2 | 0.6 | 0.55 | | Temp. x pCO ₂ | 8 | 2 | 0.4 | 0.68 |
| | Residuals | 353 | 36 | | | | Residuals | 1334 | 132 | | |
| <i>M. cavernosa</i> | Temperature | 62 | 1 | 53 | <0.001* | <i>S. hyades</i> | Temperature | 51 | 1 | 12 | 0.001* |
| | pCO ₂ | 35 | 2 | 15 | <0.001* | | pCO ₂ | 18 | 2 | 2 | 0.14 |
| | Temp. x pCO ₂ | 4 | 2 | 2 | 0.2 | | Temp. x pCO ₂ | 19 | 2 | 2 | 0.12 |
| | Residuals | 161 | 138 | | | | Residuals | 580 | 134 | | |

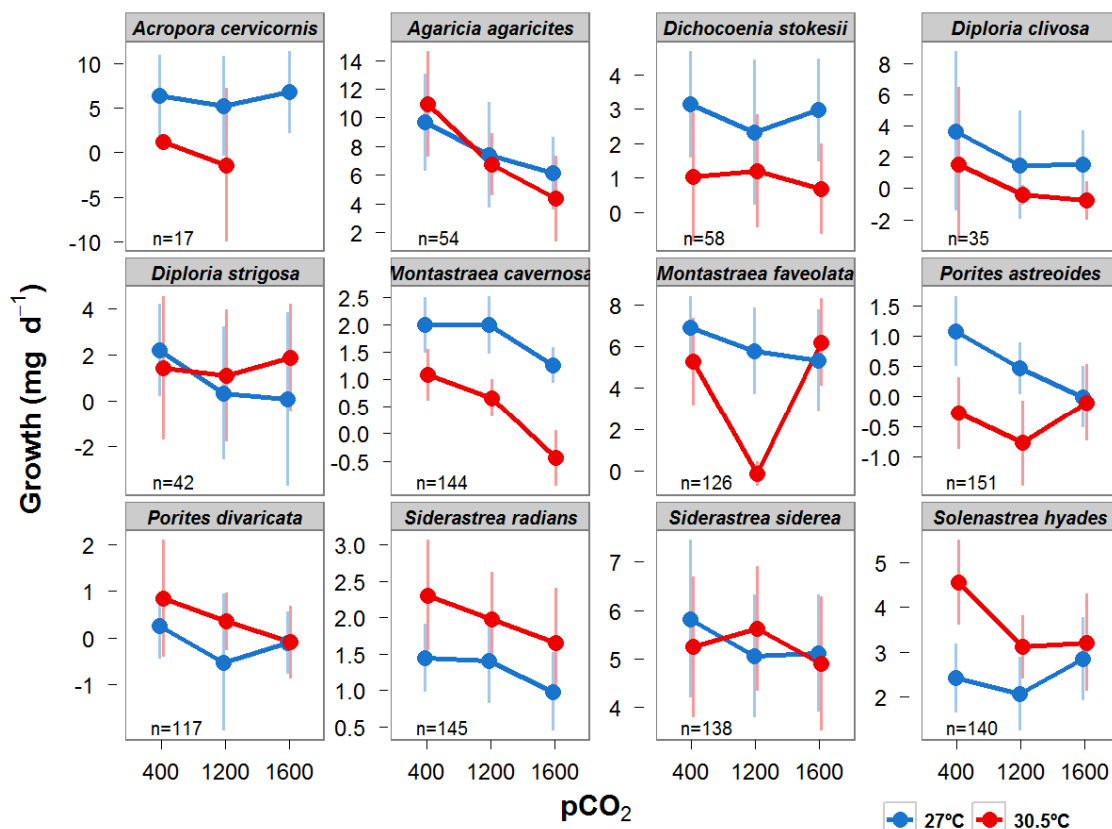


Figure 2.3. Coral growth rates across treatments. Carbon dioxide treatments are graphed on the x-axis and control and elevated temperatures are blue and red colors, respectively. Circles represent mean, and error bars are 95% confidence intervals. Total sample size for each species is listed in the bottom corner. Note: X-axis is not proportional.

Growth projections

Projected growth relative to year 2010 rates declined approximately 33-110% by 2100 for most coral species (Fig. 2.4, Table 2.5), with *P. astreoides* experiencing the largest declines of $109 \pm 22\%$, (calcification relative to present day \pm 95% confidence interval). The next most affected coral was *D. clivosa* with rates falling $16 \pm 24\%$ by 2100, followed by *A. cervicornis* ($24 \pm 30\%$) *M. cavernosa* ($31 \pm 24\%$), *D. stokesii* ($46 \pm 16\%$), and *A. agaricites* ($67 \pm 11\%$). *S. siderea* had almost no net change in projected growth ($93 \pm 6\%$) while *S. radians* and *S. hyades* had approximate increases of 30%. The

variability associated with models for *D. strigosa* and *P. divaricata* was too large to determine growth trajectories for these species. *M. faveolata*'s calcification by this model would fall to 64% by 2100, but this result is confounded by the interaction and consequently is not included in the discussion.

Table 2.4. Constants for calcification response variables. Slopes (m) represent change in calcification per unit increase in Ω_{arag} for each treatment temperature (T). *A. cervicornis* only had two data points for the regression at 30°C, hence residual mean square error (RMSE) is not applicable (NA). The other variables are regression intercepts (b) and coefficients of determination (r^2).

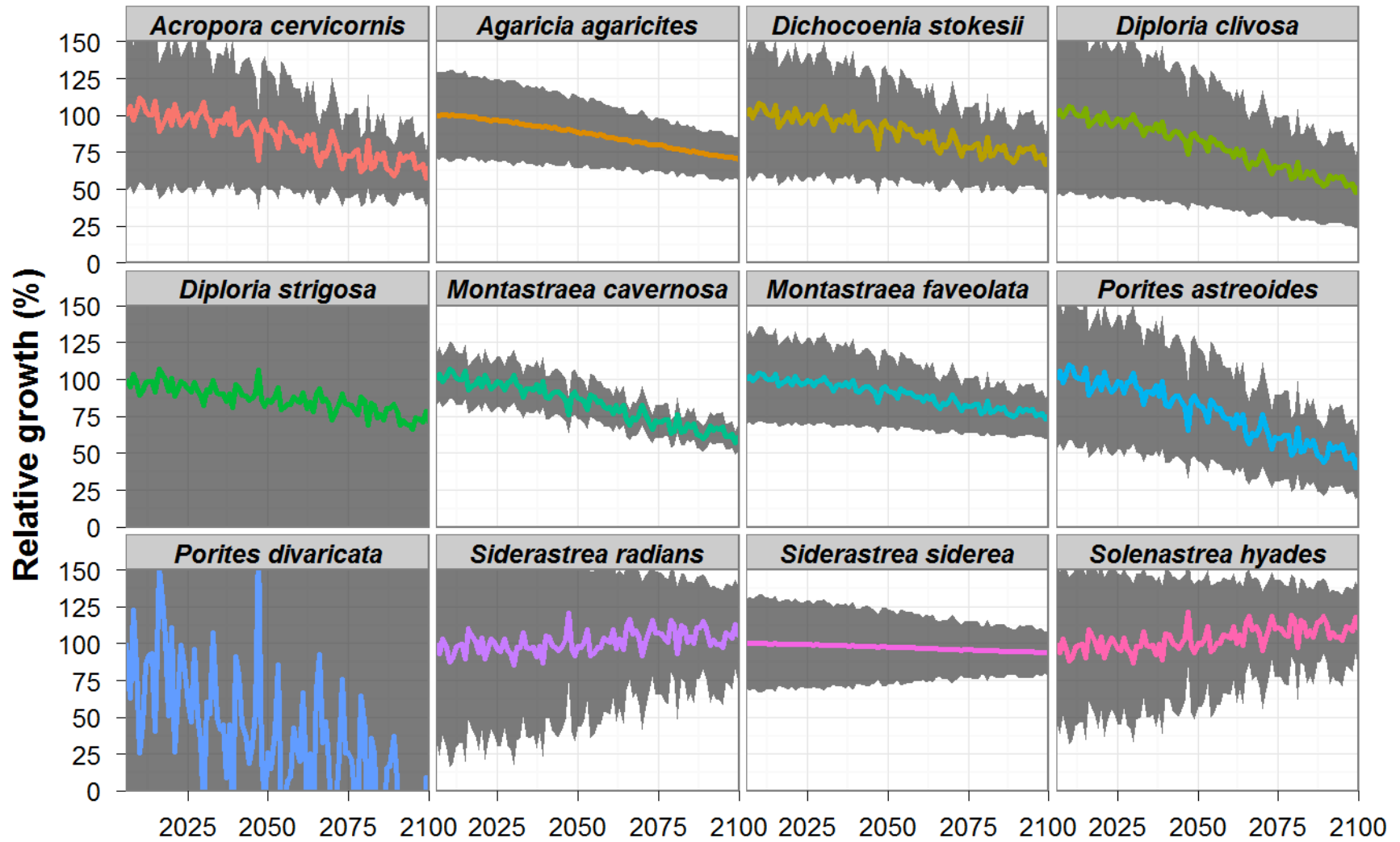
| Species | T (°C) | m | b | RMSE | r^2 |
|-----------------------|--------|-------|-------|------|-------|
| <i>A. cervicornis</i> | 27 | 0.02 | 6.14 | 1.1 | 0.0 |
| | 30.5 | 1.39 | -4.04 | NA | 1.0 |
| <i>A. agaricites</i> | 27 | 1.72 | 4.41 | 0.30 | 1.0 |
| | 30.5 | 2.72 | 0.74 | 1.12 | 0.9 |
| <i>D. stokesii</i> | 27 | 0.19 | 2.45 | 0.53 | 0.2 |
| | 30.5 | 0.07 | 0.79 | 0.36 | 0.1 |
| <i>D. clivosa</i> | 27 | 1.14 | 0.02 | 0.46 | 0.9 |
| | 30.5 | 1.04 | -2.43 | 0.03 | 1.0 |
| <i>D. strigosa</i> | 27 | 1.11 | -1.29 | 0.23 | 1.0 |
| | 30.5 | -0.07 | 1.63 | 0.56 | 0.0 |
| <i>M. cavernosa</i> | 27 | 0.28 | 1.20 | 0.43 | 0.5 |
| | 30.5 | 0.53 | -0.85 | 0.67 | 0.6 |
| <i>M. faveolata</i> | 27 | 0.77 | 4.51 | 0.04 | 1.0 |
| | 30.5 | 0.73 | 2.00 | 4.66 | 0.1 |
| <i>P. astreoides</i> | 27 | 0.51 | -0.48 | 0.16 | 1.0 |
| | 30.5 | 0.04 | -0.48 | 0.49 | 0.0 |
| <i>P. divaricata</i> | 27 | 0.26 | -0.61 | 0.40 | 0.5 |
| | 30.5 | 0.37 | -0.52 | 0.24 | 0.9 |
| <i>S. radians</i> | 27 | 0.19 | 0.92 | 0.25 | 0.6 |
| | 30.5 | 0.25 | 1.36 | 0.18 | 0.9 |
| <i>S. siderea</i> | 27 | 0.39 | 4.57 | 0.18 | 0.9 |
| | 30.5 | 0.03 | 5.18 | 0.52 | 0.0 |
| <i>S. hyades</i> | 27 | -0.11 | 2.65 | 0.53 | 0.1 |
| | 30.5 | 0.66 | 2.01 | 0.21 | 1.0 |

Table 2.5. Projected changes in coral growth by the year 2100 relative to rates in 2010 (%). Multiple linear regression constants for aragonite saturation state (Ω_{arag}), temperature, and intercepts are listed.

| Species | Year 2100 | $\pm 95\%$ CI | Ω_{arag} | T ($^{\circ}\text{C}$) | Intercept |
|-----------------------|-----------|---------------|------------------------|--------------------------|-----------|
| <i>P. astreoides</i> | -9 | 22 | 0.3 | -0.3 | 8 |
| <i>D. clivosa</i> | 16 | 24 | 0.2 | -0.6 | 19 |
| <i>A. cervicornis</i> | 24 | 30 | 3.4 | -0.1 | 1 |
| <i>M. cavernosa</i> | 31 | 7 | 0.7 | -0.4 | 12 |
| <i>D. stokesii</i> | 46 | 16 | 1.5 | -0.7 | 17 |
| <i>A. agaricites</i> | 67 | 11 | 0.1 | -2.3 | 67 |
| <i>S. siderea</i> | 93 | 10 | 0.3 | 0.2 | -6 |
| <i>S. radians</i> | 127 | 20 | 0.4 | 0.4 | -9 |
| <i>S. hyades</i> | 135 | 16 | 0.3 | 0 | 5 |

Figure 2.4. Projected relative coral growth to the year 2100 based annual average temperature and Ω_{arag} from the RCP 8.5 emissions scenario. Growth is normalized to the year 2006. Shaded area represents 95% confidence limit. These confidence bounds reflect only the error in the coral growth models and do not include uncertainty in the climate models. They narrow with time because projected annual average temperatures increase from 24.5 $^{\circ}\text{C}$ to 26.5 $^{\circ}\text{C}$ in 2100 while this experiment tested coral growth at 27 $^{\circ}\text{C}$ and 30.5 $^{\circ}\text{C}$. These treatment temperatures reflect the average projected summer temperature increases. *D. strigosa* and *P. divaricata* models reflect variable calcification rates. *M. faveolata* projections should be considered with caution given the observed interaction between temperature and pCO₂.

Caribbean coral growth projections



DISCUSSION

Calcification responses

This experiment demonstrated temperature is the dominant stressor to corals, and species vary in their growth responses to both temperature and pCO₂. Six species significantly responded only to temperature effects, and two of those species (*S. radians* and *S. hyades*) had positive calcification with increasing temperature. *P. divaricata* also had higher calcification at higher temperatures, but its rates were not significantly different across temperature treatments. *S. radians*, *S. hyades*, and *P. divaricata* are considered stress tolerant species thriving in habitats considered marginal for other species (Macintyre and Pilkey 1969; Lirman et al. 2003; Crook et al. 2012), including warm shallow waters (Chiappone and Sullivan 1994). All of the *S. hyades* and many of the *S. radians* and *P. divaricata* were collected from Florida Bay where summertime maximum temperatures can reach 34°C. Consequently the 27°C control temperature may actually be suboptimal to these corals relative to the higher 30.5°C temperature, which could explain why these corals had higher calcification rates in warmer temperatures. Temperature negatively affected the other species. All *A. cervicornis* in the highest temperature and highest pCO₂ treatment died. *P. astreoides* at 30.5°C appeared pale or bleached towards the end of the experiment.

P. astreoides exemplifies the dominance of temperature over pCO₂ as a stressor. Thirty degrees Celsius appears to surpass its thermal threshold, resulting in no net growth. Without any calcification at this temperature, a pCO₂ effect cannot be detected. However at control temperatures, calcification showed consistent decreases with increasing pCO₂. *S. hyades* had similar CO₂-induced declines at 30.5°C only, although

calcification was net positive in all treatments. Seibel et al. (2012) observed an analogous pattern in the pteropod *Limacina helicina antarctica* where starved specimens maintained constant respiration while fed specimens respired less with increasing pCO₂. The authors proposed low prey availability suppressed metabolism, masking the effects of pCO₂ for those starved pteropods. Metabolism is generally proportional to temperature, and the metabolic suppression observed by Seibel et al. (2012) could be the mechanism underlying *S. hyades*'s different CO₂ responses at different temperatures. In another coral study, *Porites rus* decreased calcification in response to high pCO₂ at elevated temperatures and no calcification change at lower temperatures (Edmunds et al. 2012).

A. agaricites was the only coral statistically responsive to pCO₂ but not temperature. This species has proven temperature resistant in regards to its zooxanthellae (Fitt and Warner 1995; Warner et al. 1996), which were not identified in those studies. Its calcification declines of approximately 44% per unit change saturation state are at the upper end of those compiled in Kleypas and Langdon (2006), indicating it is more sensitive to ocean acidification than other corals. For this any other species, the lack of statistical effects for temperature do not actually mean temperature does not affect coral. Rather, calcification rates likely follows a Gaussian distribution (Marshall and Clode 2004) for which the two temperature treatments lie on either side of the thermal optimum (Edmunds et al. 2012). More than two treatments are necessary to further elucidate temperature responses.

Both temperature and pCO₂ treatments reduced calcification in *M. cavernosa*. Consequently, this species is particularly vulnerable to climate change because it cannot

extend its range latitudinally or deeper to avoid heat stress without experiencing depressed growth conditions as optimal saturation states constrict towards shallow tropical waters. *M. faveolata* experienced no change in calcification except under the high temperature, intermediate pCO₂ treatment, where calcification stopped for almost all corals. This observation is likely not a result of the experimental methods because of the aforementioned stratified random assignment, replicate tanks, periodic random reassignment within treatments, and random periodic shuffling of treatment tanks. Reynaud et al. (2003) observed almost identical results with *Stylophora pistillata* where the pCO₂ effect was only observed at the elevated temperature and elevated pCO₂ concentration of 798 µatm. Their experiment did not include a higher pCO₂ treatment. In another study (Anthony et al. 2008), *Porites lobata* calcification rates were highest at the intermediate pH treatment and elevated temperature, though the authors did not find a significant interaction between temperature and pH. Wooldridge (2008) proposed a possible enzymatic “dead zone” at intermediate pH, but this level corresponded to 560 ppm pCO₂ rather than 800 ppm. Nonetheless, if a similar mechanism was responsible for calcification shutdown in this species, it must also be temperature-dependent.

This study demonstrates not only interspecies variability to climate change factors, but variability among closely related species. *P. astreoides* proved temperature sensitive while its congeneric *P. divaricata* was not. In contrast, massive Pacific *Porites* spp. are generally more resistant to pCO₂ while branching *P. rus* are sensitive (Edmunds et al. 2012), which supports observations of massive Pacific *Porites* spp. dominance in natural CO₂ vent areas (Fabricius et al. 2011). *P. astreoides*, the only Atlantic massive *Porites* spp., appears highly sensitive to both warming and acidification, despite its

presence near CO₂ vents in the Gulf of Mexico (Crook et al. 2012). *D. strigosa* and *D. clivosa* also followed this pattern of mixed temperature sensitivity, where *D. strigosa* was insensitive and *D. clivosa* sensitive to temperature. Opposite of those genera, *S. radians* increased calcification with increasing temperature and *S. siderea* was insensitive. These results suggest coral responses cannot be generalized to genus. Overall, temperature increases to 30.5°C negatively affected growth while CO₂ generally had secondary, negative effects on growth. This pattern is expected given many studies have documented the detrimental effects of increased temperature on coral and symbiont physiology (González-Dávila et al. 2010) but few have found CO₂ adversely affecting physiology rather than the underlying chemical conditions for calcification (Hendriks et al. 2010; Kroeker et al. 2010). Exceptions to this generalization include CO₂-induced bleaching (Anthony et al. 2008) and depressed reproduction (Kurihara 2008; Albright et al. 2010; Morita et al. 2010; Albright and Langdon 2011).

Growth projections

Modelers and managers can use these data to predict reef changes through time and assess relative vulnerability of species to climate change. Models of coral growth based on the A1b emissions scenario reveal large declines in several taxa by the end of the century (Table 2.5, Fig. 2.4). *P. astreoides* was the most sensitive species, followed in order by *D. clivosa*, *A. cervicornis*, *M. cavernosa*, *D. stokesii*, and *A. agaricites*. All of these are considered reef-builders, and therefore any slowing in their growth could have subsequent effects for the diverse assemblages of organisms that live, forage, and reproduce on reefs. Carricart-Ganivet et al. (2012) modeled coral growth of several

genera, including *P. astreoides* and *M. faveolata*, and obtained similar results though their models did not account for ocean acidification. In their study, *P. astreoides* experiences net dissolution by 2100 and *M. faveolata* calcification falls 40%. Currently, *P. astreoides* is increasing in relative abundance on Caribbean reefs (Green et al. 2008), but most of this increase was attributed to faster declines of other species (Gardner et al. 2003; Alvarez-Filip et al. 2009) as well as new recruitment rather than sustained growth.

Two species that showed no negative effects, *S. radians* and *S. hyades*, are generally small and do not contribute significantly to reef frameworks. *P. divaricata*, another minor component of Caribbean reefs, had large variability associated with its model that reflects high intraspecies variability in calcification rates relative to differences across treatments. *D. strigosa*'s growth projections were also inconclusive, likely a result of intraspecies variability and low sample size. Diversity of responses within a species can serve an adaptive purpose where over time resistant individuals preferentially reproduce and pass on their genes. However, given the rapid rate of climate change and slow generation time of corals, adaptation is unlikely (Hoegh-Guldberg 1999). In fact, coral abundance and recruitment have both fallen in the Caribbean (Hughes and Tanner 2000; Gardner et al. 2003), which can lead to positive feedbacks of coral loss (Birkeland 2004; Mumby and Steneck 2008). While the reef-builders generally fair poorly in the simulations, *S. siderea* maintains almost constant calcification through the end of the century, indicating this structural coral may persist while others falter. Managers should concentrate on protecting reefs and managing local stressors where this species is abundant.

The growth models used in this study are conservative because they do not account for bleaching and mortality from temperatures rising above upper thermal thresholds, which are usually within 1-2°C of summertime means (Coles et al. 1976; Jokiel and Coles 1977). The simulation data also utilized annual averages for temperature, instead of summertime peak temperatures. Furthermore, models do not take into consideration a host of other stressors that negatively affect coral health such as fishing pressure and eutrophication (Jackson et al. 2001). The A1b emissions scenario used in this study is conservative compared to actual emissions, which are increasing faster than the IPCC's most extreme scenarios (Raupach et al. 2007).

This study demonstrates species-specific responses to climate change and assesses the relative sensitivity of many common Caribbean corals. Responses often differed within genera, precluding generalizations at this taxonomic level. Reef-building corals are the most vulnerable to climate change, with the exception of *S. siderea*, as opposed to smaller, weedy species. Calcification rates decline faster with temperature stress than elevated pCO₂. *S. hyades* and *S. radians* were resistant to temperature and pCO₂ stress and are found in highly variable environments, hence they are ideal species for further study on resistance to climate change stressors.

Chapter 3: Stress-tolerant Corals of Florida Bay are Vulnerable to Ocean Acidification

SUMMARY

In situ calcification measurements tested the hypothesis that corals from environments (Florida Bay, USA) that naturally experience large swings in pCO₂ and pH will be tolerant or less sensitive to ocean acidification than species from laboratory experiments with less variable carbonate chemistry. The pCO₂ in Florida Bay varies from summer to winter by several hundred ppm roughly comparable to the increase predicted by the end of the century. Rates of net photosynthesis and calcification of two stress tolerant coral species, *Siderastrea radians* and *Solenastrea hyades*, were measured under the prevailing ambient chemical conditions and under conditions amended to simulate a pH drop of 0.1-0.2 units at bimonthly intervals over a two year period. Net photosynthesis was not changed by the elevation in pCO₂ and drop in pH; however, calcification declined by 52% and 50% per unit decrease in saturation state, respectively. These results indicate that the calcification rates of *S. radians* and *S. hyades* are just as sensitive to a reduction in saturation state as coral species that have been previously studied. In other words stress tolerance to temperature and salinity extremes as well as regular exposure to large swings in pCO₂ and pH did not make them any less sensitive to ocean acidification. These two species likely survive in Florida Bay in part because they devote proportionately less energy to calcification than most other species and the average saturation state is elevated relative to that of nearby offshore water due to high rates of primary production by seagrasses.

BACKGROUND

Atmospheric CO₂ has increased by over 100 ppm since the start of the industrial revolution principally as a result of the burning of fossil fuels. The world's oceans have absorbed ~33-50% of this CO₂ (Sabine et al. 2004), which has in turn caused well-documented reductions in carbonate ion concentration and concomitant decreases in pH (Dore et al. 2009; González-Dávila et al. 2010). Several studies and meta-analyses have shown varying organismal responses to ocean acidification (Ries et al. 2009; Hendriks et al. 2010; Kroeker et al. 2010). Coral calcification is consistently negatively impacted with general declines of 20-30% per unit change in aragonite saturation state (Langdon and Atkinson 2005; Kroeker et al. 2010). However, some studies suggest certain corals appear less sensitive to pCO₂ changes than others (Gattuso et al. 1998; Marubini et al. 2001; Marubini et al. 2003; Reynaud et al. 2003). Furthermore, recent work has shown factors such as feeding can mitigate the negative effects of pCO₂ on calcification (Cohen and Holcomb 2009). Altogether, these studies indicate corals have varying responses to pCO₂, but little is known about the nature of this variance.

In addition to ocean acidification, climate change is expected to increase sea surface temperatures (SSTs) past corals' thermal optimums. The dual stressors of higher temperatures and changing ocean chemistry are expected to have compounding effects on net reef growth (Hoegh-Guldberg 2005; Silverman et al. 2009). A study by Reynaud et al. (2003) illustrates these compounded effects, where calcification of *S. pistillata* declined by -38%, at elevated temperature and pCO₂, compared to -5% as a result of pCO₂ alone. The 3°C temperature increase that these corals experienced is within the annual (and diurnal) temperature range of many reefs. Consequently to understand coral

responses to ocean acidification, calcification must be measured under a range of conditions that represent the conditions that corals experience in nature and that are associated with future climate change.

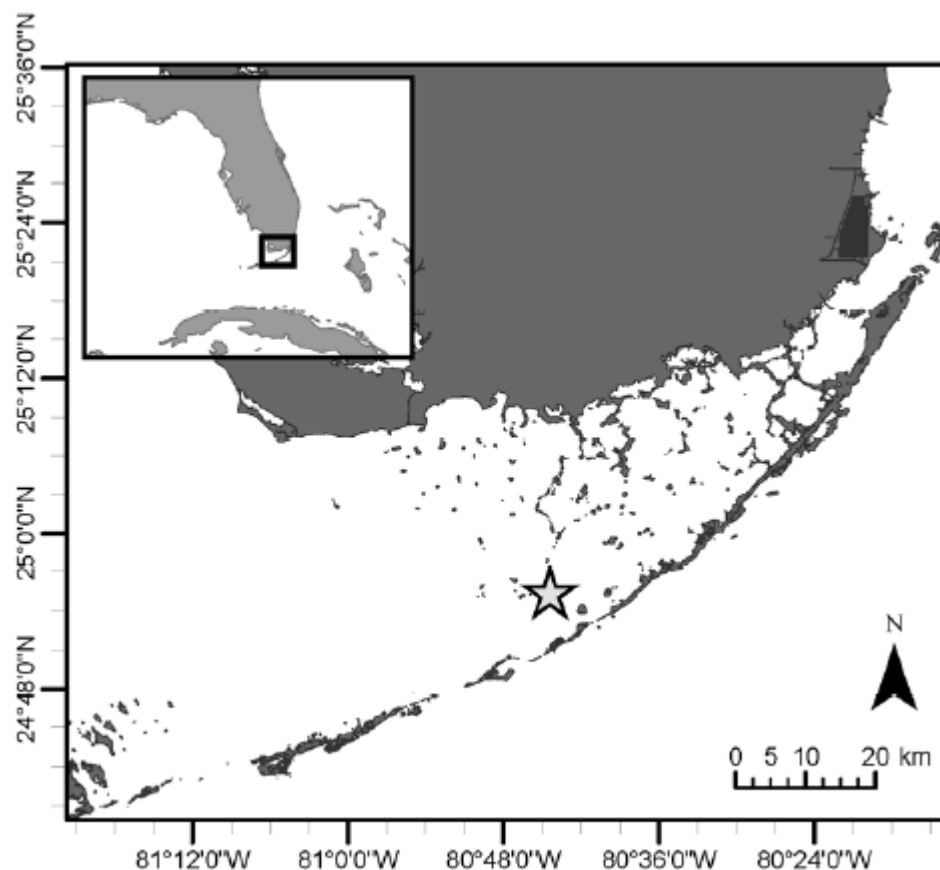


Figure 3.1. The field site, denoted by a star, is just north of Peterson Keys in Florida Bay.

Florida Bay as a natural laboratory

Florida Bay, bordered by the Everglades to the north and the Florida Keys to the south and east (Fig. 3.1), consists of a series of shallow, compartmentalized basins whose chemistry is dominated by carbonate sediment precipitation and dissolution (Ginsburg 1956; Kerr 1972; Yates et al. 2007). The relative isolation and shallow basins subject Florida Bay to more extremes in temperature and salinity (Montague and Ley 1993;

Boyer et al. 1997,1999; Millero et al. 2001). Mass seagrass dieoff and chronic ecosystem degradation beginning in the summer of 1987 have been attributed to such extremes in temperature and salinity (Fourqurean and Robblee 1999; Porter et al. 1999; Zieman et al. 1999; Koch et al. 2007). Because the depth is shallow (≤ 3 m), ambient air temperatures affect SSTs in the bay to a greater degree than offshore waters. Winter cold fronts traveling southward over the Florida peninsula cause cold spells (Roberts et al. 1982; Duever et al. 1994) whereas summer temperatures typically raise bay temperatures over 30°C for extended periods (Fig. 3.2). Two different processes heavily influence salinity variations in the bay: Everglades runoff in the northeast and evaporation/precipitation in the southwest (Swart and Price 2002).

With respect to carbonate chemistry and ocean acidification, Florida Bay acts as a natural laboratory for changing pCO_2 , with seasonal pCO_2 of 325-725 μatm (Millero et al. 2001), and diurnal swings of 100-200 μatm pCO_2 (Yates et al. 2007). Variability in pH values in Florida Bay reflect those reported in other nearshore systems (Wootton et al. 2008; Hofmann et al. 2011). Diurnal changes in carbonate chemistry of Florida Bay are driven by biogenic sediment precipitation and dissolution (Yates et al. 2007), which in turn are driven by photosynthesis and respiration effects on pCO_2 and pH (Yates and Halley 2006). Seasonal variability is also biologically driven through calcification and photosynthesis (Millero et al. 2001), as well as by oxidation of organic matter and by the exchange with marine water (Swart et al. 1996b; Swart et al. 1999). Because of this natural variation in pCO_2 , *in situ* measurements of calcification throughout the year can be used to predict coral calcification responses to future increases in atmospheric CO_2 .

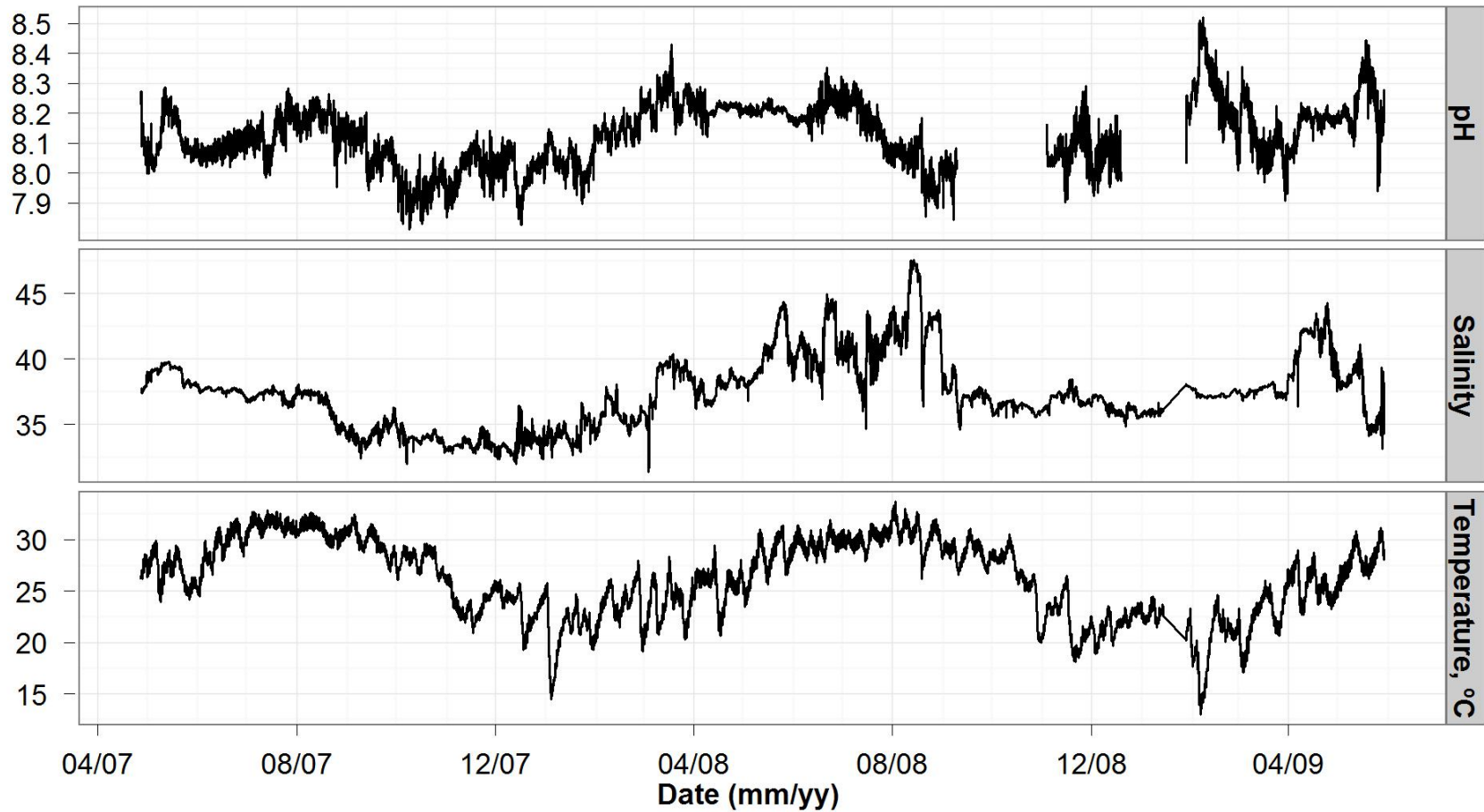


Figure 3.2. Water quality parameters over the course of the study period. This area of Florida Bay regularly experiences hypersalinity, summer temperatures in excess of 30°C, and winter cold spell temperatures below 15°C. The pH rarely fell below 8.0. Gaps in the pH record were due to sensor malfunctions.

Stress tolerant corals

Corals are not widely found throughout Florida Bay, principally as a result of the lack of suitable hard substrate. Where there is bare rock on which they can attach, corals appear healthy despite the variable pCO₂. These corals might therefore represent CO₂-resistant scleractinians. Three species of corals occur in the study area: *Siderastrea radians* (Pallas 1776), *Solenastrea hyades* (Dana 1846), and *Porites divaricata* (LeSuer 1821). Given the ability of these species to tolerate stress and marginal or disturbed habitats (Vaughan 1913; Yonge 1936; Macintyre and Pilkey 1969; Lewis 1989; Rice and Hunter 1992; Lirman et al. 2002; Lirman et al. 2003; Macintyre 2003; Chartrand et al. 2009; Lirman and Manzello 2009), they may also have the ability to tolerate changing pCO₂ levels, i.e., maintain constant calcification rates even in high pCO₂ conditions. Such corals would provide model organisms for studying how other taxa might cope with ocean acidification and physiological mechanisms that determine pCO₂ resistance. In addition, the two tropical corals examined in this study, *S. radians* and *S. hyades*, have been observed in cool, temperate waters as far north as North Carolina, USA (Macintyre and Pilkey 1969; Macintyre 2003).

METHODS

Field site

Eleven specimens of *Siderastrea radians* and nine specimens of *Solenastrea hyades* were collected near Peterson Keys (Fig. 3.1; 24.926 °N, 80.740 °W) in Florida Bay and epoxied to plastic tiles, which were attached to a platform of cinderblocks at the

collection site. Surface areas of *S. radians* and *S. hyades* were $45 \pm 17 \text{ cm}^2$ and $138 \pm 43 \text{ cm}^2$ (mean \pm standard deviation), respectively.

Environmental loggers (Yellow Springs Instruments) recorded conductivity, temperature, pressure, dissolved oxygen and pH from April 2007 to November 2010 at 30 min intervals. Between deployments, the loggers were calibrated against standards (Yellow Springs Instruments) and discrete water samples collected during field trips. Light was measured with Onset HOBO Temperature/Light Data Loggers in units of lux, which does not have an exact conversion to photosynthetically active radiation (PAR) but was approximated using a lux-PAR conversion factor of $\text{lux}/50 = \text{PAR}$. While light readings were not obtained for all visits, light levels ranged from $100\text{-}600 \mu\text{E m}^{-2} \text{ s}^{-1}$, with differences due to water quality, i.e. turbidity.

Table 3.1: Physical parameters measured during field trips. Sample sizes refer to the total number of corals measured on a particular date.

| Date (m/d/yy) | Time (h:m) | T (°C) | Sal. | O ₂ (μM) | pH _t | TA ($\mu\text{mol kg}^{-1}$ SW) | TCO ₂ ($\mu\text{mol kg}^{-1}$ SW) | Ω_{arag} | pCO ₂ (ppm) |
|------------------|---------------|-----------|------|-------------------------------------|-----------------|--|--|------------------------|-------------------------------|
| 4/27/07 | 15:00 | 26.5 | 37.7 | 224 | 8.21 | 2267 | 1821 | 4.7 | 237 |
| 5/4/07 | 11:15 | 28.3 | 39.1 | 178 | 7.99 | 2407 | 2027 | 3.8 | 465 |
| 7/11/07 | 11:00 | 30.6 | 37.4 | 163 | 8.05 | 2206 | 1822 | 4.1 | 360 |
| 7/23/07 | 11:30 | 30.8 | 36.5 | 224 | 8.12 | 2159 | 1693 | 4.4 | 293 |
| 9/12/07 | 11:30 | 29.6 | 33.1 | 203 | 8.00 | 2212 | 1884 | 3.5 | 437 |
| 9/12/07 | 14:45 | 29.9 | 33.5 | 208 | 8.02 | 2222 | 1878 | 3.6 | 422 |
| 11/19/07 | 11:30 | 22.2 | 33.4 | 237 | 8.12 | 2505 | 2168 | 3.9 | 358 |
| 11/19/07 | 13:55 | 22.5 | 33.4 | 235 | 8.11 | 2495 | 2163 | 3.8 | 368 |
| 12/12/07 | 11:15 | 23.9 | 32.2 | 214 | 8.07 | 2676 | 2338 | 4.1 | 447 |
| 12/12/07 | 14:00 | 24.2 | 32.3 | 224 | 8.08 | 2653 | 2309 | 4.2 | 430 |
| 1/30/08 | 10:30 | 19.5 | 35.3 | 239 | 8.11 | 2711 | 2370 | 3.8 | 396 |
| 1/30/08 | 13:00 | 19.9 | 35.4 | 237 | 8.10 | 2715 | 2369 | 3.8 | 406 |
| 4/9/08 | 11:00 | 25.8 | 36.6 | 204 | 8.12 | 2308 | 1935 | 4.1 | 316 |

| Date (m/d/yy) | Time (h:m) | T (°C) | Sal. | O ₂ (μM) | pH _t | TA (μmol kg ⁻¹ SW) | TCO ₂ (μmol kg ⁻¹ SW) | Ω _{arag} | pCO ₂ (ppm) |
|------------------|---------------|-----------|------|------------------------|-----------------|--|--|-------------------|-------------------------------|
| 4/9/08 | 13:00 | 26.3 | 36.6 | 217 | 8.14 | 2271 | 1885 | 4.2 | 293 |
| 4/28/08 | 11:00 | 25.1 | 38.0 | 216 | 8.23 | 2201 | 1759 | 4.9 | 234 |
| 4/28/08 | 14:00 | 25.7 | 37.9 | 212 | 8.22 | 2223 | 1777 | 4.9 | 239 |
| 6/9/08 | 11:00 | 28.1 | 39.7 | 191 | 8.20 | 2174 | 1711 | 5.0 | 244 |
| 6/9/08 | 14:00 | 28.4 | 39.5 | 200 | 8.20 | 2177 | 1714 | 5.1 | 248 |
| 8/12/08 | 11:00 | 29.9 | 46.5 | 131 | 8.03 | 2187 | 1781 | 3.9 | 366 |
| 8/12/08 | 13:30 | 30.1 | 47.2 | 131 | 8.07 | 2179 | 1733 | 4.1 | 317 |
| 11/3/08 | 11:30 | 22.7 | 36.3 | 229 | 8.14 | 2466 | 2096 | 4.1 | 326 |
| 11/3/08 | 13:00 | 23.0 | 36.4 | 231 | 8.14 | 2456 | 2083 | 4.1 | 323 |
| 1/28/09 | 10:45 | 21.8 | 38.0 | 235 | 8.23 | 2895 | 2421 | 5.4 | 297 |
| 1/28/09 | 12:45 | 22.2 | 37.9 | 241 | 8.26 | 2870 | 2361 | 5.7 | 268 |
| 3/31/09 | 10:50 | 25.7 | 37.3 | 197 | 8.05 | 2396 | 2057 | 3.8 | 415 |
| 3/31/09 | 12:45 | 26.3 | 37.3 | 212 | 8.08 | 2378 | 2012 | 4.0 | 375 |

| sample size (A = ambient, T = treatment) | | | | |
|--|-------------------|---|------------------|---|
| Date (m/d/yy) | <i>S. radians</i> | | <i>S. hyades</i> | |
| | A | T | A | T |
| 4/27/07 | - | - | - | - |
| 5/4/07 | 3 | - | 1 | - |
| 7/11/07 | - | - | - | - |
| 7/23/07 | - | - | - | - |
| 9/12/07 | 4 | 4 | 1 | 1 |
| 11/19/07 | 3 | 1 | - | - |
| 12/12/07 | 2 | 2 | 3 | 3 |
| 1/30/08 | 4 | 4 | 5 | 4 |
| 4/28/08 | 4 | 3 | 5 | 5 |
| 6/9/08 | 4 | 4 | 3 | 3 |
| 8/12/08 | 4 | 4 | 5 | 5 |
| 11/3/08 | 5 | 5 | 5 | 5 |
| 1/28/09 | 4 | 4 | 3 | 3 |
| 3/31/09 | 4 | 4 | 2 | 2 |

Chemical measurements

Total alkalinity (TA) was determined in duplicate using an automated Gran titration (Dickson et al. 2007), and accuracy was checked against certified seawater reference material (A. Dickson, Scripps Institute of Oceanography). The pH on the total scale (Dickson et al. 2007) was determined at 25.0°C using an Orion Ross combination pH electrode calibrated against Tris buffer prepared in synthetic seawater (Nemzer and Dickson 2005). Concentrations of CO_3^{2-} and Ca^{2+} as well as saturation state (Ω_{arag}) were computed from TA, pH, temperature, and salinity using the program CO2SYS (Lewis and Wallace 1998; Pierrot et al. 2006), and dissociation constants for carbonate from Mehrbach et al. (1973) as refit by Dickson and Millero (1987) and for boric acid from Dickson (1990). The pH is reported on the total scale, the scale on which K1 and K2 were determined in the Gran functions. Dissolved oxygen (DO) was determined by Winkler titration using an automated titrator that utilized amperometric endpoint detection (Langdon 2010). Salinity was measured on a Guildline 8410A Salinometer.

Incubations

At approximately bi-monthly intervals from May 2007 to March 2009, a random subset of corals from the sample population were detached from the platform that held them in place between trips and incubated *in-situ* in 2 L chambers (Fig. 3.3) for approximately 90 minutes. Under this sampling regime, certain individuals were measured multiple times over the course of the experiment. Battery-powered magnetic stirrers in the bases provided circulation within the chambers. Individual corals were incubated twice during each visit: once with the chamber filled with ambient seawater

and once with the seawater in the chamber modified to simulate mid- to end-of-century projections of $p\text{CO}_2$, i.e., 100-200 μatm above ambient conditions. The order of incubations was randomized such that half the corals were incubated under ambient conditions first while the other half under elevated $p\text{CO}_2$ conditions. The incubations were performed between 10:00 and 14:00 when daily solar insolation peaked, assuming photosynthesis would be saturating (Langdon and Atkinson 2005). Light levels were equal for both two incubations. Incubations with an empty chamber were made to account for any non-coral changes to the water chemistry, which were found to be negligible. Chambers that malfunctioned during the incubation and samples that were lost were excluded from the analyses. Water samples were withdrawn using syringes fitted to a valved port on the incubation chambers. The chambers themselves acted as large syringes, with the clear tops sliding over the bases to account for changes in volume from sampling while maintaining the separation of outside water from the inner incubation water. Water samples were then poisoned with HgCl_2 for TA or pickled Winkler reagents for DO.

CO₂ treatments

A two-part chemical injection of NaHCO_3 followed by HCl was used to elevate $p\text{CO}_2$ in the treatment incubations. This procedure was necessary for these underwater, *in-situ* incubations and is chemically identical to bubbling with $p\text{CO}_2$ (Gattuso et al. 2010). The addition of NaHCO_3 causes an increase in dissolved inorganic carbon (DIC) while the HCl cancels the increase to TA caused by the addition of the Na^+ ions. The net result is an increase in DIC and no change in TA that closely simulates what would

happen if the seawater was bubbled with CO₂ until the desired pCO₂ was achieved.

Calculation of the amounts of NaHCO₃ and HCl needed to achieve the desired chemical conditions in the 2 L chambers were computed as follows. First, present-day pCO₂ and average Florida Bay TA were used to compute present-day DIC using CO2SYS. Second, future DIC was computed holding TA constant and choosing a target pCO₂ of 750 ppm. The addition of NaHCO₃ is the desired increase in DIC and is given by Equation 3.1.

$$V_{spike} = \frac{\Delta DIC \times V_{chamber}}{N_{spike}} \quad (3.1)$$

Where V_{spike} is the volume of NaHCO₃ solution added to the chambers, ΔDIC is the difference in DIC between simulated future and present day conditions (umol L⁻¹), $V_{chamber}$ is the volume of the incubation chamber (2 L), and N_{spike} is the normality of the NaHCO₃ solution. Since the addition of NaHCO₃ increases the DIC and the TA equally Eqn. 3.1 also gives the volume of the HCl spike.

The actual achieved pCO₂ varied due to differences in ambient conditions and generally ranged from 500-800 ppm. This in turn resulted in a variable decrease in Ω_{arag} . Changes in calcification were standardized by dividing by the realized change in saturation state to account for this variation.

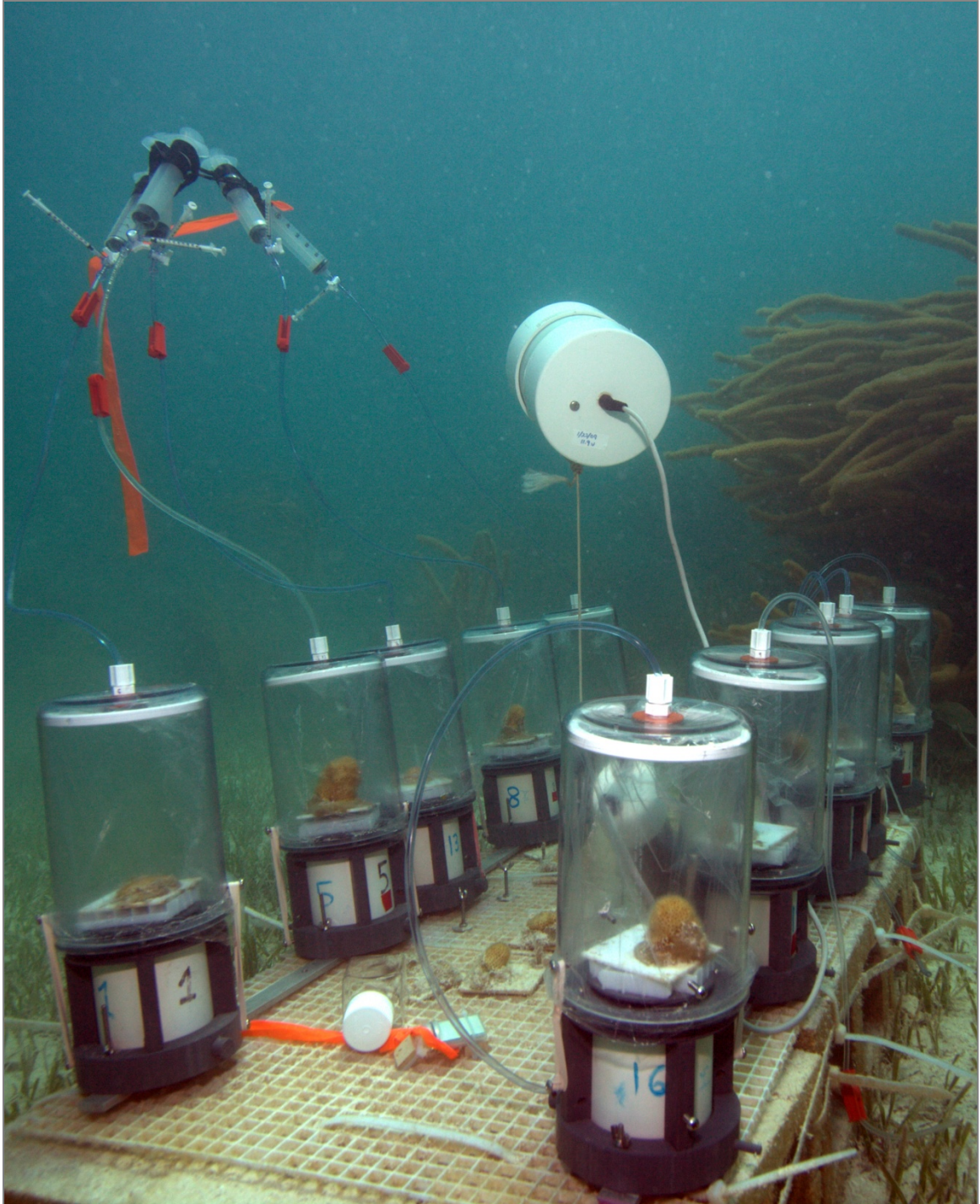


Figure 3.3. Corals were placed in incubation chambers to measure calcification and net photosynthesis. Carbon dioxide levels were elevated above ambient conditions by equimolar additions of NaHCO_3 and HCl through a sampling port at the top. Water samples were drawn from the same port. Photo credit: Evan D'Alessandro.

Biological variables

Changes in TA and DO were used to calculate calcification and net photosynthesis. Carbonate parameters and dissolved oxygen were measured as described above. Rates were normalized to coral surface area, determined from morphometric measurements. Biological variables were calculated from the following equations:

Calcification:

$$G = \frac{-0.5\rho\Delta TA \times V}{t \times SA} \quad (3.2)$$

Where G is calcification, ρ is seawater density, ΔTA is the change in total alkalinity ($\mu\text{mol kg}^{-1}$ seawater), V is chamber volume, t is the incubation time, and SA is the coral surface area.

Net photosynthesis:

$$NP = \frac{\Delta DO \times V}{t \times SA} \quad (3.3)$$

Where NP is net photosynthesis, ΔDO is the change in dissolved oxygen over the incubation period.

Coral responses to high CO_2 treatments were calculated as the change in calcification or photosynthesis between ambient and high CO_2 treatments normalized to the ambient treatment rate:

$$R_{\text{calcif}} = \left(\frac{G_{\text{ambient}} - G_{\text{CO}_2}}{G_{\text{ambient}}} \right) \quad (3.4)$$

$$R_{\text{photosyn}} = \left(\frac{NP_{\text{ambient}} - NP_{\text{CO}_2}}{NP_{\text{ambient}}} \right) \quad (3.5)$$

Dividing Equation 4 for R_{calcif} by the change in saturation ($\Delta\Omega$) state between ambient and high CO_2 treatments yields the change in calcification per unit change in saturation state, a useful metric for comparing coral growth responses across studies (Langdon and Atkinson 2005; Kleypas and Langdon 2006; Hendriks et al. 2010).

Chemical environment

The diurnal pH range was calculated from the difference between the maximum and minimum recorded value for every day from the start of the study through April 2009. Saturation state was estimated for a typical year based on pH values recorded from the environmental logger and TA values reported in this study, Millero et al. (2001), and Yates and Halley (2006). TA generally shows low interannual variation relative to seasonal variation. Monthly values were extrapolated for missing months based on neighboring dates.

Statistical analyses

Each fieldtrip measured a subset of corals from the same experimental pool, necessitating a multilevel model that could account for repeated measures, unbalanced data, and missing-at-random corals (i.e. not every coral was measured on every trip). Coral calcification and photosynthesis responses to high CO_2 treatments were analyzed as a function of pCO_2 treatment, temperature, salinity, coral, and date. The baseline null model grouped response by individual corals:

$$R_{ij} = \beta_0 + \mu_{0j} + \varepsilon_{ij} \quad (3.6)$$

Where R_{ij} is the calcification or photosynthesis response for the i^{th} measurement of the j^{th} coral, β_0 is the overall mean calcification or photosynthesis response, μ_{0j} is the residual between the individual and the overall calcification or photosynthesis response, assumed to have a mean of zero with variance σ_{u0}^2 , and ε_{ij} is the residual difference between the average j^{th} coral response and i^{th} measured response for that coral. Explanatory variables were individually forward-stepped into the model and evaluated against the simpler nested model with likelihood ratio (LR) tests. If they improved the model fit, they were retained and the next variable was added. The treatment variable $\Delta\Omega$ was first added to the null model as a fixed effect because it was the only treatment imposed on the corals:

$$R_{ij} = \beta_0 + \beta_1 \Delta\Omega_{ij} + \mu_{0j} + \varepsilon_{ij} \quad (3.7)$$

with slope term β_1 for $\Delta\Omega$. Median-zeroed time, temperature, and salinity were subsequently forward-stepped into the model as random effects with diagonal covariance structures:

$$R_{ij} = \beta_0 + \beta_1 x_{1ij} + \mu_{1j} x_{1ij} + \beta_2 x_{2ij} + \mu_{2j} x_{2ij} + \dots + \beta_k x_{kij} + \mu_{kj} x_{kij} + \mu_{0j} + \varepsilon_{ij} \quad (3.8)$$

Where β_2 through β_k are slopes for each explanatory variable x_2 to x_k . The error terms μ_{2j} to μ_{kj} for the random variables 2 to k are assumed to follow a zero-centered normal distribution with σ_{2j}^2 to σ_{kj}^2 variance. Equation 8 shows the full model with all explanatory variables though the final model would not necessarily contain all variables. Models were fit with maximum likelihood estimates of parameters. Model residuals were examined for normality. Bayesian highest probability density (HPD) 95% confidence intervals were calculated from Markov chain Monte Carlo samples of posterior distributions of the fixed effect parameters.

Statistical analyses were performed using the software program R, version 2.14.1 (R Development Core Team 2011). The statistical packages ‘stats’ and ‘lme4’ (Bates et al. 2011) within R were used for the curve-fitting and multi-level modeling, respectively. Significance thresholds were set at $\alpha = 0.05$.

RESULTS

Field conditions

Conditions recorded in Florida Bay exhibit large-scale diurnal and seasonal variability. Over the three-year deployment of the environmental loggers, temperature ranged diurnally $1.4 \pm 0.5^\circ\text{C}$ ($n = 1297$ days) with more extreme values of approximately 4°C d^{-1} . Seasonally, temperature varied approximately 15°C from summer to winter (Fig. 3.2). The average diurnal salinity range was 1.0 ± 1.4 ($n = 1297$ days). The most extreme daily salinity ranges were 10, the same as the seasonal variation. Average diurnal pH range was 0.09 ± 0.05 ($n = 1297$ days) with more extreme ranges of 0.2 to 0.3 d^{-1} . Seasonally, pH ranged from approximately 7.9 to 8.3 (Fig. 3.2). Ambient pCO_2 averaged 350 ± 70 ppm ($n = 11$ incubation dates). Treatment pCO_2 conditions were 480 ± 100 ppm ($n = 11$).

Calcification and photosynthesis

Pooled ambient calcification rates for *S. radians* were 5.24 ± 3.17 $\text{mmol CaCO}_3 \text{ m}^{-2} \text{ h}^{-1}$ over the study period, while calcification rates for *S. hyades* were 3.07 ± 1.81 $\text{CaCO}_3 \text{ m}^{-2} \text{ h}^{-1}$ (Table 3.2, Fig. 3.4). Pooled net photosynthesis was 18.70 ± 12.29 $\text{mmol O}_2 \text{ m}^{-2} \text{ h}^{-1}$ and 9.10 ± 4.28 for *S. radians* and *S. hyades*, respectively (Table 3.2, Fig. 3.4).

Ambient calcification to net photosynthesis (G:NP) ratios were 0.26 ± 0.12 for *S. radians* and 0.37 ± 0.20 for *S. hyades* (Table 3.2). Calcification rates tracked changes in temperature, light, and pH that are known to affect growth, but calcification was best explained as a function of net photosynthesis. Pooled calcification data were linearly correlated with net photosynthesis for both species. However, for *S. radians* calcification was better fit to a hyperbolic tangent function ($G = 14.59 \tanh(NP/46.34)$) than linear regression (AIC scores of 161.0 and 164.9 respectively) (Fig. 3.5). Traditionally, hyperbolic tangent functions have been used to describe calcification or photosynthesis as a function of irradiance (Chalker 1981). Multiple linear regressions with physical data did not yield significant models for predicting calcification or net photosynthesis, suggesting interactions with other unmeasured variables such as feeding or flow rates may influence these processes (Kinsey and Davies 1979; Dennison and Barnes 1988; Houlbrèque et al. 2003).

Table 3.2. Pooled calcification (G) and net photosynthesis (NP) measurements for *Siderastrea radians* and *Solenastrea hyades*. Subscripts ‘ambient’ and ‘CO₂’ indicate control and elevated pCO₂ conditions, respectively. Values are reported as mean \pm standard deviation (sample size).

| | <i>S. radians</i> | <i>S. hyades</i> |
|-------------------------------|----------------------|---------------------|
| G_{ambient} | 5.2 \pm 3.2 (41) | 3.1 \pm 1.8 (33) |
| G_{CO2} | 2.7 \pm 5.6 (35) | 2.0 \pm 2.7 (31) |
| NP_{ambient} | 18.7 \pm 12.3 (41) | 9.1 \pm 4.3 (33) |
| NP_{CO2} | 20.1 \pm 12.1 (35) | 10.0 \pm 5.6 (31) |
| G:NP_{ambient} | 0.29 \pm 0.12 (40) | 0.37 \pm 0.2 (33) |

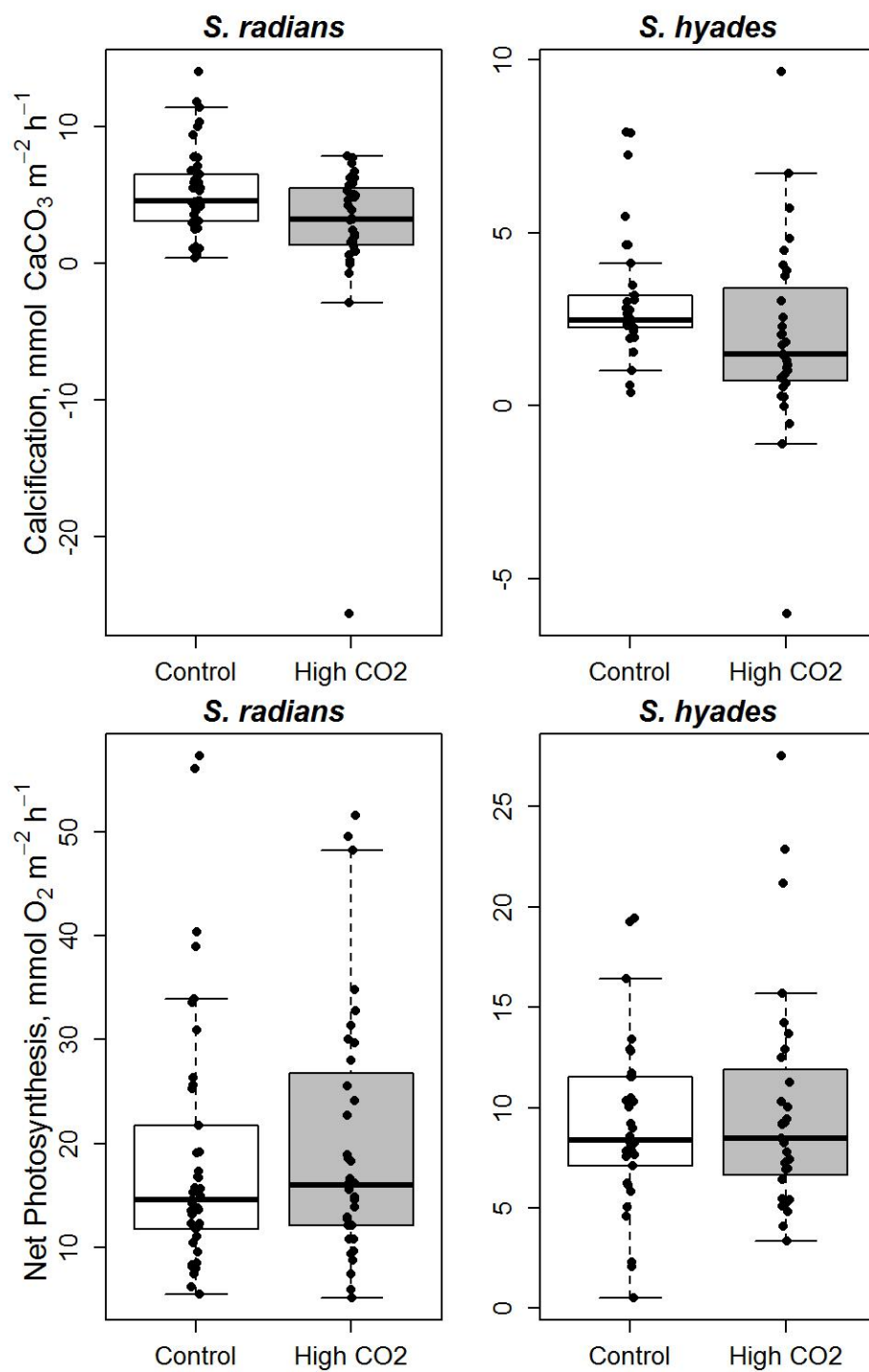


Figure 3.4. Boxplots of pooled calcification and net photosynthesis data.

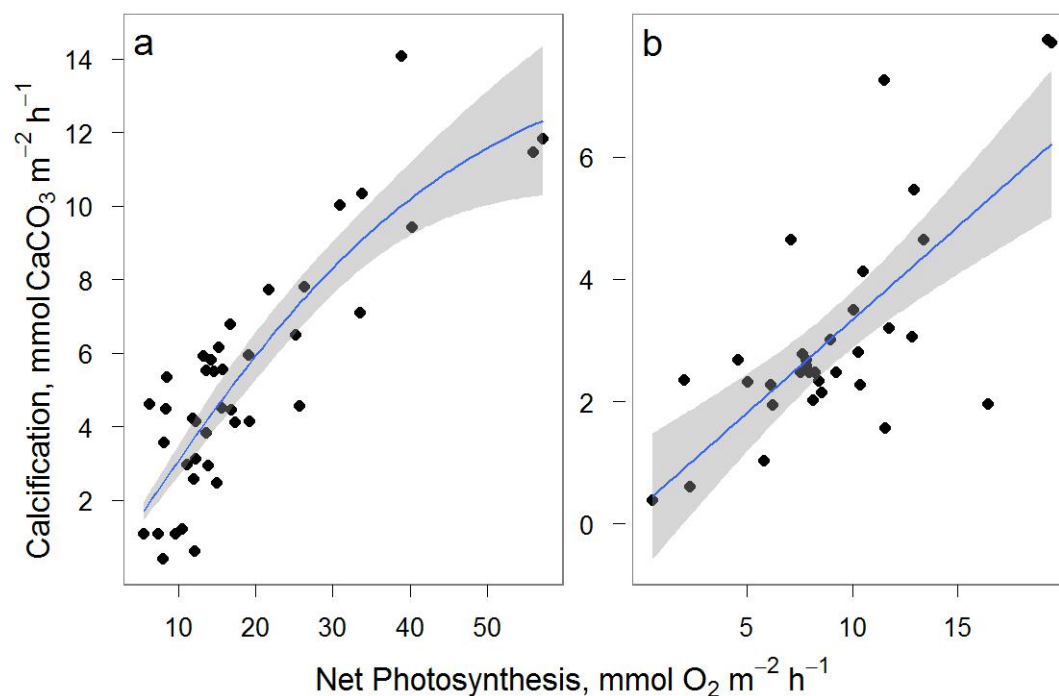


Figure 3.5. Calcification (G) correlated with net photosynthesis (NP) for a) *Siderastrea radians* and b) *Solenastrea hyades*. Lines represent best fit models while shaded regions represent 95% confidence intervals. *Siderastrea radians* is fitted to the hyperbolic tangent function: $G = 14.59 \tanh(NP/46.34)$. *Solenastrea hyades* is fitted to the linear regression: $G = 0.31 NP + 0.29$.

Calcification and net photosynthesis responses

Multilevel models of calcification responses found both species responded to $\Delta\Omega$, with calcification decreasing 52% (1-100% HPD 95% CI) and 50% (16-83% HPD 95% CI) per unit change in saturation state for *S. radians* and *S. hyades*, respectively (Table 3.3; Null model vs model 1, fixed effects $\Delta\Omega$: *S. radians* $LR_1 = 4.6$, $p = 0.03$, *S. hyades* $LR_1 = 8.6$, $p = 0.003$). Date, temperature, salinity, and initial saturation state did not improve model fits and were therefore not considered in the final model. Near-zero estimates of variances for the coral grouping variable suggest the models may be overfitted with respect to this variable, i.e. there is insufficient evidence that individual corals had unique

responses. The coral calcification responses to increased pCO₂ observed here are greater than the range of 5-40% for other species summarized by (Kleypas and Langdon 2006). None of the variables of increased pCO₂/decreased saturation state, initial saturation state, date, temperature, and salinity had detectable effects on photosynthetic responses of either species of corals.

Table 3.3: Multilevel model comparisons of the only observed significant calcification response variable, change in saturation state, against a null model accounting only for coral.

| | <i>S. radians</i> | | <i>S. hyades</i> | |
|-----------------------|-------------------|-------------------|------------------|-------------------|
| | Null model | Model 1 | Null model | Model 1 |
| Fixed effects | | | | |
| Intercept | 0.414 (0.111) | -0.073 (0.244) | 0.370 (0.130) | -0.156 (0.202) |
| ΔΩ | | 0.516 (0.234) | | 0.502 (0.160) |
| Random effects | | | | |
| Coral | 0 | 0 | 0 | 0 |
| Residual | 0.427 | 0.375 | 0.526 | 0.399 |
| Log likelihood | -34.776 | -32.498 | -34.016 | -29.73 |
| HDP 95% CI | | | | |
| ΔΩ | | (0.013 - 0.997) | | (0.157 - 0.832) |
| n Coral | | 10 | | 7 |
| n observations | | 35 | | 31 |

DISCUSSION

Calcification and net photosynthesis

The calcification rates reported here are lower than other corals and reef communities (Chave et al. 1972; Kinsey 1983; Davies 1990; Meesters et al. 1994; Ohde and van Woerik 1999; Bates et al. 2001; Langdon and Atkinson 2005). The low G:NP

ratios of <0.4 reported here relative to other studies (Jacques and Pilson 1980; Dennison and Barnes 1988; Swart et al. 1996a; Furla et al. 2000; Gattuso et al. 2000; Houlbrèque et al. 2003; Al-Horani et al. 2005; Schneider and Erez 2006) suggest Florida Bay corals' photosynthate provides energy for processes other than calcification, possibly for coping with temperature and salinity extremes or large swings in pH. *Siderastrea radians* and *S. hyades* have historically populated disturbed areas (Yonge 1936; Lewis 1989; Sorauf and Harries 2009) and the extremes in temperature and salinity posed by Florida Bay are more immediate and threatening to survival than extremes in $p\text{CO}_2$. As a result, these corals likely have most-likely developed survival strategies that favor stress-tolerance mechanisms and prioritized them over calcification processes.

Another possible explanation for the relatively low G:NP ratios is that zooxanthellae may be hoarding photosynthate and thereby slowing coral calcification. This explanation assumes calcification is driven mainly by energy from translocated photosynthate instead of the direct chemical effects of increased pH from photosynthesis. This explanation is not favored because it contradicts many studies that indicate calcification is chemically-linked to photosynthesis (Furla et al. 2000; McConnaughey et al. 2000; Al-Horani et al. 2003).

Calcification-photosynthesis curves offer insight into the nature of this relationship. A linear relationship supports a chemical response whereas an asymptotic curve indicates some biological constraint such as enzyme saturation. Calcification rates of *S. radians* fit better to an asymptotic hyperbolic tangent curve than a simple linear curve, indicating possible limits to photosynthesis-stimulated calcification (Fig. 3.5). The mechanisms underlying this limitation are unknown, but may include limitations in H^+

transport from the calcification site (Ries 2011a; McCulloch et al. 2012). This relationship may be species-specific as *S. hyades* calcification data was linearly-correlated with photosynthesis. Further studies on this relationship would better elucidate the effects of photosynthesis on calcification.

Two aspects of the calcification response findings are noteworthy: 1) Both species exhibited high variability in calcification responses, with some individuals exhibiting positive responses to increased pCO₂ on some dates, and 2) calcification rates for both species are not, on average, CO₂ resistant. Such variability in calcification responses could serve as an adaptive mechanism to increasing ocean acidification where over time colonies whose calcification rates are resistant to CO₂ increase in abundance relative to CO₂-susceptible conspecifics. However, positive responses to acidification were not consistent by coral or any other measured parameter, and no such resistant individuals were observed in this study.

Furthermore, calcification is an energy-intensive process (Chalker and Taylor 1975; Chalker 1976; Fang et al. 1989; Tambutté et al. 1996), and the hypothetically resistant corals may maintain calcification at the expense of other processes such as tissue repair or gamete production.. Comparably, Wood et al. (2008) showed echinoderms that increased calcification during ocean acidification suffered muscle wastage and increased metabolic costs. The Florida Bay corals appear to exhibit the opposite pattern where calcification decreases because of ocean acidification and is superseded by other metabolic demands. Furthermore, corals exhibited consistent declines in calcification under high pCO₂/low pH treatments despite experiencing diurnal swings in pH of 0.08 ± 0.04 units in their natural environment. This response suggests short-term variability in

pH will not mask the negative effects of incremental, long-term declines in pH on coral calcification. More studies are needed to determine how corals prioritize resource allocation and whether they might face tradeoffs between calcification and other processes.

Role of the environment

The persistence of *S. radians* and *S. hyades* in Florida Bay initially seems counterintuitive given their skeletal growth susceptibility to low saturation states and the bay's low winter saturation states (Millero et al. 2001). However, over the course of this study saturation state at the field site remained high relative to oceanic waters ($\Omega_{\text{arag}} = 4.27 \pm 0.57$ vs oceanic $\Omega_{\text{arag}} = 3.6$). The pH remained above 8.0 for 88% of the time during the study (Fig. 3.2). An annual composite of aragonite saturation state, created from recorded pH and discrete TA samples over a three-year period extending from 2007-2010 indicates aragonite saturation state would remain above 3.6 for 80% of the year (Fig. 3.6). Consequently, the environment augments the low calcification rates of *S. radians* and *S. hyades* (relative to other species) while its extremes preclude other less stress-tolerant coral species. With its low average annual pCO₂, Florida Bay could potentially serve as a refuge against ocean acidification (Boyer et al. 1999; Fourqurean and Robblee 1999; Boyer et al. 2009; Manzello et al. 2012), if not for the frequent phytoplankton blooms, persistent turbidity, and extremes in temperature and salinity (Boyer et al. 1999; Fourqurean and Robblee 1999; Boyer et al. 2009). However, seagrass areas and other highly productive habitats should be included in any management plan to deal with ocean acidification due to their ability to reduce ambient pCO₂ levels.

Future research should decouple these corals from Florida Bay to better evaluate their calcification-pCO₂ responses. If these corals direct a large portion of their resources towards survival in Florida Bay's marginal conditions, then under more benign oceanic conditions they may have more robust pCO₂ responses than observed in this study. Comparing these corals with conspecifics from the nearby reef tract might elucidate how individuals and their environments interact to affect pCO₂ responses.

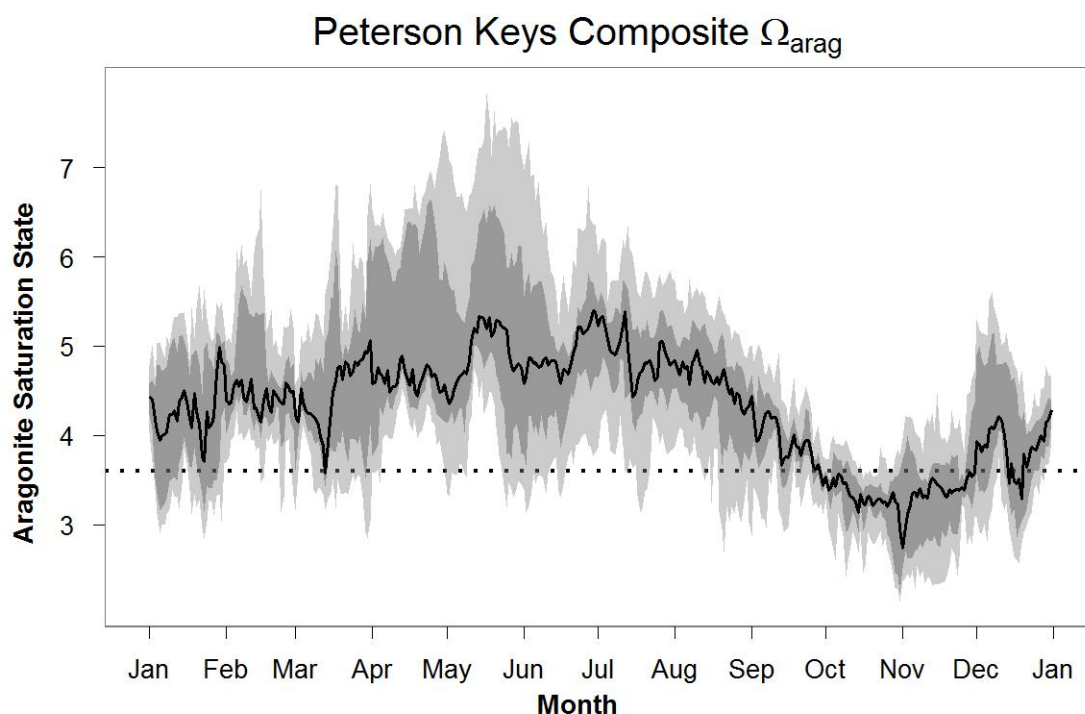


Figure 3.6. Composite monthly saturation state based on pH recorded at the field site and discrete monthly total alkalinity (TA) samples over approximately three years from 2007-2010. CO2Sys was used to calculate saturation state as discussed in the methods section. Black line represents median aragonite saturation state (Ω_{arag}), dark shaded region represents middle 50% of composite values, light shaded region represents full range of composite estimates of Ω_{arag} . Dotted horizontal line represents modern-day oceanic average saturation state of 3.6. Saturation states in Florida Bay are generally closer to pre-industrial levels of 4.6 for most of the year. As a result, Florida Bay is chemically favorable for calcification.

Despite experiments showing the importance of heterotrophy in reducing the negative effects of ocean acidification on calcification (Cohen and Holcomb 2009) and increasing photosynthesis (Borell et al. 2008), it may not be enough to buffer coral calcification under predicted future climate conditions. It is possible that the limited positive responses of calcification rates to increased $p\text{CO}_2$ observed here could be due to feeding or increased nutrient uptake by corals, which were not measured in this study. However, positive responses were not consistent for individual corals or time. Additionally, the corals in this study were kept in their natural environment and had ample opportunity to feed, yet their calcification responses were more sensitive those from many laboratory studies summarized in Kleypas and Langdon (2006).

In conclusion, increased frequency of bleaching as a result of climate change and increased local stress from growing human populations will probably favor more stress tolerant corals on reefs. For example, *Montastraea* sp. increased in prominence with respect to *Acropora cervicornis*, following the decline of *A. cervicornis* in the early 1980s (Gardner et al. 2003) and *P. astreoides* in general have increased in abundance throughout the Caribbean relative to other species (Green et al. 2008). However, the ability of reefs to cope with future warming by supporting more stress tolerant species will be undermined if those species are vulnerable to ocean acidification. This study found that the calcification rates of two stress-tolerant corals, *S. radians* and *S. hyades*, are just as sensitive to elevated $p\text{CO}_2$ as other corals previously studied, which suggests a limited ability of corals to adjust to ocean acidification. The corals from this study appear uniquely adapted to the marginal environment of Florida Bay, with their low calcification rates augmented by the environment's generally high saturation state and

their physiologies adapted to frequent extremes in water quality. As a result, calcification appears to be a secondary priority compared to survival in Florida Bay. The sensitivity of calcification rates of *S. radians* and *S. hyades* to pCO₂ discounts the notion that reefs can adjust to climate change by shifting to eurytopic species.

Chapter 4: Corals May Face a Tradeoff Between Stress Tolerance and Calcification

SUMMARY

The response of stress tolerance corals to increased pCO₂ is confounded when their environment is simultaneously conducive for calcification but marginal for survival. A reciprocal transplant study separated *Solenastrea hyades* corals from their historical environments, measured their calcification and photosynthesis in ambient and elevated pCO₂ incubations, and found a possible tradeoff between growth and survival. Florida Bay corals had lower calcification and net photosynthesis rates than conspecifics from the more stable Triangles patch reef, regardless of which environment they were located. The 2010 cold spell resulted in disproportionately more mortality in the Triangles corals than Florida Bay, indicating a potential tradeoff between stress tolerance and calcification rates. Despite these differences in growth strategies, coral growth was suppressed equally across treatments under high pCO₂.

BACKGROUND

Despite highly variable physical conditions (Millero et al. 2001) that preclude most species from establishing, Florida Bay's average conditions are quite conducive for calcification. Consequently, Florida Bay is paradoxically a favorable environment for stress-tolerant corals: they can cope with physical extremes without cost to calcification thanks to consistently high saturation states. The goal of this study was to decouple a prominent Florida Bay species, *Solenastrea hyades*, from its environment to determine if

it would have a more robust $p\text{CO}_2$ response when ambient conditions were less extreme and what role the environment plays in mediating $p\text{CO}_2$ responses. *S. hyades* from Florida Bay were reciprocally transplanted with conspecifics from the oceanic, nearshore Triangles patch reef, where conditions are generally more stable (Table 4.1). Conversely, transplanting corals from Triangles to Florida Bay tested whether those corals from a traditionally more favorable environment would increase growth rates in Florida Bay's high saturation state waters or decrease growth due to other environmental stressors.

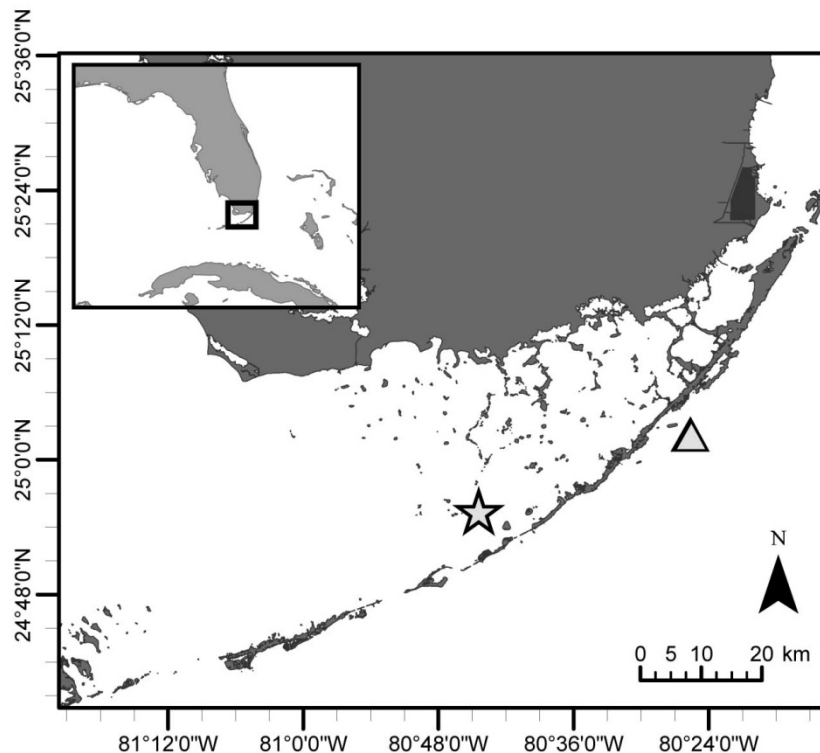


Figure 4.1. Reciprocal transplant field sites. The star denotes Peterson Keys and the triangle denotes Triangles patch reef. The sites are approximately 30 km apart.

Table 4.1. Environmental conditions at the Florida Bay and Triangles patch reef field sites. The parameters pH_t , Ω_{arag} , and pCO_2 are reported at ambient temperature. Light is converted from a Lux sensor into PAR using an assumed conversion of $\text{PAR} = \text{Lux}/50$.

| Date m/d/yyyy | T °C | S | DO μM | pH_t | TA μmol kg ⁻¹ SW | TCO ₂ μmol kg ⁻¹ SW | Ω_{arag} | pCO_2 ppm | PAR μE m ⁻² s ⁻¹ |
|--------------------|---------|------|----------|---------------|--------------------------------------|--|------------------------|-----------------------|---|
| Florida Bay | | | | | | | | | |
| 5/7/2009 12:30 | 26.6 | 38.4 | 188 | 8.16 | 2245 | 1826 | 4.4 | 273 | 548 |
| 5/7/2009 14:30 | 27.1 | 38.5 | 212 | 8.22 | 2221 | 1763 | 4.8 | 225 | 563 |
| 5/8/2009 12:00 | 27.1 | 38.4 | 203 | 8.20 | 2222 | 1781 | 4.6 | 241 | 636 |
| 5/9/2009 11:30 | 27.3 | 38.3 | 188 | 8.15 | 2222 | 1812 | 4.3 | 278 | 460 |
| 5/9/2009 14:00 | 28.0 | 38.6 | 191 | 8.17 | 2209 | 1780 | 4.5 | 261 | 525 |
| 5/9/2009 22:00 | 28.8 | 38.9 | 203 | 8.14 | 2229 | 1807 | 4.4 | 287 | 0 |
| 5/10/2009 12:00 | 28.3 | 38.9 | 173 | 8.10 | 2242 | 1852 | 4.1 | 328 | 628 |
| 5/10/2009 15:00 | 29.1 | 38.9 | 201 | 8.12 | 2221 | 1809 | 4.3 | 301 | 510 |
| 5/11/2009 11:00 | 29.0 | 39.1 | 181 | 8.12 | 2217 | 1809 | 4.3 | 304 | 626 |
| 5/11/2009 14:00 | 29.4 | 38.9 | 200 | 8.12 | 2219 | 1809 | 4.3 | 307 | 599 |
| 7/15/2009 10:55 | 31.5 | 39.3 | 176 | 8.12 | 2140 | 1701 | 4.6 | 285 | 388 |
| 7/15/2009 14:00 | 32.3 | 39.4 | 177 | 8.11 | 2161 | 1716 | 4.7 | 296 | 425 |
| 7/22/2009 10:50 | 30.1 | 40.0 | 145 | 8.05 | 2174 | 1792 | 4.0 | 365 | 397 |
| 7/22/2009 13:50 | 30.6 | 40.0 | 157 | 8.09 | 2149 | 1735 | 4.3 | 316 | 402 |
| 9/22/2009 11:10 | 29.6 | 40.1 | 182 | 8.07 | 2253 | 1858 | 4.1 | 353 | 416 |
| 9/22/2009 13:55 | 30.1 | 40.1 | 198 | 8.10 | 2253 | 1834 | 4.4 | 325 | 429 |
| 9/24/2009 10:15 | 29.6 | 39.9 | 168 | 8.10 | 2247 | 1829 | 4.4 | 325 | 365 |
| 9/24/2009 12:35 | 30.1 | 40.0 | 200 | 8.15 | 2243 | 1784 | 4.8 | 279 | 352 |
| 11/23/2009 10:30 | 25.1 | 38.4 | 207 | 8.05 | 2495 | 2138 | 3.9 | 429 | 146 |
| 11/23/2009 13:30 | 25.2 | 38.1 | 209 | 8.06 | 2486 | 2125 | 4.0 | 416 | 109 |
| 3/9/2010 11:20 | 17.7 | 34.2 | 259 | 8.26 | 2838 | 2411 | 4.9 | 278 | 184 |
| 3/9/2010 13:55 | 18.2 | 34.1 | 260 | 8.28 | 2841 | 2395 | 5.2 | 265 | 187 |
| 6/24/2010 10:30 | 29.1 | 41.1 | 162 | 8.17 | 2115 | 1651 | 4.6 | 241 | 299 |
| 6/24/2010 12:30 | 29.7 | 41.1 | 185 | 8.21 | 2145 | 1640 | 5.0 | 216 | 306 |
| Triangles | | | | | | | | | |
| 4/15/2009 10:30 | 26.7 | 36.8 | 219 | 8.13 | 2370 | 1976 | 4.3 | 326 | 217 |
| 4/15/2009 12:35 | 27.2 | 36.8 | 231 | 8.16 | 2370 | 1950 | 4.6 | 296 | 378 |

| | | | | | | | | | |
|------------------|------|------|-----|------|------|------|-----|-----|-----|
| 9/28/2009 11:05 | 30.1 | 36.1 | 215 | 7.96 | 2331 | 2021 | 3.6 | 521 | 165 |
| 9/28/2009 13:50 | 30.2 | 36.1 | 197 | 7.98 | 2347 | 2018 | 3.8 | 494 | 229 |
| 9/30/2009 11:20 | 30.1 | 35.3 | 178 | 7.94 | 2356 | 2065 | 3.4 | 571 | 183 |
| 9/30/2009 13:40 | 30.1 | 35.8 | 175 | 7.98 | 2356 | 2036 | 3.7 | 502 | 163 |
| 11/21/2009 10:50 | 24.4 | 36.6 | 205 | 7.96 | 2495 | 2221 | 3.2 | 555 | 116 |
| 11/21/2009 13:45 | 24.7 | 36.6 | 205 | 7.97 | 2538 | 2254 | 3.3 | 556 | 84 |
| 3/13/2010 12:05 | 22.3 | 36.6 | 223 | 8.06 | 2411 | 2101 | 3.4 | 402 | 154 |
| 3/13/2010 13:55 | 22.2 | 36.5 | 227 | 8.09 | 2412 | 2088 | 3.6 | 375 | 120 |
| 7/9/2010 9:30 | 30.1 | 36.2 | 193 | 8.04 | 2342 | 1971 | 4.2 | 416 | 151 |
| 7/9/2010 11:10 | 30.2 | 36.1 | 199 | 8.07 | 2321 | 1936 | 4.4 | 379 | 36 |

METHODS

Collections and transplantation

S. hyades colonies were collected from Peterson Keys, Florida Bay (24.926 °N, 80.740 °W) and Triangles patch reef, Key Largo (25.038 °N, -80.427 °W) (Fig. 4.1).

Florida Bay is described in the previous chapter. Triangles is a nearshore patch 3 km southeast of Rodriguez Key at approximately 4 m depth. The patch reef is broken into clumps stretching a few hundred meters and isolated by seagrass beds. The nearest offshore reef is Molasses reef. It was chosen as the transplant site because it was a close analog to the Florida Bay site in terms of depth and proximity to shore, as well as its presence of *S. hyades*.

Colonies were chiseled from the substrate and epoxied to labeled acrylic tiles. Half were randomly assigned for transplantation. All corals, including controls, were transported to the other site to account for any possible transportation effects, and control corals were returned to their original site. All corals appeared healthy and had extended polyps shortly after transplantation. Once the corals were reciprocally transplanted, corals were periodically incubated *in situ* for calcification and net photosynthesis rates

every 2-3 months from May 2009 to July 2010. Visits to each site were timed as close together as possible to account for any seasonal changes in the environment. Weather and scheduling conflicts prevented a visit to Triangles in July 2009. Results from the July 2010 Triangles reef field trip were not used for high pCO₂ comparisons because a brief rainstorm blocked light during one incubation. A cold spell during January 2010 resulted in partial and full mortality in ~90% of Triangles corals in Florida Bay. Consequently, surface area was adjusted to account for remaining live tissue of the corals used in incubations.

Incubations

Incubation chambers and methods are described in Chapter 3. Briefly, elevated pCO₂ treatments were achieved through a two-part equimolar addition of HCO₃⁻ and HCl. Calcification was measured by change in total alkalinity. Total alkalinity was measured via an open-cell Gran titration with a pH probe (Orion) calibrated in Tris seawater buffer (Nemzer and Dickson 2005) as described in SOP3b in Dickson et al. (2007). The other carbonate parameters were calculated with CO2Sys (Pierrot et al. 2006), using total alkalinity and pH as input parameters and K1 and K2 from Mehrbach et al. (1973), refitted by Dickson and Millero (1987). Dissolved oxygen was determined by Winkler titration utilizing an amperometric endpoint detection method (Langdon 2010). Salinity was measured with a Guildline 8410A Portable Salinometer. Light was measured with Onset HOBO Temperature/Light Data Loggers in units of lux, which does not have an exact conversion to photosynthetically active radiation (PAR) but can be

approximated. Assuming a lux-PAR conversion factor of $\text{lux}/50 = \text{PAR}$, light levels ranged from $100\text{-}600 \mu\text{E m}^{-2} \text{s}^{-1}$.

Calcification (G) and net photosynthesis (NP) were calculated following Equations 3.2 and 3.3 respectively, with rates normalized to morphometrically-determined surface areas. Calcification response (R_{calcif}) was computed from Equation 3.4. The calcification:net photosynthesis ratio is reported as G:NP.

“Triangles corals” refer to any corals originally from Triangles while “Florida Bay corals” refer to corals originally collected from Florida Bay. The term “populations” refers to corals from each site rather than distinct genetically-defined groups.

Statistics

Calcification, net photosynthesis and calcification responses were natural log (ln)-transformed to meet assumptions of normality and homoscedasticity as determined by D’Agostino-Pearson and Levene tests, respectively. An offset was added to calcification responses to make all values positive so they could be ln-transformed. These variables, along with G:NP, were compared in two-way analyses of variance (ANOVA) ($\alpha = 0.05$) with Type II sum-of-squares calculations. No trends were observed over time, so data were aggregated by treatment without temporal analyses. Pooled calcification responses were compared in a one-way t-test against the generalized species value of -0.22 (Kleypas and Langdon 2006). All analyses were conducted in the software program R (Team 2011).

Table 4.2. Biological variables (mean \pm SD) measured for the four treatments with sample size (n) in the adjacent column.

| Coral | Treatment | n | Control | Treatment | R_{change} | Ambient Net | Treatment Net | G:NP |
|--------------|------------------|----------|---|---|---------------------------|---|---|-----------------|
| | | | Calcification | Calcification | | Photosynthesis | Photosynthesis | |
| | | | mmol CaCO ₃ m ⁻² h ⁻¹ | mmol CaCO ₃ m ⁻² h ⁻¹ | | mmol O ₂ m ⁻² h ⁻¹ | mmol O ₂ m ⁻² h ⁻¹ | |
| Florida Bay | control | 28 | 2.60 \pm 1.74 | 2.07 \pm 1.26 | -0.14 \pm 0.31 | 8.65 \pm 3.97 | 8.74 \pm 5.07 | 0.33 \pm 0.15 |
| Florida Bay | transplant | 12 | 3.73 \pm 2.05 | 2.58 \pm 2.92 | -0.25 \pm 0.53 | 10.61 \pm 7.29 | 10.02 \pm 5.43 | 0.38 \pm 0.08 |
| Triangles | control | 17 | 5.37 \pm 2.26 | 3.86 \pm 3.22 | -0.37 \pm 0.40 | 12.72 \pm 8.14 | 10.38 \pm 4.84 | 0.50 \pm 0.24 |
| Triangles | transplant | 25 | 5.51 \pm 3.30 | 3.68 \pm 3.16 | -0.28 \pm 0.43 | 18.93 \pm 12.56 | 17.65 \pm 13.92 | 0.39 \pm 0.20 |

RESULTS

Biological rates

Calcification rates, calcification responses, photosynthesis rates, and G:NP ratios for the four treatments are summarized in Table 4.2. Both calcification and net photosynthesis rates were higher for Triangles corals versus Florida Bay corals (Fig 4.2a,c, Table 4.3, two-way ANOVA. Calcification $F_{1,78}=31.31$, $p<0.001$; net photosynthesis $F_{1,75}=15.36$, $p<0.001$) while environment had no effect ($F_{1,78}=2.05$ and $F_{1,75}=0.91$ respectively). G:NP ratios are generally lower than reported for other species (as reported in Chapter 2). Like calcification and photosynthesis, corals from Triangles had higher G:NP ratios (Fig 2d, $F_{1,78}=4.08$, $p=0.047$) while corals at Triangles reef had higher, though not significant, G:NP ratios than corals at Florida Bay. Calcification responses were the same across treatments (Fig 4.2b, Table 4.3), and the pooled overall response (-0.25 ± 0.40) was not significantly different from the generalized coral response of -0.22 compiled by Kleypas and Langdon (2006) (one-way t-test, $t_{79}=-0.66$, $p>0.05$).

Mortality

Corals from Triangles experienced greater mortality than their Florida Bay counterparts following the anomalous cold water event in early 2010 (Lirman et al. 2011). Approximately 90% of transplanted Triangles colonies in Florida Bay had partial or full mortality following these stress events while none of the other experimental colonies were visibly affected. The minimum water temperature recorded in Florida Bay

during that time was 8°C for six hours. Rates of the affected corals were consistent with previously measured rates after adjusting for remaining live tissue area.

Incidentally, nearly all other coral species at the Triangles patch reef site died, and a large 1m diameter *Solenastrea bournoni* colony in Florida Bay (discussed in Chapter 5) bleached later that summer 2010 but eventually recovered.

Table 4.3. Two-way analysis of variance (ANOVA) results tables for calcification, calcification responses, net photosynthesis and calcification:net photosynthesis ratios for the reciprocal transplant experiment.

| log(Calcification) | SS | df | F | p |
|--------------------------------------|-----------|-----------|----------|----------|
| Coral origin | 8.05 | 1 | 31.31 | <0.001 |
| Environment | 0.53 | 1 | 2.06 | 0.16 |
| Origin * Environment | 0.57 | 1 | 2.22 | 0.14 |
| Residuals | 20.06 | 78 | | |
| log(R_{change} + 4.3) | SS | df | F | p |
| Coral origin | 0.02 | 1 | 2.18 | 0.14 |
| Environment | 0.01 | 1 | 1.24 | 0.27 |
| Origin * Environment | 0 | 1 | 0.05 | 0.82 |
| Residuals | 0.81 | 76 | | |
| log(Net photosynthesis) | SS | df | F | p |
| Coral origin | 4.82 | 1 | 15.36 | <0.001 |
| Environment | 0.29 | 1 | 0.91 | 0.34 |
| Origin * Environment | 0.84 | 1 | 2.69 | 0.11 |
| Residuals | 23.52 | 75 | | |
| G:NP | SS | df | F | p |
| Coral origin | 0.13 | 1 | 4.08 | 0.047 |
| Environment | 0.13 | 1 | 3.93 | 0.05 |
| Origin * Environment | 0.02 | 1 | 0.54 | 0.47 |
| Residuals | 2.46 | 75 | | |

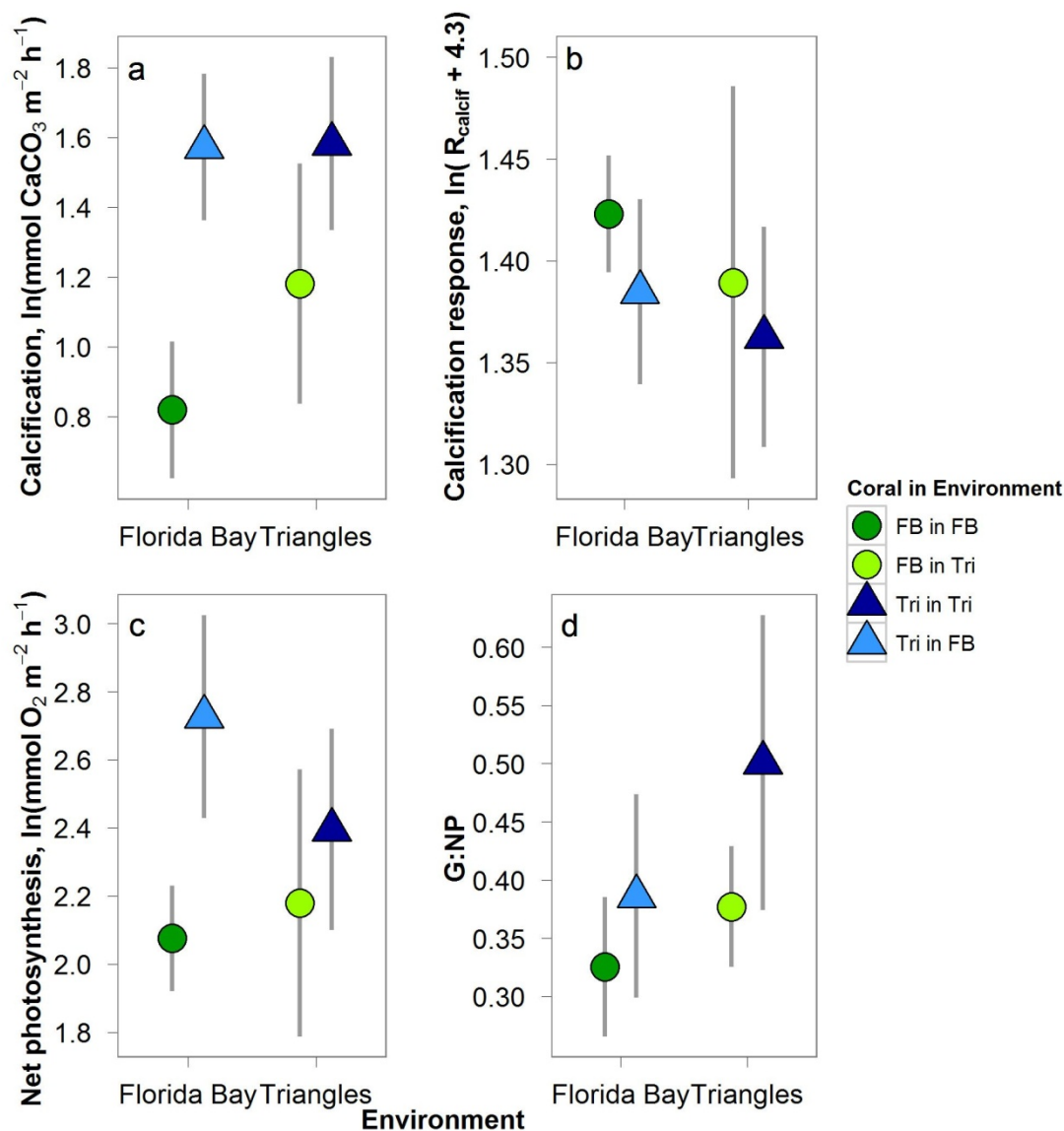


Figure 4.2. Calcification (a), calcification response (b), net photosynthesis (c), and calcification:net photosynthesis ratios (d) for control Florida Bay corals (FB in FB, dark green circles, $n=28$), Florida Bay corals transplanted to Triangles (FB in Tri, light green circles, $n=12$), control Triangles corals (Tri in Tri, dark blue triangles, $n=17$), and Triangles corals transplanted to Florida Bay (Tri in FB, light blue triangles, $n=25$). Rates and responses were natural log-transformed to meet assumptions of ANOVA. R_{calcif} included negative numbers, hence 4.3 was added to shift numbers so they could be ln-transformed. Points are means \pm 95% confidence interval bars.

DISCUSSION

This reciprocal transplant experiment revealed a potential tradeoff between growth and stress tolerance in *S. hyades*. Triangles corals generally had greater rates of calcification and photosynthesis than their Florida Bay counterparts but also increased bleaching and mortality following an extreme stress event. Chapter 3 presented evidence that *S. hyades* from Florida Bay direct less photosynthate towards calcification than other species, suggesting they may apply these resources towards surviving Florida Bay's marginal environment. *S. hyades* from the more stable Triangles patch reef, on the other hand, appear to invest more photosynthetic products in growth. This potential difference in resource investment may reflect the corals' adaptation to their local environments to optimize growth.

While this species shows some plasticity in its growth strategies, neither population showed conclusive evidence of a shift in resource investment strategy. The experiment duration might have been shorter than the timeframe in which such acclimatization could occur. Corals were transplanted approximately eight months prior to the cold spell event, and growth rates were only assessed over a year. Alternatively, a stress event such as a cold spell or bleaching summer may be required to initiate a shift in growth strategies, similar to the shifts in zooxanthellae populations towards more heat tolerant types following bleaching events (Buddemeier and Fautin 1993; Baker 2001; Glynn et al. 2001). Furthermore, like this study, Little et al. (2004) demonstrated a tradeoff between heat tolerance and coral growth that was determined by the zooxanthellae types the coral hosted. Zooxanthellae types were not assessed in this experiment, so their role in the coral responses is unknown.

These data suggest the corals themselves exert enough control over calcification and net photosynthesis to distinguish the two populations, regardless of their environment. Triangles corals had higher rates than Florida Bay corals in both environments. Environments differed in their chemical conditions but had little effect on calcification and photosynthesis. Saturation states were generally 0.5 units higher in Florida Bay than Triangles, which would theoretically increase calcification by 11%, all else equal. Despite more favorable chemical conditions in Florida Bay, Triangles corals' calcification was consistent across environments while transplanted Florida Bay corals actually had slightly higher, though non-significant, rates than the control Florida Bay corals (Fig. 4.2a). Consequently other factors likely depress calcification in Florida Bay, such as the aforementioned chronic sub-lethal stressors of temperature and salinity.

The cold snap of January 2010 tested the stress tolerance of the corals, especially in Florida Bay where water temperatures were likely colder due to the shallower, more isolated basin environment. As a whole, the species is relatively stress tolerant: *S. hyades* survived while almost all other species died at the relatively diverse Triangles patch reef. However, Triangles corals in Florida Bay experienced mortality while all other treatments survived. Hence, though Triangles corals have higher rates of growth, they are more susceptible to acute stress events than Florida Bay corals. In their home environments, the corals have ideal growth strategies. Florida Bay corals persist in the bay because they prioritize survival but are at a competitive disadvantage in more stable environments because of their low growth rates compared to Triangles corals.

Corals in all treatments had calcification responses to elevated pCO₂ that were insignificantly different from one another and the overall coral response summarized in

Kleypas and Langdon (2006). The lack of species-specific responses across studies and the lack of difference among treatments in this study suggest pCO₂ likely affects the underlying chemical conditions rather than some biological process such as hypercapnia, at least for levels of pCO₂ less than 1000 ppm. Conversely, variability among individuals may obscure differences across treatments and species. Though biological processes like heterotrophy can mitigate ocean acidification effects on growth (Cohen and Holcomb 2009), corals in this study still responded negatively to increased pCO₂ despite growing in natural conditions with ample feeding opportunities. Additionally, bicarbonate and acid additions resulted in immediate reductions in calcification. This observation further supports the idea that growth responses are largely determined by the chemical environment, with declines in [CO₃²⁻] resulting in proportionately less calcification.

Chapter 5: Insights into Past Florida Bay Conditions from a 190-year old *Solenastrea bournoni* coral

SUMMARY

The carbon isotope ($\delta^{13}\text{C}$), oxygen isotope ($\delta^{18}\text{O}$), and trace metal (Sr, Mg, Ba, Ca) record of a specimen of *Solenastrea bournoni* coral was compared with a 19-year record of temperature, salinity, and water oxygen isotopes to develop proxies for historical salinity and saturation state conditions. These proxies were then applied to the full 190-year skeletal record of the same coral. First, the skeletal chronology was determined by using seawater temperature and $\delta^{18}\text{O}$ to calculate expected coral skeletal $\delta^{18}\text{O}$ and matching them to actual coral skeletal $\delta^{18}\text{O}$. This method yielded a chronology that could be continually checked against the water quality record, thereby avoiding misalignments that amplify further back into the chronology. The coral skeletal $\delta^{18}\text{O}$ was then used to reconstruct historical salinity, which in turn was used to calculate past aragonite saturation states. This reconstruction indicates saturation states were elevated relative to oceanic waters and may be one factor responsible for the coral's stable growth rates over the last 60 years. However, the reconstruction assumes temperatures in Florida Bay have not changed over the life of the coral because an annual temperature composite based on the long-term water measurements was used instead of a coral skeletal Sr/Ca paleothermometer. The coral skeletal Sr/Ca could not accurately record temperature because the underlying seawater variability in Sr/Ca likely masked any temperature effects in the coral skeleton. These results illustrate how past conditions can be inferred from coral skeletal geochemistry in a highly variable environment.

BACKGROUND

Geochemical records have been used over the past 50 years as proxies for temperature, light, coral growth, sea level, salinity, pH and many other parameters (Keith and Weber 1965; Weber and Woodhead 1970; Weber 1973; Fairbanks and Dodge 1979; Smith et al. 1979; Swart 1983; McConnaughey 1989). Corals' annual density bands (Knutson et al. 1972) provide a chronological framework with which isotopes and trace metal proxies can estimate historical conditions (Weber and Woodhead 1970; Fairbanks and Dodge 1979; McConnaughey 1989; de Villiers et al. 1994; Guzman and Tudhope 1998; Gagan et al. 2000). However, a limitation of previous studies is the lack of concurrent environmental data by which these geochemical proxies can be calibrated. A long-term collection of monthly water samples from 1989 to 2008 by the Southeast Environmental Research Center of Florida International University (SERC-FIU) in addition to carbon and oxygen isotope data from those same water samples by the University of Miami overcomes this limitation of short-term environmental records. A 190-year old *Solenastrea bournoni* colony located near Peterson Keys, Florida allows for calibrations of skeletal proxies over this approximately 20-year record that can then be applied to the preceding 170 years of the coral's history. This coral and the SERC-FIU water record therefore present a unique opportunity to explore past conditions.

Florida Bay

Florida Bay is a shallow water basin located between peninsular Florida and the Florida Keys (Fig. 5.1). The bay is divided into semi-isolated subbasins less than 3 m deep by a network of carbonate mudbanks and islands (Enos and Perkins 1979). These

mudbanks restrict water exchange and create a north-to-south gradient of Everglades freshwater to reef-tract seawater. The monthly SERC-FIU water quality samples were collected from 28 of these subbasins. As a result of its shallow depths, proximity to the Everglades, and compartmentalized mudbanks, Florida Bay experiences greater variability in temperature, salinity, and other environmental parameters relative to the ocean as well distinct zonation within the bay (Montague and Ley 1993; Boyer et al. 1997,1999; Millero et al. 2001).

Hydrology in Florida Bay is influenced by multiple processes. Everglades runoff adds freshwater and organic matter to northern Florida Bay while the Florida reef tract and Gulf of Mexico moderate the waters of south and west Florida Bay. Evaporation and precipitation play a larger role in the southwest compared to the runoff-influenced north (Lloyd 1964; Swart and Price 2002). This study focuses on Lignumvitae Basin, a southwestern sub-basin of Florida Bay whose western boundary connects to a more open expanse of the Bay that opens up to the Gulf of Mexico. Channels between Upper and Lower Matecumbe Keys allow water exchange between Lignumvitae Basin and the reef tract.

In the late 1980s the bay experienced mass seagrass dieoffs attributed to a number of stressors including hypersalinity, temperature, loss of large herbivores, and phosphorous pollution (Robblee et al. 1991; Fourqurean and Robblee 1999; Zieman et al. 1999; Koch et al. 2007). This loss of seagrasses resulted in a transition from a bay with clear waters with extensive seagrass coverage to one with frequent algal-blooms and sediment-dominated benthos (Gunderson 2001). In addition to the mass sea-grass dieoff, Florida Bay has experienced changes from upstream land use including reductions of

water flows from the Everglades and increased nutrient inputs from agriculture (Walters et al. 1992; Gunderson 2001) as well as restricted water exchange with the reef tract from the construction of the Overseas railroad in 1912 (Swart et al. 1996b).

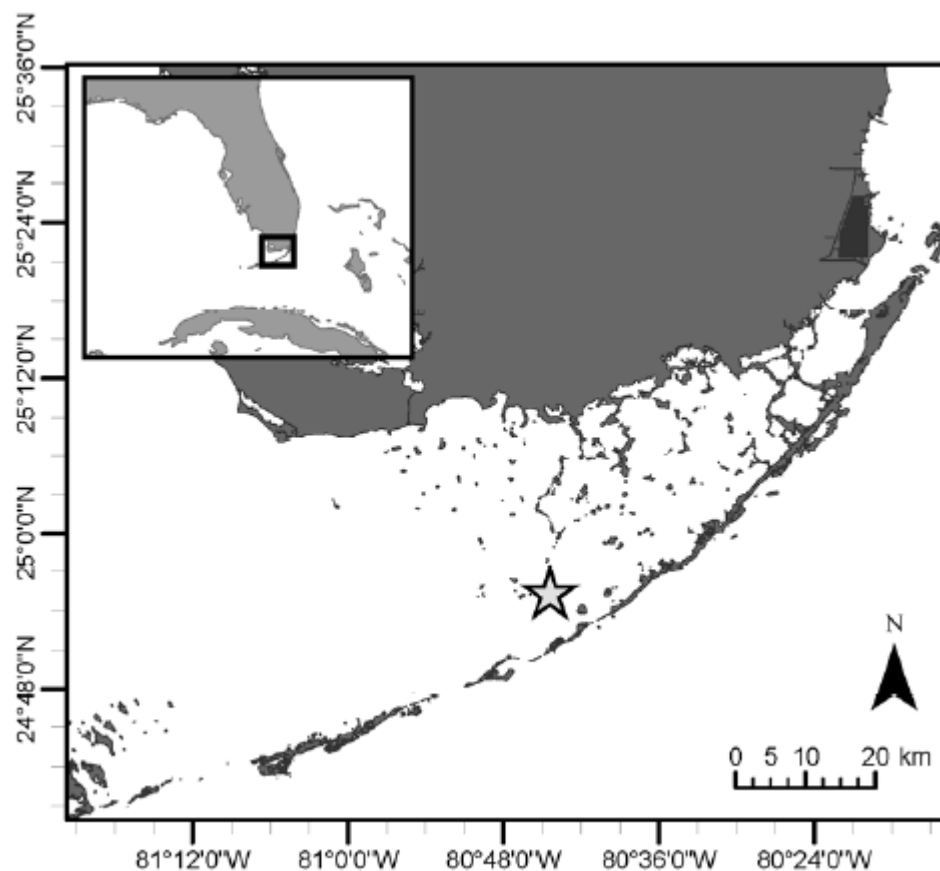


Figure 5.1. The field site, denoted by a star, is just north of Peterson Keys in Florida Bay.

Coral

The coral that is the subject of this study is located at 24.93 °N, 80.74 °W near Peterson Keys in Lignmvitae Basin, Florida Bay (Fig. 5.1). This coral, named FB6, was previously cored in October 1986 (Hudson et al. 1989) and again in May 1993 (Healy 1996). Previous studies of this coral concluded 1) Florida Bay experienced no long-term

increases in salinity based on the lack of increase in skeletal oxygen-18 isotopes ($\delta^{18}\text{O}$), 2) the Overseas railroad restricted exchange with oceanic waters based on decreased skeletal fluorescence amplitude and a sudden decrease in carbon-13 isotopes ($\delta^{13}\text{C}$), and 3) oxidation has increased with the buildup of organic matter from restricted circulation and infrequent hurricanes based on decreasing skeletal carbon-13 ($\delta^{13}\text{C}_\text{C}$) (Healy 1996; Swart et al. 1996b; Swart et al. 1999). Since the last coring in 1993, the aforementioned SERC-FIU dataset of monthly water samples from Peterson Keys provides an opportunity to calibrate the coral skeletal proxies for temperature and salinity and to extend them to aragonite saturation state.

Skeletal proxies for environmental conditions

These proxies for historical salinity and temperature are based on the skeletal $\delta^{18}\text{O}$ and $\delta^{13}\text{C}$ and ratios of strontium, magnesium, and barium to calcium. Prior work has shown these geochemical tracers record temperature, salinity, carbon dynamics, and freshwater inputs. Coral skeletal $\delta^{18}\text{O}$ is negatively correlated with temperature and has been used in numerous studies as a paleothermometer (Weber and Woodhead 1972; Fairbanks and Dodge 1979; McConnaughey 1989). The $\delta^{18}\text{O}$ of biogenic calcium carbonates also reflects water $\delta^{18}\text{O}$ at the time of deposition (Epstein et al. 1953), which in turn is dependent on salinity (Lowenstam and Epstein 1957; Swart and Coleman 1980).

Carbon isotopic ratios in corals reflect the interdependent processes of photosynthesis, insolation, and growth (Weber and Woodhead 1970; Land et al. 1975; Fairbanks and Dodge 1979; Swart and Coleman 1980; Swart 1983; McConnaughey

1989; Allison et al. 1996; Grottoli 2000), as well as other processes such as heterotrophy (Grottoli 2000) that influence the carbon pool from which calcification draws. In prior studies of this *S. bournoni* coral, $\delta^{13}\text{C}$ recorded the buildup and oxidation of isotopically-depleted organic matter in Florida Bay that accumulated after water exchange with the Florida reef tract was restricted (Swart et al. 1996b).

Concentrations of several trace metals (ex. Ca, Sr, U) in coral skeletons generally reflect concentrations in seawater at the time of skeletal deposition (Amiel et al. 1973; Shen and Boyle 1988; Linn et al. 1990; Gaetani and Cohen 2006) while others (ex. Mg, Ba) are depleted with respect to seawater (Gaetani and Cohen 2006). Strontium:calcium ratios vary inversely with temperature and have been used as paleothermometers in several coral taxa (Houck et al. 1977; Smith et al. 1979; Beck et al. 1992; Marshall and McCulloch 2002; Quinn and Sampson 2002; Swart et al. 2002; Fallon et al. 2003; Montaggioni et al. 2006; Reynaud et al. 2007). Despite these numerous Sr/Ca-temperature calibrations, some workers have proposed growth rate and other processes indirectly affecting growth rate such as symbiont density alter the calibration slopes (Weber 1973; Cohen et al. 2001; Cohen et al. 2002). Nonetheless, Sr/Ca is considered one of the more robust paleothermometers relative to other trace metal ratios (Quinn and Sampson 2002; Fallon et al. 2003; Mitsuguchi et al. 2003).

Magnesium:calcium ratios have also been used as paleothermometers (Mitsuguchi et al. 1996; Wei et al. 2000; Watanabe et al. 2001) and show positive correlations with temperature (Chave 1954). As with strontium, other factors can influence Mg/Ca ratios such as coral growth rates. Increased coral growth has resulted in higher skeletal Mg/Ca ratios (Reynaud et al. 2007). Increased pCO_2 , which slows growth, has led to decreased

skeletal Mg/Ca (Cohen et al. 2009). Furthermore, variable Mg/Ca ratios across taxa led Weber (1974) to discount the role of temperature or calcification over physiology.

In contrast to strontium and magnesium, increased Ba/Ca ratios generally signal upwelling (Lea and Boyle 1989; Fallon et al. 1999; Montaggioni et al. 2006) and freshwater runoff (Hanor and Chan 1977; Alibert et al. 2003; McCulloch et al. 2003; Sinclair and McCulloch 2004; Montaggioni et al. 2006; Prouty et al. 2008), which in turn is a proxy for anthropogenic activity along coasts. Previous work on the FB6 coral from this study corroborated the inverse relationship of Ba/Ca to salinity (Swart et al. 1999) and found enriched Ba/Ca relative to other corals in the region, including conspecifics (Anderegg 1998).

Previous calibrations of geochemical proxies for environmental conditions

The goals of this chapter are to determine whether skeletal $\delta^{18}\text{O}$, $\delta^{13}\text{C}$, Sr/Ca, Mg/Ca, and Ba/Ca can predict past environmental conditions, such as carbonate chemistry, by comparing these skeletal data against the long-term water sample record. Previous calibrations provide starting points for initial comparison. One such calibration developed by Leder et al. (1996) estimated temperature from oxygen isotopes of *Montastraea annularis* skeleton and water (Eqn 5.1):

$$\text{Temperature} = -4.519 * (\delta^{18}\text{O}_C - \delta^{18}\text{O}_W) + 5.33 \quad (5.1)$$

Where temperature is in Celsius degrees, $\delta^{18}\text{O}_C$ and $\delta^{18}\text{O}_W$ are the $\delta^{18}\text{O}$ of the coral and water reported in ‰ Vienna Pee Dee Belemnite (V-PDB) and Standard Mean Ocean Water (V-SMOW), respectively. Swart et al. (1999) later combined this equation with a

salinity- $\delta^{18}\text{O}_w$ calibration from Healy (1996) (Eqn. 5.2) to obtain salinity as a function of $\delta^{18}\text{O}_C$ and temperature (Eqn 5.3).

$$\text{Salinity} = 4.98 \delta^{18}\text{O}_w + 25.89 \quad (5.2)$$

$$\text{Salinity} = 4.98 \delta^{18}\text{O}_C + 1.18 \text{Temperature} + 19.62 \quad (5.3)$$

Equation 5.3 indicates salinity can be estimated if temperature and $\delta^{18}\text{O}_C$ are known. While oxygen-18 is preserved in the coral skeleton, temperature is not. However, the Sr/Ca of the coral skeleton can be substituted for temperature (Beck et al. 1992), thereby enabling the calculation of salinity. This study updates the salinity- $\delta^{18}\text{O}_w$ calibration (Eqn. 5.2) for Peterson Keys (Swart and Price 2002) and utilizes a temperature- ^{18}O proxy similar to Equation 5.1 that is based on *S. bournoni* rather than *M. annularis* (Leder et al. 1996).

Chronology resolution and hurricanes

In a previous study of this same coral, Swart et al. (1996b) attributed $\delta^{13}\text{C}$ shifts in the coral skeletal record to variations in hurricane frequency on a decadal scale. Building on these observations, this study investigated whether hurricanes might have a shorter-term, more immediate impact on the coral $\delta^{13}\text{C}$ skeletal signal on the order of months to years. Seven category 3 or higher hurricanes passed through Florida Bay during the period from 1910 to 1948, and the skeletal $\delta^{13}\text{C}$ was marked by consistent increases. Conversely, the period from 1948 to 1986 saw low hurricane activity and declining $\delta^{13}\text{C}_C$. Swart et al. (1996b) attributed the ability of hurricanes to build up or flush out organic matter from the Bay as the driver of decadal movements of the carbon isotopic signal. To detect hurricane signals at finer temporal resolutions, a highly accurate

chronology is necessary because inaccuracies in year assignments of growth bands towards the coral surface can amplify further back in time and even misalignments of months within a year can alter statistical conclusions. This study compares several different methods of establishing coral chronology, including visual assessment of density bands and applying the environmental water sampling record to predict coral ^{18}O -oxygen values. The latter method is unique because it requires the long-term record of water ^{18}O -oxygen, which often is unavailable for many coral skeletal studies.

METHODS

Environmental data

Water quality data (hereafter referred to as SERC data) were provided by the SERC-FIU Water Quality Monitoring Network supported by SFWMD/SERC Cooperative Agreement #4600000352 as well as EPA Agreement #X7-96410603-3. Records extend from June 1989 to September 2008. Methods for measurements of those data, including temperature (T), salinity (S) (Fig. 5.2), chlorophyll *a* (Chl *a*), and total organic carbon (TOC) have been described by Boyer et al. (1999). Seawater oxygen ($\delta^{18}\text{O}$) and hydrogen (δD) isotopes were measured by the Stable Isotope Lab at the University of Miami following methods reported in Swart and Price (2002).

Between April 2007 and November 2010, environmental loggers (Yellow Springs Instruments) were continually deployed on an experimental platform next to the *S. bournoni* coral and recorded conductivity, temperature, and pH at 30 minute intervals. Loggers were exchanged every 2-3 months and were calibrated against standards (Yellow Springs Instruments) and discrete water samples collected during visits to the coral.

These water samples were analyzed in the lab for pH and salinity. Measurements of pH on the total scale (Dickson et al. 2007) were determined at 25.0°C using an Orion Ross combination pH electrode calibrated against Tris buffer prepared in synthetic seawater (Nemzer and Dickson 2005). Salinity was measured on a Guildeline 8410A Salinometer.

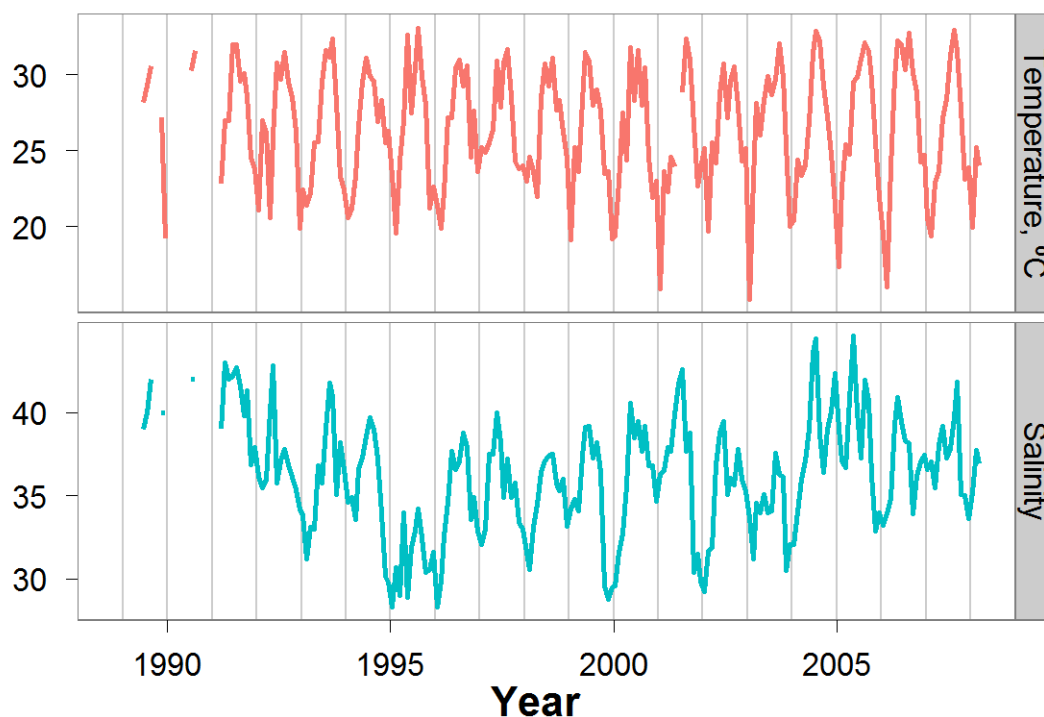


Figure 5.2. Temperature and salinity data from the SERC monthly water sample data for Peterson Keys (Station 20).

SERC data

The assumption that the monthly SERC water samples were representative of the entire month in which they were collected was examined by correlating the SERC salinity and temperature data against the high-temporal resolution salinity and temperature data from environmental logger. The environmental logger data were averaged by month to match the SERC temporal resolution. Though the temperature and salinity were logged every

half hour at the site continuously from 2007 to 2010, only April 2007 to March 2008 overlapped with the coral and SERC data. Consequently, only 12 months of overlapping data were available for comparison. To evaluate whether temperature or salinity better reflected environmental conditions, the correlation coefficients of the logger and SERC data for both variables ($r_{T.\text{logger},T.\text{SERC}}$ and $r_{S.\text{logger},S.\text{SERC}}$) were converted to z-scores by Fisher's Z transformations. If any statistically significant difference existed between the two non-overlapping dependent correlation coefficients ($r_{T.\text{logger},T.\text{SERC}}$ and $r_{S.\text{logger},S.\text{SERC}}$), i.e. the 95% confidence interval for the difference between the coefficients did not include zero, the variable with the higher correlation to the environmental logger record was used to build an annual composite for further analyses. The SERC values were averaged by month for all available years to create the annual composite.

Coral data

In April 2008, the *S. bournoni* colony (FB-6) from Peterson Keys, Florida was cored to a depth of approximately 50 cm using a 10 cm diameter coring bit attached to a hydraulic drill. The hole was filled with a cement plug and edges smoothed with epoxy to facilitate healing of the scar. The core was slabbed and x-rayed (Fig. 5.4) using standard methods (Dodge et al. 1984). The slab was subsequently impregnated with resin and divided into sections approximately 7 cm long to enable polishing of the resin surface. The first two sections were drilled along the length of a thecal wall at 120 μm intervals using a Micromil drill to a cumulative depth of approximately 10 cm from the coral surface. Drilling was shifted to a second thecal wall (Transect 2B) on the second section 2 cm in lateral distance from the original transect (Transect 1A) and 7 cm depth

(from the coral surface) (Fig. 5.4). The second section was drilled to include an overlap of skeletal density bands from the first section's thecal wall. The first section was subsequently redrilled on another thecal wall (Transect 1B) closer to Transect 2B because trace element ratios were variable on the original Transect 1A. Skeletal powder was collected with a dental pick and separated for isotopic and trace metal analyses.

Skeletal powder was dissolved in phosphoric acid to liberate CO_2 from the carbonate material and analyzed in batches of 27 samples per run. Carbon-13 and oxygen-18 were measured on a Delta-PLUS with Kiel following Swart et al. (1991) with isobaric corrections and an internal CaCO_3 standard to correct for drift. Coral $\delta^{13}\text{C}$ and $\delta^{18}\text{O}$ are reported relative to V-PDB. Analytical error has been determined to be $\pm 0.046\text{‰}$ and $\pm 0.119\text{‰}$ standard deviations for $\delta^{13}\text{C}$ and $\delta^{18}\text{O}$, respectively (Rosenberg 2011).

Calcium, strontium, magnesium, and barium were measured on an inductively coupled plasma optical emission spectrometer (ICP-OES) (Varian), calibrated to IAPSO standard seawater (Ocean Scientific International Ltd.). Samples were dissolved in 4% nitric acid and metal concentrations were measured in batches of 115 samples. Concentrations were measured once then samples were diluted to a uniform calcium concentration (approximately 3000 ppm) and measured again to account for dilution-dependent changes in elemental ratios. Strontium, magnesium, and barium concentrations are reported as ratios relative to calcium. Strontium/calcium ratios were normalized to an internal standard from Florida State University to account for machine drift over the course of an analysis session run. Barium is reported in $\mu\text{M}/\text{M}$ ratios for

barium while magnesium and strontium are reported in mM/M ratios. Laboratory analytical precision for Sr/Ca is $\pm 0.45\%$ relative standard deviation (Rosenberg 2011).

Chronology

Unique to this study, the coral skeletal chronology could be determined by calculating expected $\delta^{18}\text{O}_C$ and matching it to actual $\delta^{18}\text{O}_C$. Expected $\delta^{18}\text{O}_C$ was calculated from Eqn 5.1 using a 3-point moving average of T (to account for missing data) from the SERC data and $\delta^{18}\text{O}_W$ from Stable Isotope Lab measurements (Fig. 5.3). This chronology was compared against other chronologies, including 1) counting density bands and assigning the summer maximum to the densest region, 2) assigning annual temperature maximums and minimums to density maximums and minimums, respectively, that were determined from CoralXDS+ software (Kohler 2002), and 3) assigning the temperature maximums and minimums to $\delta^{18}\text{O}_C$ troughs and peaks, respectively.

Once anchor dates were established based on the annual density bands or $\delta^{18}\text{O}_C$ maxima and minima, dates were assigned to the remaining samples evenly assuming uniform coral growth between the biannual anchor samples. Spatiotemporal resolution averaged 38 samples per year and ranged from 19 to 68 samples per year. Chemical data were then rectangularly interpolated (Davis 1973) to a monthly basis to match the temporal resolution of the water sample data.

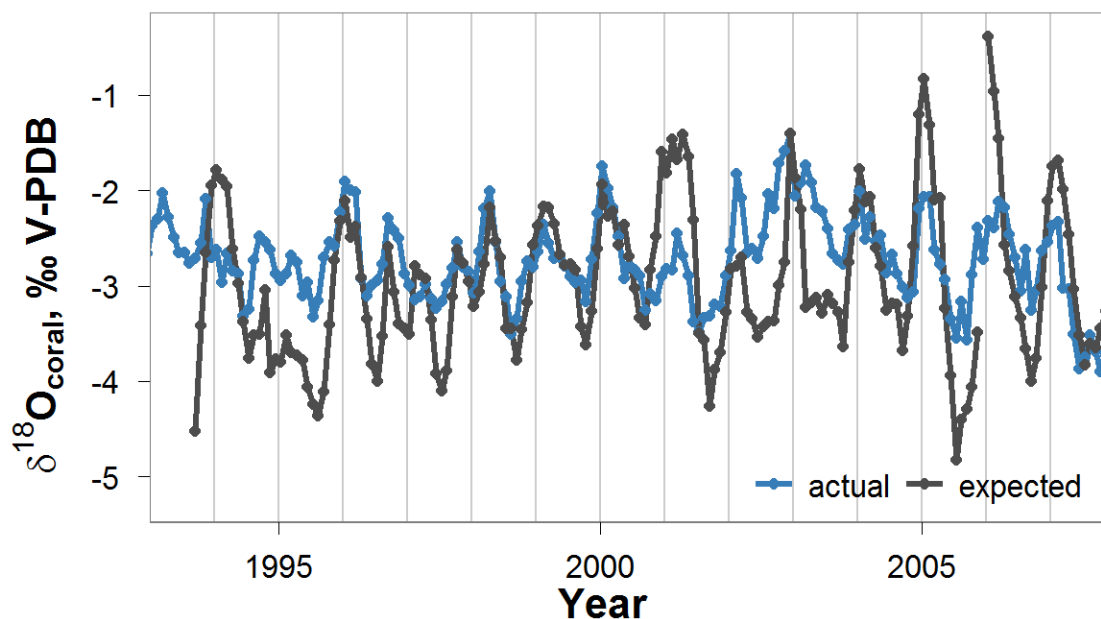


Figure 5.3. Chronology established by matching actual and expected $\delta^{18}\text{O}_C$. First, the $\delta^{18}\text{O}_W$ and a 3-point moving average of water temperatures were used to calculate expected $\delta^{18}\text{O}_C$ following (Leder et al. 1996). Second, actual $\delta^{18}\text{O}_C$ was assigned dates so that the peaks, troughs, and interannual variability matched as closely as possible the dates associated with the expected $\delta^{18}\text{O}_C$.

Carbon isotopes

The coral skeletal $\delta^{13}\text{C}_C$ record was corrected for two known anthropogenic forcings. The background long-term decline in $\delta^{13}\text{C}_C$ due to the global increase in atmospheric carbon derived from ^{13}C -depleted fossil fuels, i.e. the ^{13}C Suess effect (Druffel and Suess 1983), was subtracted from the coral skeletal carbon signal using slope constants from Swart et al. (2010). In addition to this gradual decrease in $\delta^{13}\text{C}_C$, skeletal carbon was corrected for the sudden -0.9 ‰ shift during construction of the Overseas Railroad from 1905 to 1912, which restricted water movement in the Bay and resulted in a buildup of organic matter (Swart et al. 1996b). First, the ^{13}C Suess effect was subtracted from the coral carbon record to 1905. Then the average $\delta^{13}\text{C}_C$ from 1909-

1912, when construction neared completion and $\delta^{13}\text{C}_\text{C}$ values stabilized, was used as a new baseline from which the ^{13}C Suess effect was subtracted to the present. The anomaly between actual $\delta^{13}\text{C}_\text{C}$ and long-term average $\delta^{13}\text{C}_\text{C}$ (corrected for those anthropogenic signals) was used to determine if hurricanes influenced the $\delta^{13}\text{C}_\text{C}$.

Hurricane data

Hurricane and tropical storm records obtained from the U.S. National Oceanic and Atmospheric Administration (Downloaded February 2011 from <http://www.srh.noaa.gov/gis/kml/>), including information on direction, strength (category), wind speed, and distance from coral. Hurricanes were coded as strongly likely or likely to flush organic matter depending on whether they passed through the bay within or over 30 km of the coral, respectively. Flushing of organic matter results in less oxidation than normal, hence fewer carbon-12 isotopes in seawater and subsequent $\delta^{13}\text{C}$ increases in the coral skeleton. Hurricanes passing over the Everglades were coded as likely to cause increased runoff from the Everglades, increasing organic matter, and ultimately driving $\delta^{13}\text{C}_\text{C}$ down. The full skeletal $\delta^{13}\text{C}$ and $\delta^{18}\text{O}$ record for the FB6 coral was obtained from Swart et al. (1996b). Scores of 0 or 1 were assigned according to whether expected $\delta^{13}\text{C}_\text{C}$ change matched actual change, both immediately after a hurricane passed and with a six-month lag. Data were analyzed using Fisher's exact tests on various combinations of hurricane strength, wind speed, distance, date bins, and lag time for signal to become incorporated into the skeleton. Analyses were conducted in the software program (R Development Core Team 2011).

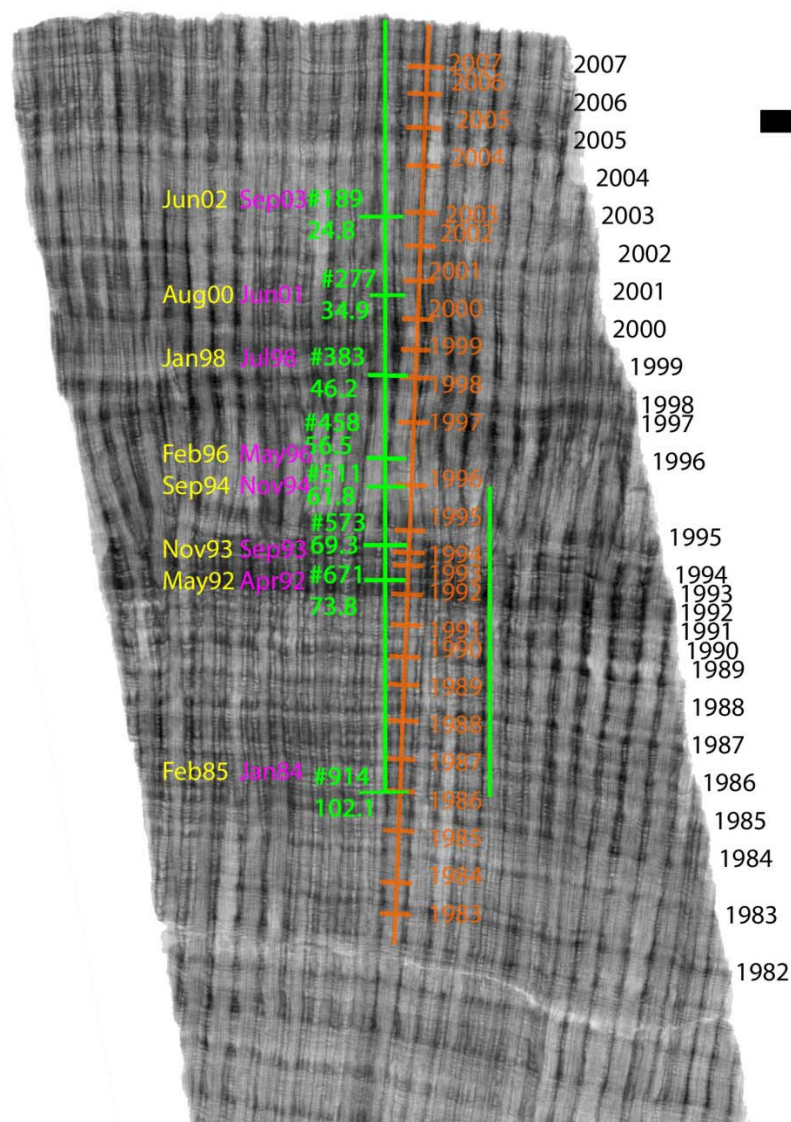


Figure 5.4. Positive x-radiograph of the *S. bournoni* skeleton from Peterson Keys, cored April 2008. The green line signifies the approximate location and lengths of the drilling transects, with sample number (#) and distance in mm annotated in green. The smaller green line represents Transect 2B. The larger line represents Transect 1A and 2B combined. Transect 1B (not shown) was drilled above Transect 2B. Several chronologies are shown based on different methodologies: (black) visual assessment of density bands, (orange) derivatives of density splines calculated in CoralXDS+, (purple) $\delta^{18}O_C$ minima correspond to annual maximum temperatures on September 1, (yellow) actual $\delta^{18}O_C$ are aligned with expected $\delta^{18}O_C$ calculated from temperature and $\delta^{18}O_W$ records. Purple and yellow dates are annotated based on measured distances (green line). The chronology based on actual/expected $\delta^{18}O_C$ (yellow) was used for all analyses. The double-band marked 1982 in the black, visual-based chronology was also demarked as 1982 in Healy (1996). This figure illustrates the complexities of deriving the exact chronology.

Skeletal data and proxy relationships

Coral skeletal $\delta^{18}\text{O}$ and Sr/Ca ratios were linearly regressed against environmental parameters to construct proxies for temperature and salinity. Salinity was determined as a function of $\delta^{18}\text{O}_\text{W}$, updating Equation 5.2. Second, seawater $\delta^{18}\text{O}_\text{W}$ was determined as a function of $\delta^{18}\text{O}_\text{C}$ and temperature, i.e. determining Equation 5.1 for *S. bournoni*. This equation for $\delta^{18}\text{O}_\text{W}$ was substituted into the previous salinity as a function of $\delta^{18}\text{O}_\text{W}$ equation to yield salinity as a function of $\delta^{18}\text{O}_\text{C}$ and temperature (i.e. Equation 5.3 calculated for *S. bournoni*). Temperature was determined from skeletal Sr/Ca ratios for the years 1997-2008 because skeletal Sr/Ca ratios in earlier years were variable and possibly decoupled from temperature. Coral skeletal Sr/Ca was substituted for temperature in the previous equation 5.3 to yield salinity as a function of coral $\delta^{18}\text{O}$ and coral Sr/Ca. Given the variability with coral Sr/Ca pre-1997, the temperature composite was also used in place of the Sr/Ca paleothermometer. The relative goodness of fit of the two salinity relationships were compared using Akaike information criteria (AIC) scores.

Once an estimate of salinity was obtained from the $\delta^{18}\text{O}_\text{C}$ and temperature, it was used to estimate aragonite saturation state from linear regressions for the two variables reported by Millero et al. (2001) for Florida Bay waters:

$$\Omega_{\text{arag}} = 1.14 + 0.083 \text{ Salinity} \quad (5.4)$$

where Ω_{arag} is aragonite saturation state.

RESULTS

Water quality data comparisons

Comparisons of continuous logger versus monthly SERC samples indicated the monthly SERC sampling regime accurately represented average monthly values for temperature but not salinity. Temperature yielded a higher coefficient of determination ($r^2 = 0.63$, $p = 0.002$) between continuous logger versus monthly SERC samples than salinity ($r^2 = 0.02$, $p = 0.62$) (Fig. 5.5). The 95% confidence intervals for the Fisher Z-transformed difference between the coefficients of correlation, $[0.04, 1.25]$, do not overlap 0 and therefore indicate the SERC temperatures are likely more representative of average environmental conditions than the salinities.

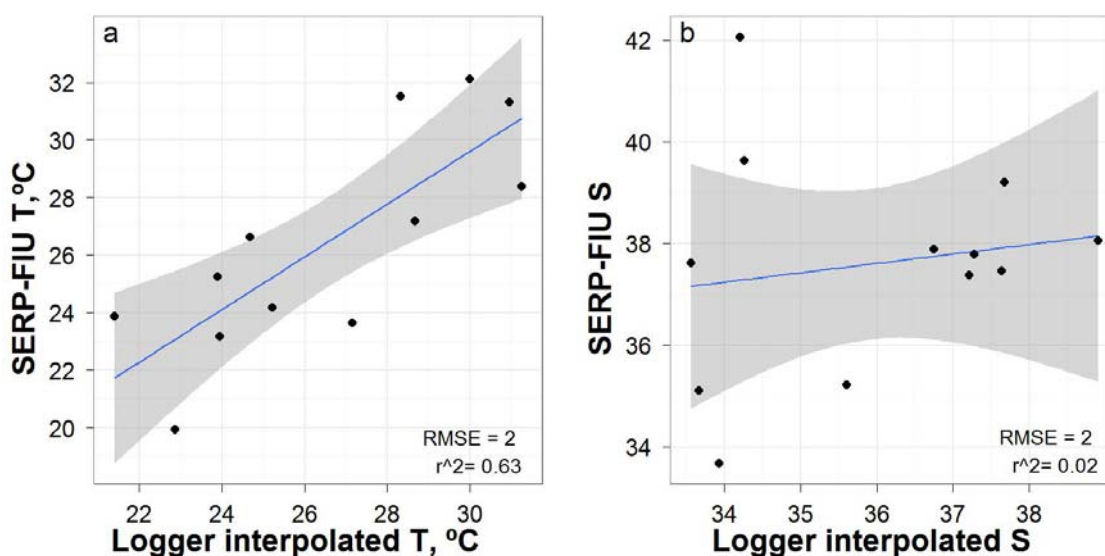


Figure 5.5. Comparisons of high frequency environmental logger data to SERC data for (a) temperature and (b) salinity, with coefficients of determination and residual mean square error (RMSE).

Chronology and coral growth rates

Chronologies based on expected $\delta^{18}\text{O}_\text{C}$ from water chemistry data and visual assessment of the coral growth bands ended in the same year of 1985 (Fig. 5.4) though a few years were misaligned (ex. 2002, 1994). In contrast, the method of assuming both highest temperature and lowest $\delta^{18}\text{O}_\text{C}$ fall at the same time each year and the density spline method were consistently offset from the other two methods (Fig. 5.4).

Annual coral calcification rates averaged $0.57 \pm 0.13 \text{ g cm}^{-2} \text{ y}^{-1}$ (mean \pm SD) and ranged from 0.27 to 0.93 $\text{g cm}^{-2} \text{ y}^{-1}$ for the period covered by the core, 1944-2008 (Fig. 5.6). Linear extension rates were $0.54 \pm 0.16 \text{ cm y}^{-1}$ and ranged from 0.17 to 1.08 cm y^{-1} . Average annual density was $1.07 \pm 0.17 \text{ g cm}^{-3}$ and ranged from 0.75 to 1.59 g cm^{-3} . Calcification remained constant, extension decreased slightly, and density increased steadily over time (Fig 5.5).

Coral skeleton

Both $\delta^{18}\text{O}_\text{C}$ and $\delta^{13}\text{C}_\text{C}$ demonstrate annual periodicity (Figs. 5.6-5.9). Average $\delta^{18}\text{O}_\text{C}$ was -2.68‰ and ranged from -4.10 to -1.55 ‰. Mean annual range was 1.23‰ with a minimum of 0.80 and maximum of 2.36‰ (Fig. 5.8). Coral $\delta^{13}\text{C}$ showed a shift to more enriched values of -3‰ in the early 1990s before stabilizing back to -4 to -5‰. Average $\delta^{13}\text{C}_\text{C}$ was -4.41‰ and ranged from -6.26 to -2.83‰. Mean annual range was 1.27‰ with a minimum of 0.56 and maximum of 2.66‰ (Fig. 5.8).

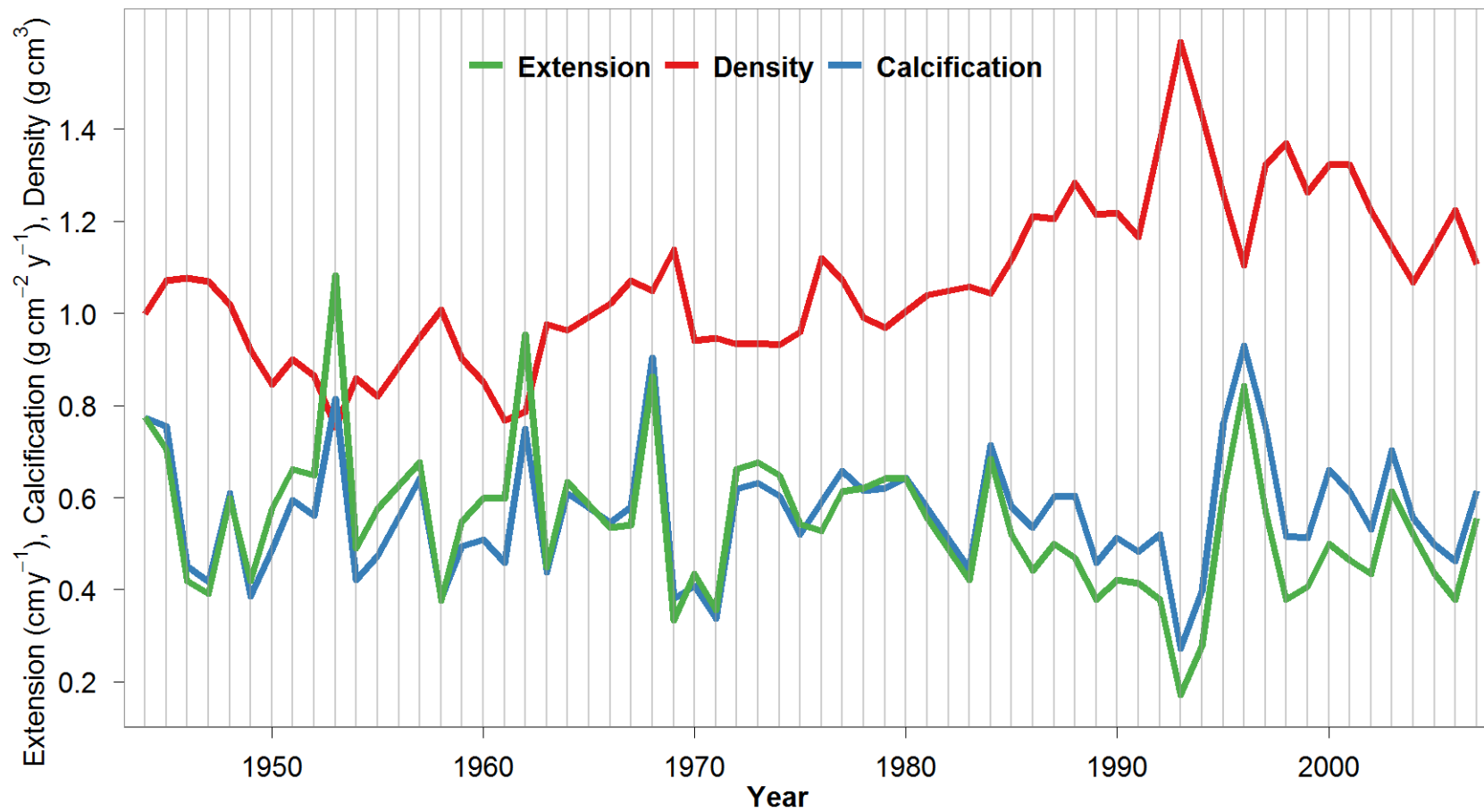


Figure 5.6. Annual extension, density, and growth for the coral core. Extension and calcification decreased slightly from 1950 to 2000 while density increased. (Courtesy of K. Helmle)

Coral elemental ratios exhibited greater inter- and intra-annual variation than the isotopic data. Barium ratios from the second slab piece (Transect 2B in Fig. 5.4, 1984-1994) showed regular annual cycles, but both Transects 1A and 1B on the first slab (1994-2008) yielded more variable ratios (Fig. 5.9). Mean Ba/Ca was 19.43 $\mu\text{M}/\text{M}$ and ranged from 2.79 to 93.48 $\mu\text{M}/\text{M}$, increasing towards the coral surface. Mean Mg/Ca was 5.50 mM/M and ranged from 3.64 to 14.37 mM/M, increasing towards the coral surface. Mean Sr/Ca was 9.13 mM/M and ranged from 8.77 to 9.56 mM/M. Magnesium had larger variability on the first slab while strontium had similar variability across all transects.

Coral $\delta^{13}\text{C}$ isotopes and hurricane frequency

Coral $\delta^{13}\text{C}$ anomalies do not appear to respond immediately to hurricanes (Fig. 5.10), even after they were corrected for declines due to the ^{13}C Suess effect and construction of the Overseas railroad. Fisher's exact tests of predicted hurricane effects at the $\alpha = 0.05$ significance level did not support the hypothesis that carbon isotopes would record hurricane signals on an annual or sub-annual basis. This outcome was the same no matter what combination of hurricanes was examined, including hurricanes in different time periods, hurricanes that passed near the coral, hurricanes expected to flush Florida Bay, hurricanes expected to add organic matter to the bay, category 3+ hurricanes, or storms greater than 50 knots.

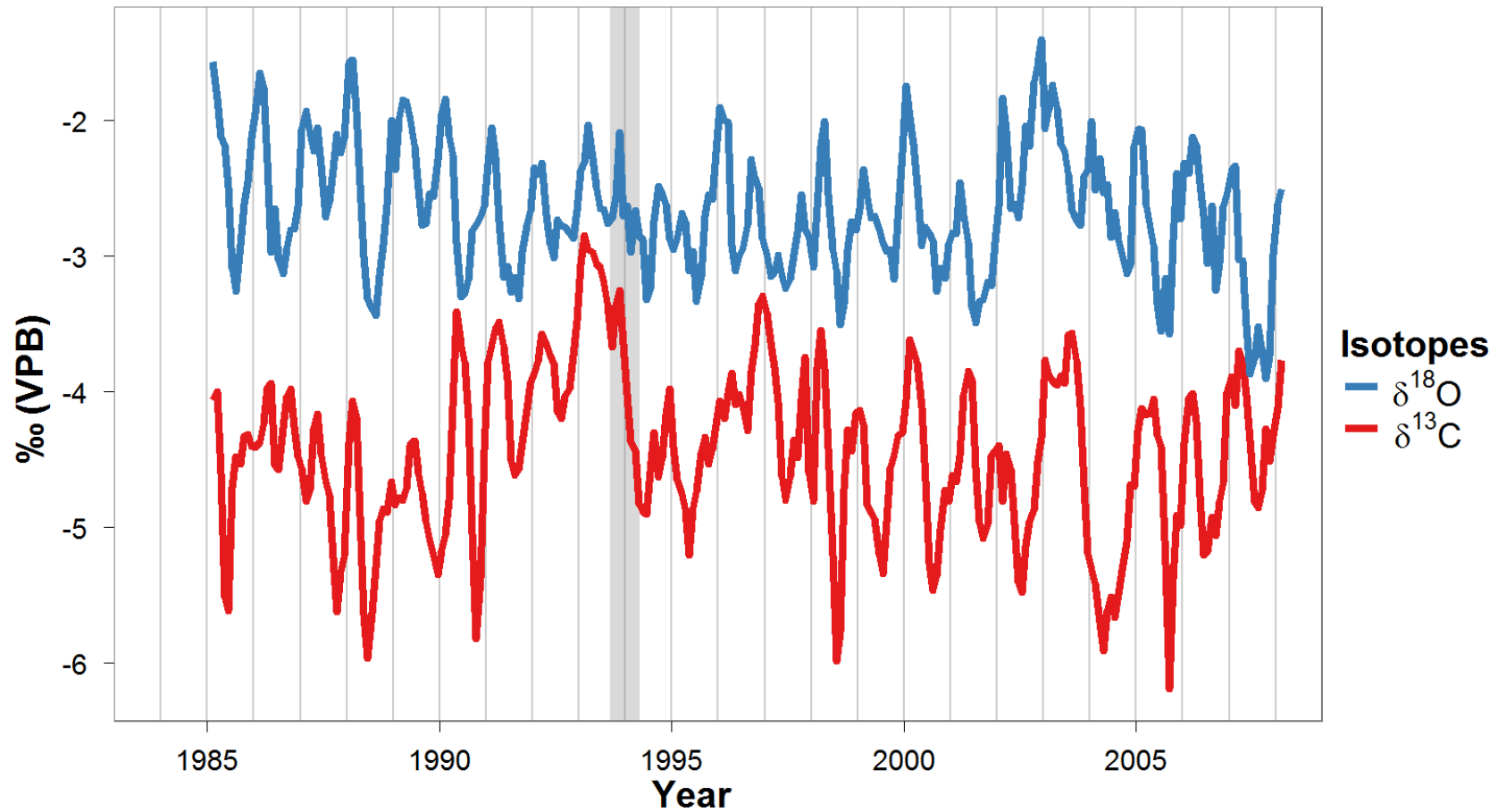


Figure 5.7. Coral oxygen and carbon isotopic data from the coral core extending from 1985 to 2008. Transect 1A transitions to Transect 2B in 1994. Overlapping isotopic values were similar, indicating carbon and oxygen isotopes are spatially consistent and movements in signals represent true conditions rather than sampling artifact.

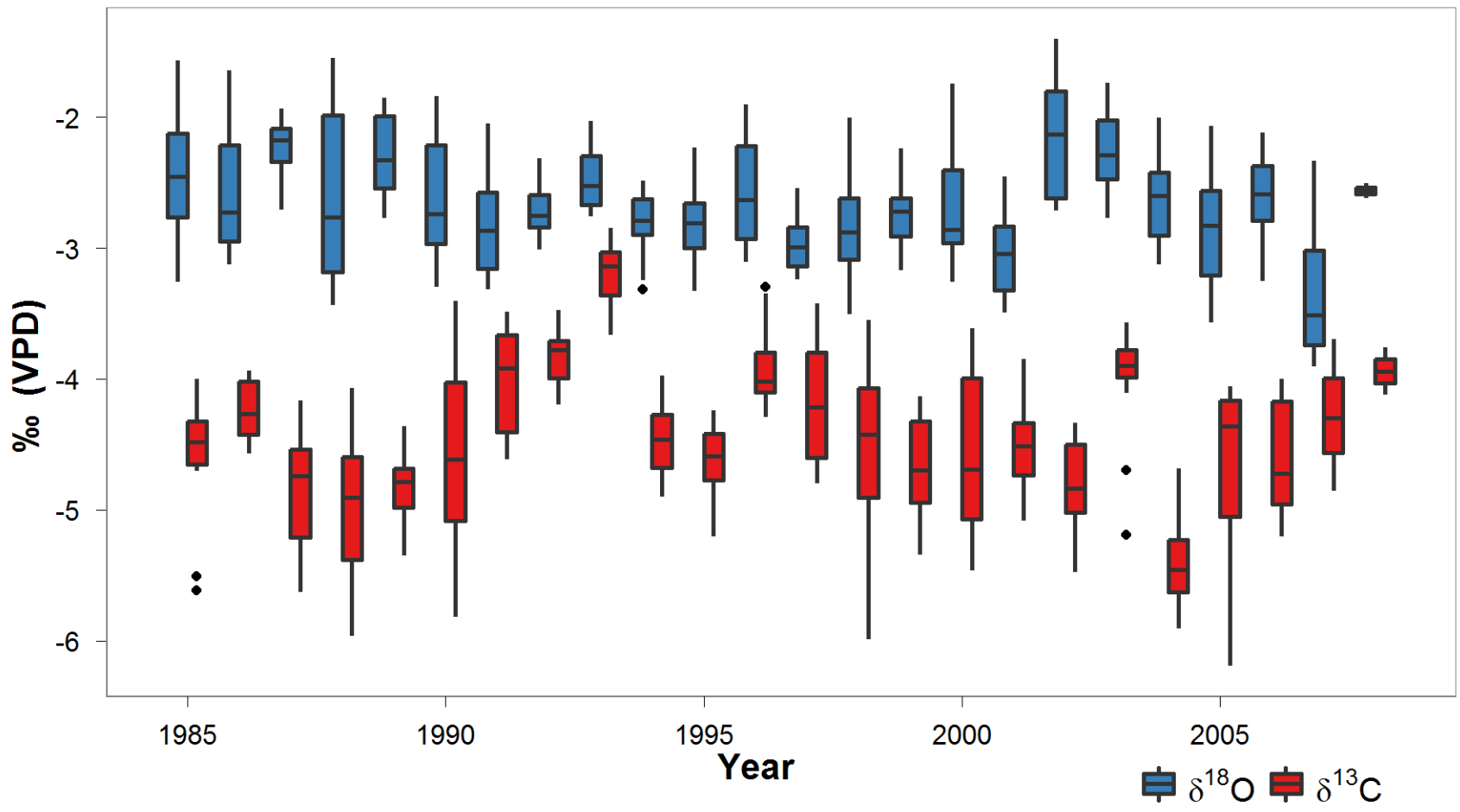


Figure 5.8. Boxplots of annual coral oxygen and carbon isotopic data. Carbon isotopes exhibit a large increase from 1990 to 1993 before settling back into a regular long-term average pattern. In comparison, oxygen has less interannual variation.

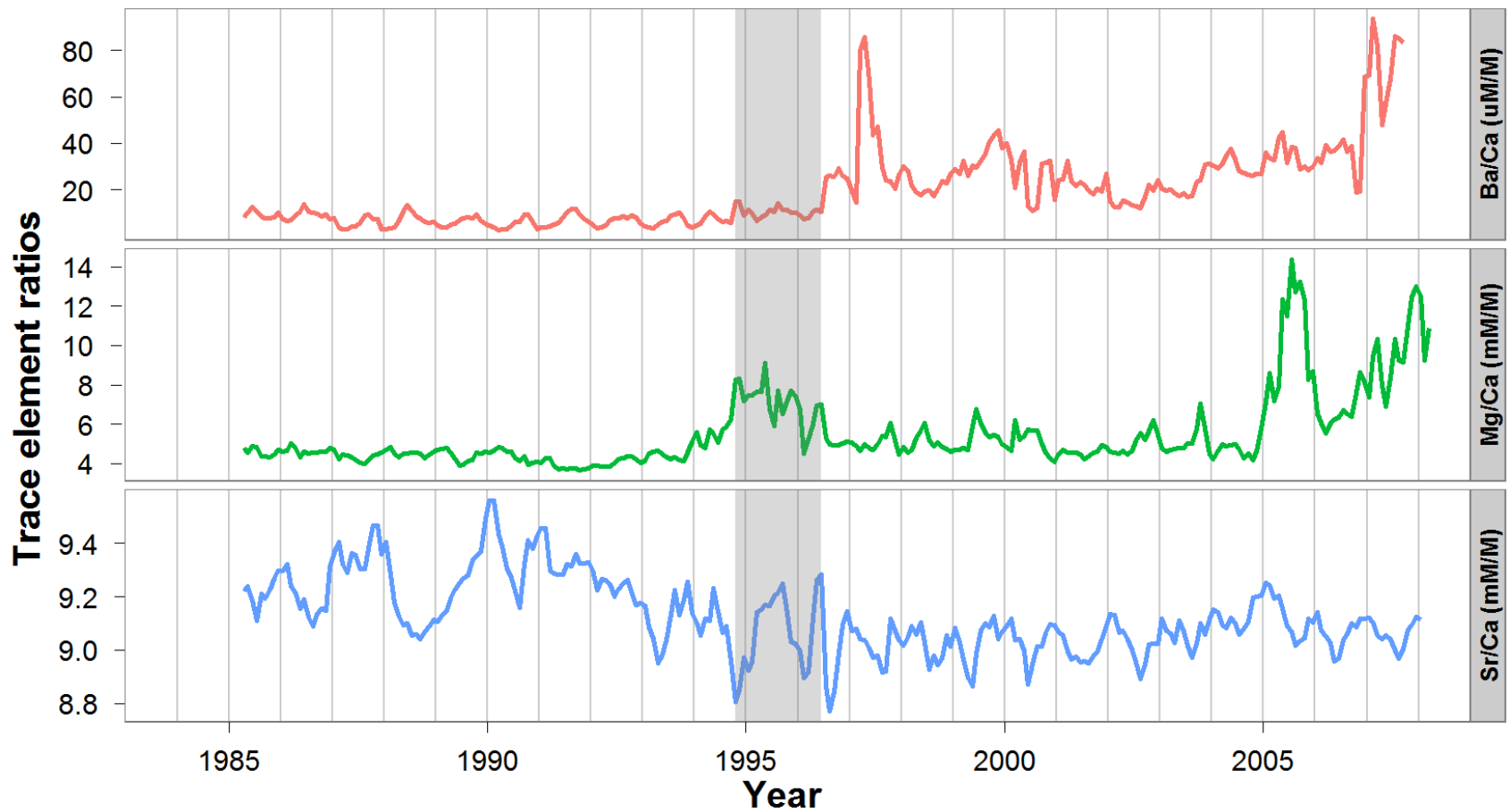


Figure 5.9. Trace metal ratios for the coral. Transect 2B extends from 1985-1994 and Transect 1B extends from 1996-2008. The values bridging the gap between the two sections in 1995 are from Transect 1A (shaded gray).

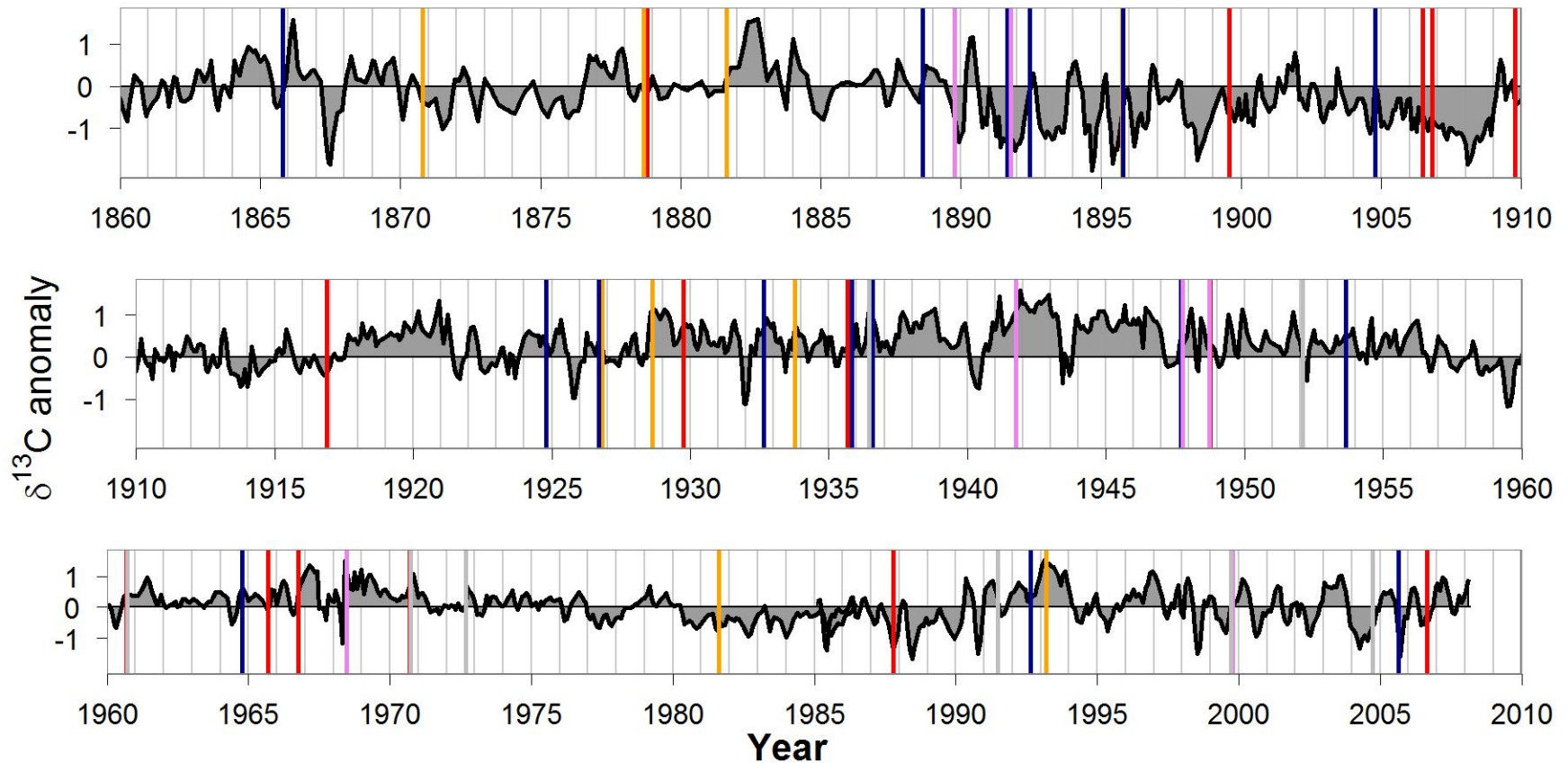


Figure 5.10. Carbon isotopic anomalies spanning 1860-2008, adjusted for the Flagler railroad construction and background anthropogenic signal. The lines represent hurricanes that passed <30 km from the coral (red), through Florida Bay >30 km from the coral (orange), across the Everglades (blue), across the bay and Everglades (purple), far from the coral (grey). Skeletal $\delta^{13}\text{C}$ is expected to increase after red and orange lines, and decrease after blue lines. Purple and grey lines were ignored because carbon isotopes could shift in either direction or have no effect following those storms.

Paleoreconstructions of temperature, salinity, and saturation state

Updating Leder et al.'s (1996) *M. annularis* temperature equation (Eqn. 5.1) for *S. bournoni* yields:

$$T = -2.26 * (\delta^{18}\text{O}_C - \delta^{18}\text{O}_W) + 16.81 \quad (5.4)$$

which also has a weaker relationship (Fig 5.10b, $r^2 = 0.23$, $p < 0.001$) and dependence on $\delta^{18}\text{O}$ (slope of -2.26 vs -4.52) than Leder et al. (1996). Similarly, salinity was positively correlated with bay water $\delta^{18}\text{O}$ (Fig . 5.10a, $r^2=0.33$, $p < 0.001$) with the slope exhibiting less dependence on $\delta^{18}\text{O}_W$, i.e. shallower slope, that reported by Healy (1996):

$$S = 2.62 \delta^{18}\text{O}_W + 31.43 \quad (5.5)$$

Of the three skeletal trace metal ratios, Sr/Ca generally had the most consistent seasonal signal (Fig. 5.9) and was the only one used in any analyses. However, skeletal Sr/Ca ratios exhibit large interannual variations and lack periodicity in most of the years preceding 1996. Hence only skeletal Sr/Ca data after 1996 were used to calibrate thermometers, though this model fit ($r^2 = 0.25$, Fig. 5.11c) was significantly lower than Swart et al.'s (2002) calibration for *M. annularis* (95% confidence interval for the difference in Fisher's Z-transformed coefficients of determination between this study and Swart et al. (2002) = [0.08, 0.76]). This *S. bournoni* Sr/Ca thermometer had a shallower slope (-0.009) than found in other studies (-0.033 to -0.080, summarized in Table 1 of Swart et al. (2002)):

$$\text{Sr/Ca} = -0.009 * T - 9.285 \quad (5.8)$$

Despite using the post-1996 skeletal Sr/Ca ratios to determine a temperature relationship, an accurate salinity reconstruction could not be obtained. The reconstruction based on $\delta^{18}\text{O}_C$ and ambient temperatures concurs with actual recorded

values of salinity (Fig. 5.12a). However, noise increases once Sr/Ca paleothermometry is added to the equation (Fig. 5.12b). Consequently, the temperature composite was used in place of skeletal Sr/Ca (Fig. 5.12c). The AIC scores for the Sr/Ca-based and temperature composite-based salinity were 1382 and 1159, respectively, supporting use of the temperature composite (Fig. 5.13) over Sr/Ca.

With salinity determined from $\delta^{18}\text{O}_\text{C}$ and the monthly temperature composite, aragonite saturation states were determined for the history of the coral skeleton (Fig 5.13). Average aragonite saturation states appear constant through time, close to the oceanic pre-industrial average of 4.6. These results correspond with observations from the environmental loggers over two years (Fig. 3.8), where saturation states were elevated relative to oceanic waters ($\Omega_{\text{arag}} = 3.6$) for most of the year. Saturation state appears to decline from 4.2 to 3.9 in the years from 2000 to 2008, when the coral was cored.

Table 5.1. Relationships between interpolated monthly coral skeletal values and SERC environmental data. The Leder et al. (1996) calibration is derived from *Montastraea annularis* while the calibrations from this study are based only on *Solenastrea bournoni*. T = Temperature (°C), S = Salinity, $\delta^{18}\text{O}_\text{C}$ = coral oxygen isotopes (‰), $\delta^{18}\text{O}_\text{W}$ = water oxygen isotopes (‰), Sr/Ca = Strontium/Calcium (mM/M). RMSE = residual mean square error.

| Proxy | RMSE | Eqn | Source |
|---|------|------|-----------------------|
| $T = -4.519 * (\delta^{18}\text{O}_\text{C} - \delta^{18}\text{O}_\text{W}) + 5.33$ | | 5.1 | Leder et al. (1996) |
| $T = -2.26 * (\delta^{18}\text{O}_\text{C} - \delta^{18}\text{O}_\text{W}) + 16.81$ | 3.5 | 5.6 | this study |
| $S = 4.98 \delta^{18}\text{O}_\text{W} + 25.89$ | | 5.2 | Healy (1996) |
| $S = 2.62 \delta^{18}\text{O}_\text{W} + 31.43$ | 2.8 | 5.7 | this study |
| $S = 4.98 \delta^{18}\text{O}_\text{C} + 1.18T + 19.62$ | | 5.3 | Swart et al. (1999) |
| $S = 2.62 \delta^{18}\text{O}_\text{C} + 1.16T + 12.65$ | 4.0 | 5.8 | this study |
| $\text{Sr/Ca} = -0.047 * T - 10.165$ | | 5.4 | Swart et al. (2002) |
| $\text{Sr/Ca} = -0.009 * T - 9.285$ | 0.06 | 5.9 | this study |
| $T = -28.06 * \text{Sr/Ca} - 280.17$ | 3.5 | 5.10 | this study |
| $\Omega_{\text{arag}} = 0.083 * S + 1.14$ | | 5.5 | Millero et al. (2001) |

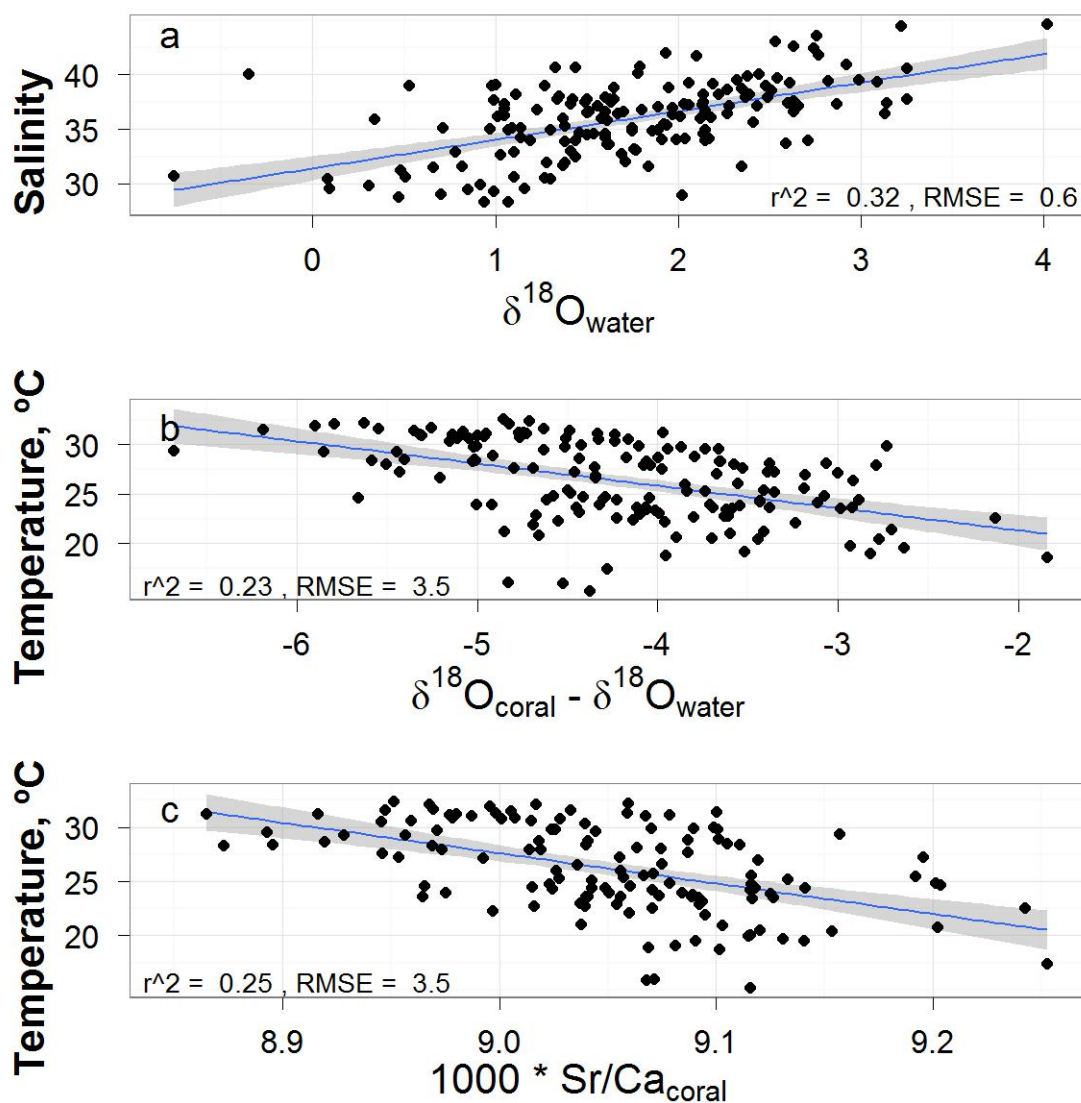


Figure 5.11. Proxies used in salinity reconstructions reconstructions: (a) salinity from $\delta^{18}\text{O}_{\text{w}}$, (b) temperature from the difference between coral and water $\delta^{18}\text{O}$, and (c) temperature from Sr/Ca ratios. Salinity reconstructions were fairly accurate from (a) and (b), but not when (a)-(c) were combined. Plots are annotated with coefficients of determination and residual mean square error (RMSE).

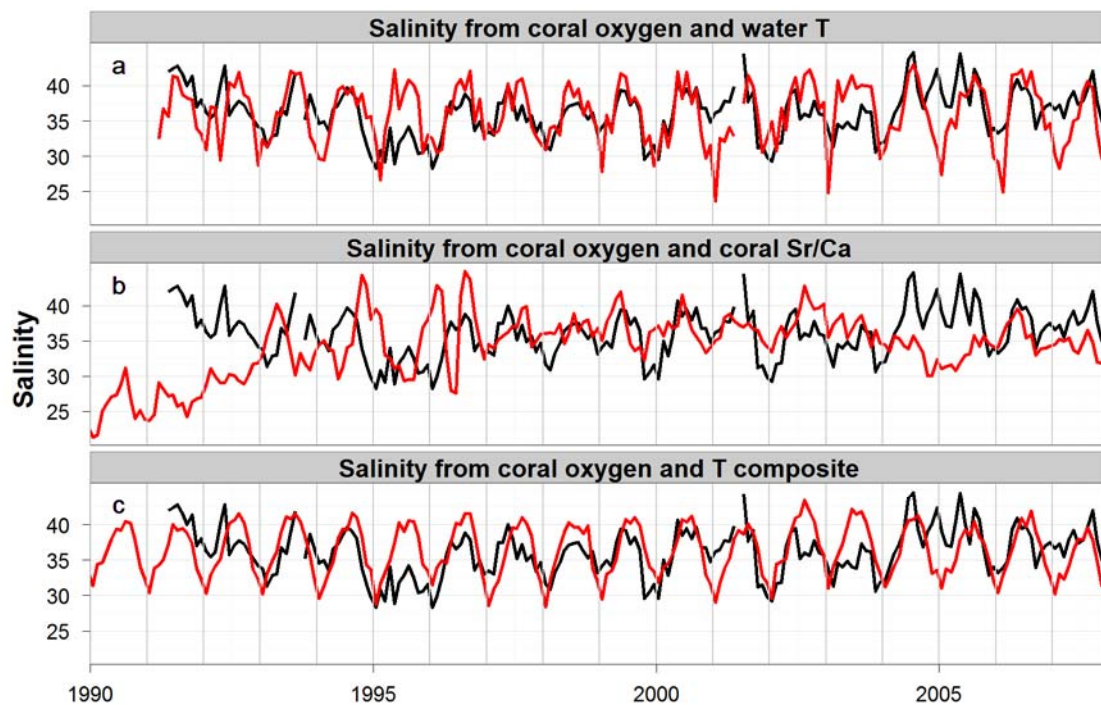


Figure 5.12. Reconstructed salinity (red) compared to actual salinity (black) from SERC records (a) before and (b) after the Sr/Ca paleothermometer is added, as well as from the (c) temperature composite substituting for the Sr/Ca paleothermometer.

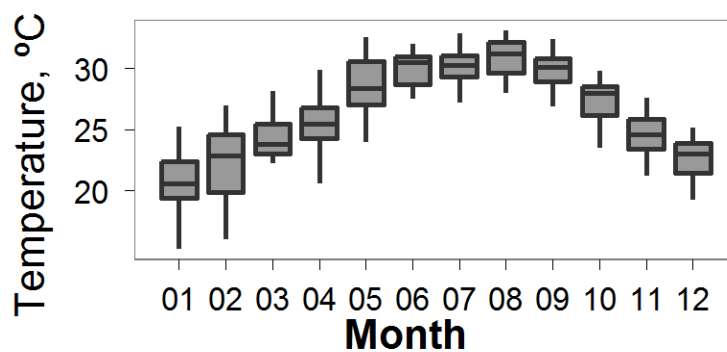


Figure 5.13. Monthly composite temperature from SERC data for Peterson Keys (Station 20) for 1991-2008 where January is Month 01.

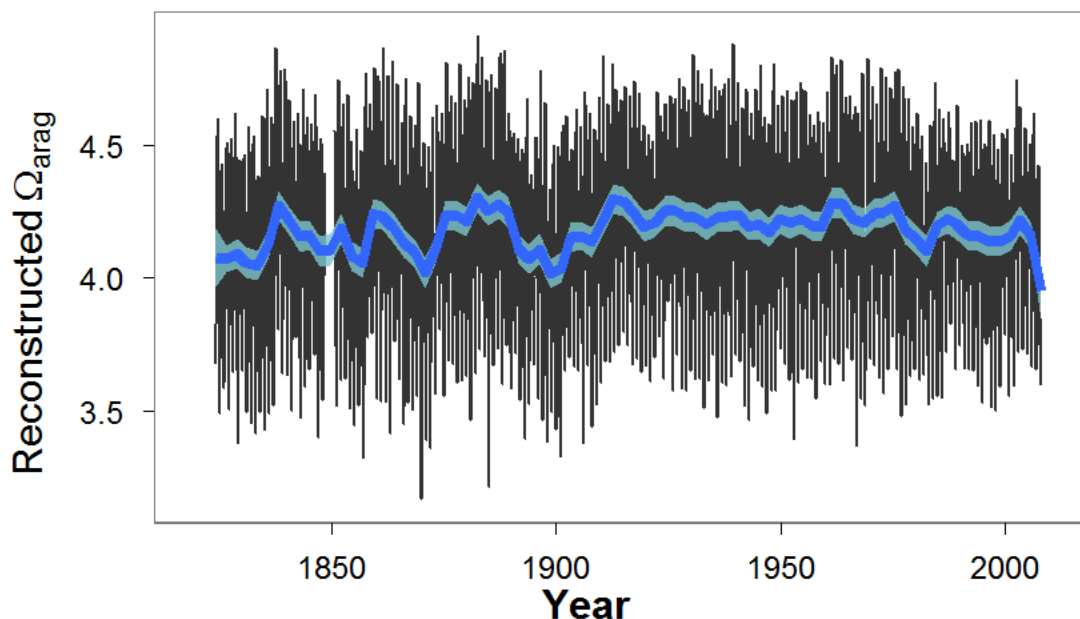


Figure 5.14. Reconstructed Ω_{arag} using $\delta^{18}\text{O}_{\text{C}}$ and composite temperature. Shaded light blue area represents the 95% confidence interval for the local regression smoothed curve (blue line, span = 0.05).

DISCUSSION

Chronology

The method of establishing coral chronology in this study is unique in that it requires a long-term record of temperature and $\delta^{18}\text{O}_{\text{w}}$, the latter of which is often unavailable. The chronology produced from this method matched visual estimates of chronology from coral density with the exception of a few years, suggesting the method is a promising means of dating coral skeletal growth. It is assumed to be the most accurate means of dating coral skeletal values because it groundtruths $\delta^{18}\text{O}_{\text{C}}$ based on expected $\delta^{18}\text{O}_{\text{C}}$ (which in turn is calculated from recorded environmental data on temperature and $\delta^{18}\text{O}_{\text{w}}$, and the expected $\delta^{18}\text{O}_{\text{C}}$ closely matched the interannual variation of the actual $\delta^{18}\text{O}_{\text{C}}$ (Fig 5.2). The other methods make assumptions on timing of annual

$\delta^{18}\text{O}_C$ and temperature peaks or are not continually verified against expected coral $\delta^{18}\text{O}_C$. However, Fisher's exact tests failed to detect hurricane signals, indicating these chronologies were inadequate in detecting individual events at an annual resolution. Numerous factors can contribute to imprecise chronologies including stress bands that obscure actual density bands, lack of growth (i.e. lack of band formation) in a given year, variable growth rates that alter skeletal linear extension and weight the sampling in favor of high growth seasons, and incorrect years early in chronology assignment that promulgate into further year misalignments (Carricart-Ganivet 2011). For example, if the chronology was off by one year, the Fisher's exact tests would not likely detect any hurricanes unless they were regular events. Conversely, if events such as hurricanes can be conclusively shown to affect the $\delta^{13}\text{C}_C$, these events could conceivably be used as markers to validate chronologies. Despite the differences in annual year assignments, the different methodologies yielded chronologies that were misaligned from a few months to about two years but ended within a year apart after 25 years (Fig. 5.4). This convergence after two decades indicates $\delta^{18}\text{O}_C$ and density bands both follow the same annual pattern. However, the variability within years among chronologies indicates $\delta^{18}\text{O}_C$ minima, density bands, and water temperatures do not necessarily all occur together or at the same time from year to year. Together, these results suggest the coral skeletal $\delta^{13}\text{C}$ may better resolve environmental patterns on interannual to decadal scales rather than monthly scales.

Proxies for past temperature and salinity

Overall, coral skeletal $\delta^{18}\text{O}$ generally exhibit lower spatial and intra-annual variability than the trace metal ratios of Ba/Ca, Mg/Ca, and Sr/Ca. Model fits derived from the SERC water quality data and skeletal isotopic records for *S. bournoni* were comparable to previous work in the area with *M. annularis* (Table 5.1) though with less predictive capability. The low coefficients of determination observed in this study (Table 5.1; Fig. 5.11) relative to those observed in other studies in the region (Table 5.1) may be a result of inaccuracies of date assignments in the coral chronology. Such inaccuracies, even of only a few months, will erode relationships with environmental variables. As discussed with the hurricane signals, misalignment of early years can amplify across older years and mask interannual trends.

Of the three skeletal elemental ratios of strontium, magnesium, and barium to calcium, Sr/Ca had a clear seasonal pattern (Fig. 5.9) and was used for paleothermometry. However, the relationship of skeletal Sr/Ca to temperature had lower regression slopes and coefficients of determination than those established for other corals (Swart et al. 2002). Consequently, the skeletal Sr/Ca-derived temperatures could not be used to reconstruct historical salinity, as shown in the comparison of modeled salinities against actual values (Fig. 5.12). Before skeletal Sr/Ca is added to the model, actual temperature and $\delta^{18}\text{O}_\text{C}$ appear to be close predictors of salinity (Fig. 5.12a). However, temperature is not recorded in the coral skeleton and cannot be used for reconstructions beyond the period of recorded temperatures. Once skeletal Sr/Ca-derived temperature is added to the salinity model in place of actual temperature, noise increases (Fig. 5.12b), reflecting the inability of skeletal Sr/Ca to adequately record environmental conditions. The variable skeletal Sr/Ca values could be a result of large temperature changes in the

bay or natural variability in seawater Sr/Ca. From 1988 to 1990 coral skeletal Sr/Ca increased from 9.04 to 9.56 mmol/mol (Fig. 5.9), which would correspond to a decrease in temperature of 11 to 15°C, depending on whether the calibrations from Swart et al. (2002) or this study were used, respectively. While this range in temperature is possible for Florida Bay, no such drop in temperature occurred over this time (Boyer et al. 1999). Instead, the coral skeletal Sr/Ca likely reflects natural variation in seawater Sr/Ca in the bay. In Peterson Keys alone, seawater Sr/Ca ranges from 8.7 to 9.7 mmol/mol (Fig. 5.15). This range in values is unlikely a result of increases in [Ca] of 5 ppm (Fig. 5.15) from groundwater intrusion because such increases were too small to significantly lower seawater Sr/Ca within the range of salinities common to Peterson Keys. Furthermore, increases in seawater calcium concentrations can only lower seawater Sr/Ca from approximately 9.0 mmol/mol while about half the observed seawater Sr/Ca values are above 9.0 mmol/mol (Fig. 5.15), indicating strontium enrichment relative to calcium. An example of such an enrichment could be increased precipitation of calcite by seagrass epiphytes that would deplete seawater calcium at a faster rate than strontium. In a completely closed system and assuming a conservative distribution coefficient for strontium (D_{Sr}) of 0.16, calcification rates for calcite-depositing epiphytes would need to increase by approximately $85 \text{ g CaCO}_3 \text{ m}^{-2} \text{ y}^{-1}$ to cause the observed increase in skeletal Sr/Ca from 9 to 9.6 mmol/mol from 1988 to 1990. While this value is comparable to carbonate production rates observed in Florida Bay from 1991-1992 (Frankovich and Zieman 1994), in a more realistic open system epiphyte calcification rates would need to be much higher. Consequently, strontium is not likely conserved in Florida Bay. As a

result, the utility of skeletal Sr/Ca as an indicator of temperature and as an indirect indicator of salinity remains limited.

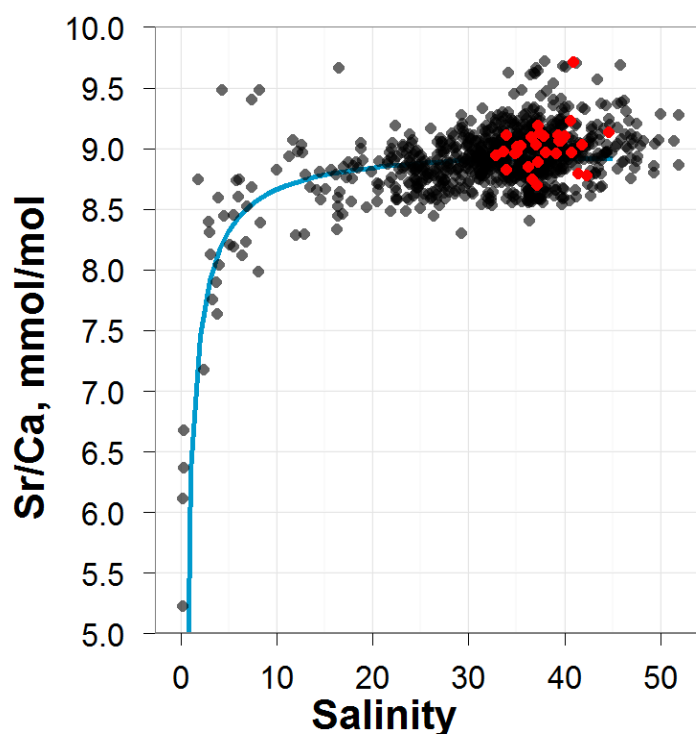


Figure 5.15. Seawater Sr/Ca values in Florida Bay. Gray dots represent values for all 28 subbasins for all available dates, and red dots represent Peterson Keys. The blue line is the modeled Sr/Ca due to 5 ppm increase in [Ca] from groundwater.

Magnesium-based thermometry (Mitsuguchi et al. 1996) was also limited here due to increasing skeletal Mg/Ca towards the coral surface despite no such trend in temperatures. This increase in skeletal Mg/Ca may be an indicator of brucite formation from photosynthesizing endoliths (Nothdurft et al. 2005; Buster and Holmes 2006) or growth-dependent effects (Mitsuguchi et al. 2003; Reynaud et al. 2007). This coral's growth record remained constant through time (Fig. 5.6) which discounts the latter mechanism. As a result of these uncertainties, magnesium was not explored further for paleothermometry.

Like magnesium, barium to calcium ratios increased towards the coral surface from 1995 to 2008, possibly a result of residual organic matter in the coral skeleton (Shen and Boyle 1988; Hart and Cohen 1996; Anderegg et al. 1997; Anderegg 1998). During these years, skeletal Ba/Ca is highly variable and does not exhibit annual periodicity. Skeletal barium records exhibit an annual cycle between 1985-1994 (Fig. 5.9), which only leaves three years of overlap with the SERC record. Because of the incomplete record and possible residual organic matter, barium was not analyzed.

As a result of the inability to calibrate Sr/Ca and Mg/Ca coral skeletal thermometers to resolve past salinity, a temperature composite (Fig. 5.13) was used instead to infer past salinity. This composite assumed temperatures followed the same annual pattern over the history of the coral with little interannual variation. This assumption was supported by the coefficient of determination between SERC temperatures with the high-resolution environmental logger data ($r^2 = 0.63$; Fig. 5.5a). The salinity record derived from this average monthly composite was then used to estimate aragonite saturation state.

Historical aragonite saturation states were consistently high in Florida Bay relative to modern-day oceanic values of 3.6, which supports the findings from the environmental loggers and discrete water samples (Fig 3.8). Additionally, the saturation state of these bay waters is consistently higher than on the reef tract Manzello et al. (2012). The most recent years reveal a drop in Florida Bay saturation state from 4.2 to 3.9, but in this study the decline is not attributable to increasing atmospheric $p\text{CO}_2$. The saturation state reconstruction is decoupled from the effects of increasing atmospheric $p\text{CO}_2$ (Feely et al. 2004; Cao et al. 2007; Doney et al. 2009) because it is based on

salinity, which itself is based on $\delta^{18}\text{O}_C$. Consequently as atmospheric pCO_2 increases while salinity is unaffected, the relationship of saturation state to salinity will deteriorate. In fact, Millero et al. (2001) collected the data to establish this relationship from 1997-2000, when saturation state was already falling from pre-industrial values to approximately 4.0. Therefore, the assumption that the S- Ω_{arag} relationship is consistent through time may require reexamination, especially in this case because Ω_{arag} is calculated indirectly using an unchanging temperature composite. Revisiting this correlation between S and Ω_{arag} periodically over time may provide some insight as to whether they are truly coupled. Nonetheless, constant aragonite saturation states in Florida Bay through time may explain the stable growth rates in this coral over the past half century (Fig 5.5). While corals from other parts of the world have experienced declines over the same period of time (Cooper et al. 2008; De'ath et al. 2009; Tanzil et al. 2009; Manzello 2010), specimens of *M. faveloata* from the Florida Keys have also maintained calcification rates (Helmle et al. 2011). Florida Bay's high saturation state waters may support the growth rates of these reef tract corals Manzello et al. (2012).

This study provides an alternative means of establishing a coral chronology using a time series of the $\delta^{18}\text{O}_W$. Despite the precision of this new method, specific events, i.e. hurricanes, could not be detected in the coral skeletal carbon isotopic record. Rather, $\delta^{13}\text{C}_C$ appears to record hurricane signals on annual-to-decadal rather than monthly-to-annual bases. Unlike many other studies, skeletal Sr/Ca ratios were not predictive of temperature, possibly due to misaligned chronology or complex processes affecting strontium concentrations in Florida Bay. Aragonite saturation states in Florida Bay have

been consistently elevated and stable relative to global oceanic waters and therefore may have augmented this coral's growth rates.

Chapter 6: Conclusions

Intra-species results

These experiments demonstrated variable responses across coral species, as well as the role of the environment in mediating those responses. Additionally, results differed for the same species across experiments, potentially due to methods used to quantify calcification. In the field studies (Chapter 3 and 4), *S. radians* and *S. hyades* both decreased calcification with increased pCO₂ similarly to the generalized coral response (Kleypas and Langdon 2006). Their responses were assessed using the alkalinity anomaly (AA) method, which quantifies instantaneous, light-enhanced calcification over a period of 1-2 h. *S. radians* from the lab study (Chapter 2) did not show statistically significant declines from pCO₂ while *S. hyades*'s calcification declined with pCO₂ only at its elevated, more optimal temperature. These growth measurements were obtained using the buoyant weight (BW) method (Davies 1989), which incorporates mass gain over a longer time period (every two-weeks in the case of this experiment). These rates generally reflect both light and dark calcification hence are generally lower than AA-calcification. For example, assuming the lab corals have uniform surface areas of 4.9 cm², the mean BW rate for *S. radians* is 1.3 compared to 5.2 mmol m⁻² h⁻¹ measured by AA in Chapter 3. Likewise, *S. hyades* growth is 3.0 versus 4.1 mmol m⁻² h⁻¹ for BW and AA, respectively. It's possible that because the BW method records calcification at lower rates, the pCO₂ signal may not appear over natural variability. Additionally, the BW method measures mass increase, which is subject to error if other encrusting organisms add to the weight of the coral. AA measures the direct uptake of

carbonate ions as they are incorporated into the coral skeleton over a shorter time period, meaning the measurement is more sensitive to changes in ambient chemistry. This may be one explanation for the discrepancies observed between the AA and BW methods.

The experiments yielding consistent declines in calcification generally measure coral growth through AA (Langdon et al. 2000; Leclercq et al. 2000; Langdon and Atkinson 2005; Schneider and Erez 2006) while the studies with more variable results generally utilize BW (Reynaud et al. 2003; Anthony et al. 2008; Ries et al. 2009). The difference may be a result of the different timescales of measurement, where corals have time to adjust calcification rates, for example by gene expression or increased heterotrophy (Cohen and Holcomb 2009), although long-term experiments using AA still detected strong CO₂ effects (Langdon et al. 2000).

More simply, experimental power may have been too low to detect pCO₂ effects for certain corals in the laboratory experiment. Given the variability of growth rate of *S. radians* encountered in the lab experiment a difference in the relative growth in excess of 100% would have been necessary to be statistically significant at $\alpha = 0.05$. Based on the field study a decrease of 60-80% [unit Δ calcification * Δ unit $\Omega_{\text{arag}} = -0.4 * (3.1-1.6)$ or $-0.4 * (3.1-1.1)$] would have been expected at the intermediate and high CO₂ treatment and hence would not have been statistically detectable.

Potential mechanisms for calcification resistance to pCO₂

These experiments presented evidence that some corals are resistant to ocean acidification. The means by which corals might achieve CO₂-resistant calcification are unknown. Many researchers have shown calcification is a linear function of saturation

state (Langdon et al. 2000; Leclercq et al. 2000; Marubini et al. 2001; Leclercq et al. 2002; Ohde and Hossain 2004; Langdon and Atkinson 2005), which is directly proportional to carbonate ion concentration. As more CO_2 dissolves in the ocean, $[\text{CO}_3^{2-}]$ decreases while $[\text{HCO}_3^-]$ increases, causing saturation state reductions and depressed calcification (Langdon et al. 2000; Schneider and Erez 2006; Marubini et al. 2008). Hence, one possible mechanism of calcification-resistance could involve corals switching from CO_3^{2-} to HCO_3^- as the primary substrate used for calcification. If corals were able to utilize ambient bicarbonate, they would have more substrate available for calcification under ocean acidification scenarios. To date, only *Madracis auretenra* has been shown to utilize bicarbonate instead of carbonate for calcification (Jury et al. 2010). Chapters 3 and 4 did not support this hypothesis because bicarbonate levels increased under elevated pCO_2 conditions while calcification decreased.

Many models of calcification posit that Ca^{2+} -ATPase proton pumps drive pH gradients that create favorable calcification conditions (Adkins et al. 2003; Al-Horani et al. 2003; McConnaughey 2003; Cohen and Holcomb 2009; McCulloch et al. 2012). Workers have focused on these pumps as the mechanism through which organisms respond to ocean acidification (Ries 2011a; McCulloch et al. 2012), with organisms that maintain tight control over calcifying space and have strong proton pumps as more likely to resist ocean acidification. Ries (2011a) split this mechanism into two models, with proton pumps: 1) pumping out a fixed number of protons against the external seawater gradient, or 2) maintaining a constant proton gradient between internal and external conditions. Reduced ambient seawater pH would increase the metabolic cost of maintaining the pH gradients under the first model, while in the second corals would still

maintain elevated pH but at a reduced energetic cost because they would not have to pump out as many protons to achieve the target gradient. This mechanism could apply to many different organisms and could be the means by which some taxa resist ocean acidification.

The stimulation of photosynthesis by increased $p\text{CO}_2$ is another proposed potential CO_2 -calcification resistance mechanism. Increased CO_2 concentrations could reduce photorespiration in symbiotic zooxanthellae's form II Rubisco leading to a more efficient Calvin cycle or indirectly reduce the metabolic costs of operating a carbon-concentrating mechanism (CCM) (Leggat et al. 1999; Bertucci et al. 2010). Increased photosynthesis might then boost calcification (Gattuso et al. 1999; Furla et al. 2000; Marubini et al. 2001; Al-Horani et al. 2003; Allemand et al. 2004; Al-Horani et al. 2005), likely through 1) the production of CO_3^{2-} as carbonic anhydrase dehydrates HCO_3^- to supply CO_2 for photosynthesis, 2) removal of CO_2 elevating pH and essentially countering ocean acidification, and 3) additional photosynthates for calcification. The basis for this mechanism requires photosynthetic stimulation in higher $p\text{CO}_2$, for which evidence is equivocal: some researchers have shown potential CO_2 -fertilization (Marubini et al. 2008) while others, including this study, have not (Langdon et al. 2003; Reynaud et al. 2003; Schneider and Erez 2006). Often CO_2 does not increase photosynthesis because it is not the limiting variable (Oren et al. 2001). Whether or not CO_2 fertilizes photosynthesis, photosynthesis generally does not buffer calcification declines from increased CO_2 (Langdon and Atkinson 2005; Kroeker et al. 2010).

Tradeoffs in coral calcification

Chapter 3 presents evidence of two different growth strategies between *S. hyades* from locations with different environmental histories. *S. hyades* from Florida Bay tolerated stress better while conspecifics from Triangles patch reef were faster calcifiers. Corals were tested by extreme cold stress seven months into the transplant experiment; therefore, it is unknown whether corals can adjust growth strategies over a longer time or with more gradual stress (acclamatory response) or if they are genetically predisposed towards a growth strategy (adaptive response). This study did not track the zooxanthellae types hence their role in this tradeoff is unknown. The limited studies of coral growth tradeoffs (Little et al. 2004; Jones and Berkelmans 2010) focused on zooxanthellae dynamics and did not document coral mortality. Assuming individuals follow one strategy or another, this could complicate efforts to characterize coral responses to climate change. Regardless, climate change presents corals with a dilemma: increase stress tolerance or maintain high growth rates when both temperature and acidity are increasing.

Coral growth records and proxies

Chapter 5 details how *Solenastrea* might have coped with the dilemma of stress tolerance versus growth by comparing its skeletal record to a long-term water quality dataset. The species studied, *Solenastrea bournoni*, may be the same as the *Solenastrea hyades* examined in the laboratory and field experiments based on intermediate forms observed by Zlatarski and Martínez (1982). This coral confirmed the utility of oxygen isotopes in reconstruction work and presented evidence for carbon isotopes as indicators

of productivity. Temperature reconstructions showed most high temperature events occurred before 1900. The coral's persistence through those past conditions combined with knowledge of Florida Bay's present conditions (summarized in Chapters 3 and 4) including high saturation states, suggests Florida Bay corals prioritize stress tolerance over calcification. This strategy makes sense given that ambient chemistry is generally favorable for calcification and there is little competition for substrate because other coral species are not present in Florida bay.

Significance and applications

This dissertation demonstrates how corals are intimately connected to their environmental history, recording it in their skeletons and retaining the same growth strategies best-suited to their native environment even when transplanted to a new environment. If other coral genera also employ different growth strategies that are shaped by long-term environmental history and do not change in the short-term (months to years), these results have implications for marine reserves, connectivity, and refugia. Based on these experiments, reefs with more variable conditions whose corals better tolerate stress are more ideal source populations for reef replenishment than corals from stable environments, as climate change is expected to exacerbate future temperature and pH stress. Similarly Soto et al. (2011) noted Florida Keys sites with moderate temperature variance experienced smaller coral cover declines than sites with little or extreme variance.

Furthermore, resistance to high temperatures takes precedence over maintaining high calcification rates given 1) most corals responded to temperature before CO₂

(Chapter 2), 2) projected end-of-century summer temperatures (Sheppard and Rioja-Nieto 2005) will likely exceed bleaching thresholds (Manzello et al. 2007), and 3) species that exert more control over their calcifying fluid may be able to mitigate changes in chemistry due to ocean acidification (Ries 2011a; Ries 2011b; Rodolfo-Metalpa et al. 2011).

The calcification responses of stress tolerant corals to ocean acidification were characterized through a combination of field, laboratory and coral skeleton studies. These experiments indicate Florida Bay corals, while still vulnerable to ocean acidification, are more resilient to stresses than their oceanic counterparts and are likely to persist longer under climate change scenarios.

WORKS CITED

- Adkins JF, Boyle EA, Curry WB, Lutringer A (2003) Stable isotopes in deep-sea corals and a new mechanism for "vital effects". *Geochimica et Cosmochimica Acta* 67:1129-1143
- Al-Horani FA, Al-Moghrabi SM, de Beer D (2003) The mechanism of calcification and its relation to photosynthesis and respiration in the scleractinian coral *Galaxea fascicularis*. *Marine Biology* 142:419
- Al-Horani FA, Ferdelman T, Al-Moghrabi SM, de Beer D (2005) Spatial distribution of calcification and photosynthesis in the scleractinian coral *Galaxea fascicularis*. *Coral Reefs* 24:173
- Albright R, Langdon C (2011) Ocean acidification impacts multiple early life history processes of the Caribbean coral *Porites astreoides*. *Global Change Biology* 17:2478-2487
- Albright R, Mason B, Langdon C (2008) Effect of aragonite saturation state on settlement and post-settlement growth of *Porites astreoides* larvae. *Coral Reefs* 27:485-490
- Albright R, Mason B, Miller M, Langdon C (2010) Ocean acidification compromises recruitment success of the threatened Caribbean coral *Acropora palmata*. *Proceedings of the National Academy of Sciences of the United States of America* 107:20400-20404
- Alibert C, Kinsley L, Fallon SJ, McCulloch MT, Berkelmans R, McAllister F (2003) Source of trace element variability in Great Barrier Reef corals affected by the Burdekin flood plumes. *Geochimica et Cosmochimica Acta* 67:231-246
- Allemand D, Ferrier-Pagès C, Furla P, Houlbrèque F, Puverel S, Reynaud S, Tambutté E, Tambutté S, Zoccola D (2004) Biomineralisation in reef-building corals: from molecular mechanisms to environmental control. *Comptes Rendus Palevol* 3:453-467
- Allison N, Tudhope A, Fallick A (1996) Factors influencing the stable carbon and oxygen isotopic composition of *Porites lutea* coral skeletons from Phuket, South Thailand. *Coral Reefs* 15:43-57
- Alvarez-Filip L, Dulvy NK, Gill JA, Cote IM, Watkinson AR (2009) Flattening of Caribbean coral reefs: region-wide declines in architectural complexity. *Proceedings of the Royal Society B-Biological Sciences* 276:3019-3025
- Amiel AJ, Friedman GM, Miller DS (1973) Distribution and nature of incorporation of trace elements in modern aragonitic corals. *Sedimentology* 20:47-64
- Anderegg D (1998) Barium and carbon and oxygen isotope chronologies from two southeast Florida coral species - environmental implications. Nova Southeastern University, p117
- Anderegg D, Dodge RE, Swart PK, Fisher L (1997) Barium chronologies from south Florida reef corals - environmental implications
- Anthony KRN, Kline DI, Diaz-Pulido G, Dove S, Hoegh-Guldberg O (2008) Ocean acidification causes bleaching and productivity loss in coral reef builders. *Proceedings of the National Academy of Sciences of the United States of America* 105:17442-17446
- Bak RPM, Engel MS (1979) Distribution, abundance, and survival of juvenile hermatypic corals (Scleractinia) and the importance of life-history strategies in the parent coral community. *Marine Biology* 54:341-352

- Baker AC (2001) Ecosystems: reef corals bleach to survive change. *Nature* 411:765
- Baker AC, Glynn PW, Riegl B (2008) Climate change and coral reef bleaching: an ecological assessment of long-term impacts, recovery trends and future outlook. *Estuarine, Coastal and Shelf Science* 80:435-471
- Baker AC, Starger CJ, McClanahan TR, Glynn PW (2004) Coral reefs: corals' adaptive response to climate change. *Nature* 430:741-741
- Bates D, Maechler M, Bolker BM (2011) lme4: linear mixed-effects models using Eigen and Eigenfaces. *Journal of Statistical Software* 65:1-18
- Bates NR, Samuels L, Merlivat L (2001) Biogeochemical and physical factors influencing seawater fCO₂ and air-sea CO₂ exchange on the Bermuda coral reef. *Limnology and Oceanography* 46:833-846
- Beck JW, Edwards RL, Ito E, Taylor FW, Recy J, Rougerie F, Joannot P, Henin C (1992) Sea-surface temperature from coral skeletal strontium/calcium ratios. *Science* 257:644-647
- Berkelmans R, van Oppen MJH (2006) The role of zooxanthellae in the thermal tolerance of corals: a 'nugget of hope' for coral reefs in an era of climate change. *Proceedings of the Royal Society B-Biological Sciences* 273:2305-2312
- Bertucci A, Tambutté E, Tambutté S, Allemand D, Zoccola D (2010) Symbiosis-dependent gene expression in coral-dinoflagellate association: cloning and characterization of a P-type H⁺-ATPase gene. *Proceedings of the Royal Society B-Biological Sciences* 277:87-95
- Birkeland C (2004) Ratcheting down the coral reefs. *BioScience* 54:1021-1027
- Bohnsack JA (1993) The impacts of fishing on coral reefs. In: Ginsburg RN (ed) *Proceedings of the Colloquium on Global Aspects of Coral Reefs: Health, Hazards and History, 1993*, pp196-200
- Borell EM, Yuliantri AR, Bischof K, Richter C (2008) The effect of heterotrophy on photosynthesis and tissue composition of two scleractinian corals under elevated temperature. *Journal of Experimental Marine Biology and Ecology* 364:116-123
- Boyer JN, Fourqurean JW, Jones RD (1997) Spatial characterization of water quality in Florida Bay and Whitewater Bay by multivariate analyses: zones of similar influence. *Estuaries* 20:743-758
- Boyer JN, Fourqurean JW, Jones RD (1999) Seasonal and long-term trends in the water quality of Florida Bay (1989-1997). *Estuaries* 22:417-430
- Boyer JN, Kelble CR, Ortner PB, Rudnick DT (2009) Phytoplankton bloom status: chlorophyll a biomass as an indicator of water quality condition in the southern estuaries of Florida, USA. *Ecological Indicators* 9:S56-S67
- Buddemeier RW, Fautin DG (1993) Coral bleaching as an adaptive mechanism - a testable hypothesis. *Bioscience* 43:320-326
- Buster NA, Holmes CW (2006) Magnesium content within the skeletal architecture of the coral *Montastraea faveolata*: locations of brucite precipitation and implications to fine-scale data fluctuations. *Coral Reefs* 25:243-253
- Caldeira K, Wickett ME (2003) Oceanography: anthropogenic carbon and ocean pH. *Nature* 425:365-365
- Caldeira K, Wickett ME (2005) Ocean model predictions of chemistry changes from carbon dioxide emissions to the atmosphere and ocean. *Journal of Geophysical Research-Oceans* 110

- Cao L, Caldeira K, Jain AK (2007) Effects of carbon dioxide and climate change on ocean acidification and carbonate mineral saturation. *Geophysical Research Letters* 34
- Carricart-Ganivet JP (2011) Coral skeletal extension rate: an environmental signal or a subject to inaccuracies? *Journal of Experimental Marine Biology and Ecology* 405:73-79
- Carricart-Ganivet JP, Cabanillas-Teran N, Cruz-Ortega I, Blanchon P (2012) Sensitivity of calcification to thermal stress varies among genera of massive reef-building corals. *PLoS One* 7:e32859, 32851-32858
- Chalker BE (1976) Calcium-transport during skeletogenesis in hermatypic corals. *Comparative Biochemistry and Physiology A-Physiology* 54:455-459
- Chalker BE (1981) Simulating light-saturation curves for photosynthesis and calcification by reef-building corals. *Marine Biology* 63:135-141
- Chalker BE, Taylor DL (1975) Light-enhanced calcification, and role of oxidative-phosphorylation in calcification of the coral *Acropora cervicornis*. *Proceedings of the Royal Society of London Series B-Biological Sciences* 190:323-331
- Chappell J (1980) Coral morphology, diversity, and reef growth. *Nature* 286:249-252
- Chartrand K, Durako M, Blum J (2009) Effect of hyposalinity on the photophysiology of *Siderastrea radians*. *Marine Biology* 156:1691-1702
- Chave KE (1954) Aspects of the biogeochemistry of magnesium 1. Calcareous marine organisms. *The Journal of Geology* 62:266-283
- Chave KE, Smith SV, Roy KJ (1972) Carbonate production by coral reefs. *Marine Geology* 12:123-140
- Cheal AJ, Wilson SK, Emslie MJ, Dolman AM, Sweatman H (2008) Responses of reef fish communities to coral declines on the Great Barrier Reef. *Marine Ecology-Progress Series* 372:211-223
- Chiappone M, Sullivan KM (1994) Ecological structure and dynamics of nearshore hard-bottom communities in the Florida Keys. *Bulletin of Marine Science* 54:747-756
- Cohen AL, Holcomb M (2009) Why corals care about ocean acidification: uncovering the mechanism. *Oceanography* 22:118-127
- Cohen AL, Layne GD, Hart SR, Lobel PS (2001) Kinetic control of skeletal Sr/Ca in a symbiotic coral: implications for the paleotemperature proxy. *Paleoceanography* 16:20-26
- Cohen AL, Owens KE, Layne GD, Shimizu N (2002) The effect of algal symbionts on the accuracy of Sr/Ca paleotemperatures from coral. *Science* 296:331-333
- Cohen AL, McCorkle DC, de Putron S, Gaetani GA, Rose KA (2009) Morphological and compositional changes in the skeletons of new coral recruits reared in acidified seawater: insights into the biomineralization response to ocean acidification. *Geochemistry Geophysics Geosystems* 10
- Coles SL, Jokiel PL, Lewis CR (1976) Thermal tolerance in tropical versus subtropical Pacific reef corals. *Pacific Science* 30:159-166
- Cooper TF, De 'Ath G, Fabricius KE, Lough JM (2008) Declining coral calcification in massive *Porites* in two nearshore regions of the northern Great Barrier Reef. *Global Change Biology* 14:529-538

- Costanza R, d'Arge R, de Groot R, Farber S, Grasso M, Hannon B, Limburg K, Naeem S, O'Neill RV, Paruelo J, Raskin RG, Sutton P, van den Belt M (1997) The value of the world's ecosystem services and natural capital. *Nature* 387:253-260
- Crook ED, Potts D, Rebolledo-Vieyra M, Hernandez L, Paytan A (2012) Calcifying coral abundance near low-pH springs: implications for future ocean acidification. *Coral Reefs* 31:239-245
- Davies SP (1989) Short-term growth measurements of corals using an accurate buoyant weighing technique. *Marine Biology* 101:389-395
- Davies SP (1990) A rapid method for assessing growth rates of corals in relation to water pollution. *Marine Pollution Bulletin* 21:346-348
- Davis JC (1973) *Statistics and data analysis in geology*. Wiley, New York 550 pp
- De'ath G, Lough JM, Fabricius KE (2009) Declining coral calcification on the Great Barrier Reef. *Science* 323:116-119
- de Villiers S, Shen GT, Nelson BK (1994) The Sr/Ca-temperature relationship in coralline aragonite - influence of variability in $(\text{Sr}/\text{Ca})_{\text{seawater}}$ and skeletal growth-parameters. *Geochimica et Cosmochimica Acta* 58:197-208
- Dennison WC, Barnes DJ (1988) Effect of water motion on coral photosynthesis and calcification. *Journal of Experimental Marine Biology and Ecology* 115:67-77
- Dickson AG (1990) Thermodynamics of the dissociation of boric acid in synthetic seawater from 273.15 K to 318.15 K. *Deep-Sea Research Part A Oceanographic Research Papers* 37:755-766
- Dickson AG, Millero FJ (1987) A comparison of the equilibrium constants for the dissociation of carbonic acid in seawater media. *Deep-Sea Research Part A Oceanographic Research Papers* 34:1733-1743
- Dickson AG, Sabine CL, Christian JR (2007) *Guide to best practices for ocean CO₂ measurements*. North Pacific Marine Science Organization, Sidney, British Columbia 176
- Dodge RE, Jickells TD, Knap AH, Boyd S, Bak RPM (1984) Reef-building coral skeletons as chemical pollution (phosphorus) indicators. *Marine Pollution Bulletin* 15:178-187
- Doney SC, Fabry VJ, Feely RA, Kleypas JA (2009) Ocean acidification: the other CO₂ problem. *Annual Review of Marine Science* 1:169-192
- Donner SD, Skirving WJ, Little CM, Oppenheimer M, Hoegh-Guldberg O (2005) Global assessment of coral bleaching and required rates of adaptation under climate change. *Global Change Biology* 11:2251-2265
- Dore JE, Lukas R, Sadler DW, Church MJ, Karl DM (2009) Physical and biogeochemical modulation of ocean acidification in the central North Pacific. *Proceedings of the National Academy of Sciences of the United States of America* 106:12235-12240
- Doropoulos C, Ward S, Diaz-Pulido G, Hoegh-Guldberg O, Mumby PJ (2012) Ocean acidification reduces coral recruitment by disrupting intimate larval-algal settlement interactions. *Ecology Letters* 15:338-346
- Duever MJ, Meeder JF, Meeder LC, McCollom JM (1994) Ch 9 The climate of South Florida and its role in shaping the Everglades ecosystem. In: Davis SM, Ogden JC (eds) *Everglades: the ecosystem and its restoration*. St. Lucie Press, Delray Beach, pp225-248

- Edmunds PJ, Brown D, Moriarty V (2012) Interactive effects of ocean acidification and temperature on two scleractinian corals from Moorea, French Polynesia. *Global Change Biology* 18:2173-2183
- Enos P, Perkins RD (1979) Evolution of Florida Bay from island stratigraphy. *Geological Society of America Bulletin* 90:59-83
- Epstein S, Buchsbaum R, Lowenstam HA, Urey HC (1953) Revised carbonate-water isotopic temperature scale. *Geological Society of America Bulletin* 64:1315-1326
- Fabricius KE, Langdon C, Uthicke S, Humphrey C, Noonan S, De'ath G, Okazaki R, Muehllehner N, Glas MS, Lough JM (2011) Losers and winners in coral reefs acclimatized to elevated carbon dioxide concentrations. *Nature Clim Change* 1:165-169
- Fairbanks RG, Dodge RE (1979) Annual periodicity of the $^{18}\text{O}/^{16}\text{O}$ and $^{13}\text{C}/^{12}\text{C}$ ratios in the coral *Montastrea annularis*. *Geochimica et Cosmochimica Acta* 43:1009-1020
- Fallon SJ, McCulloch MT, Alibert C (2003) Examining water temperature proxies in *Porites* corals from the Great Barrier Reef: a cross-shelf comparison. *Coral Reefs* 22:389-404
- Fallon SJ, McCulloch MT, van Woesik R, Sinclair DJ (1999) Corals at their latitudinal limits: laser ablation trace element systematics in *Porites* from Shirigai Bay, Japan. *Earth and Planetary Science Letters* 172:221-238
- Fang LS, Chen YWJ, Chen CS (1989) Why does the white tip of stony coral grow so fast without zooxanthellae. *Marine Biology* 103:359-363
- Feely RA, Sabine CL, Lee K, Berelson W, Kleypas J, Fabry VJ, Millero FJ (2004) Impact of anthropogenic CO_2 on the CaCO_3 system in the oceans. *Science* 305:362-366
- Fitt WK, Warner ME (1995) Bleaching patterns of four species of Caribbean reef corals. *Biological Bulletin* 189:298-307
- Fitt WK, Brown BE, Warner ME, Dunne RP (2001) Coral bleaching: interpretation of thermal tolerance limits and thermal thresholds in tropical corals. *Coral Reefs* 20:51-65
- Fourqurean JW, Robblee MB (1999) Florida Bay: a history of recent ecological changes. *Estuaries* 22:345-357
- Frankovich TA, Zieman JC (1994) Total epiphyte and epiphytic carbonate production on *Thalassia testudinum* across Florida Bay. *Bulletin of Marine Science* 54:679-695
- Furla P, Galgani I, Durand I, Allemand D (2000) Sources and mechanisms of inorganic carbon transport for coral calcification and photosynthesis. *Journal of Experimental Biology* 203:3445-3457
- Gaetani GA, Cohen AL (2006) Element partitioning during precipitation of aragonite from seawater: a framework for understanding paleoproxies. *Geochimica et Cosmochimica Acta* 70:4617-4634
- Gagan MK, Ayliffe LK, Beck JW, Cole JE, Druffel ERM, Dunbar RB, Schrag DP (2000) New views of tropical paleoclimates from corals. *Quaternary Science Reviews* 19:45-64
- Gardner TA, Cote IM, Gill JA, Grant A, Watkinson AR (2003) Long-term region-wide declines in Caribbean corals. *Science* 301:958-960
- Gates RD, Baghdasarian G, Muscatine L (1992) Temperature stress causes host-cell detachment in symbiotic cnidarians - implications for coral bleaching. *Biological Bulletin* 182:324-332

- Gattuso J-P, Allemand D, Frankignoulle M (1999) Photosynthesis and calcification at cellular, organismal and community levels in coral reefs: a review on interactions and control by carbonate chemistry. *American Zoologist* 39:160-183
- Gattuso J-P, Gao K, Lee K, Rost B, Schulz KG (2010) Chapter 2 Approaches and tools to manipulate the carbonate chemistry. In: Riebesell U, Fabry VJ, Hansson L, Gattuso J-P (eds) Guide to best practices for ocean acidification research and data reporting. Publications Office of the European Union, Luxembourg, pp41-52
- Gattuso J-P, Reynaud-Vaganay S, Furla P, Romaine-Lioud S, Jaubert J, Bourge I, Frankignoulle M (2000) Calcification does not stimulate photosynthesis in the zooxanthellate scleractinian coral *Stylophora pistillata*. *Limnology and Oceanography* 45:246-250
- Gattuso JP, Frankignoulle M, Wollast R (1998) Carbon and carbonate metabolism in coastal aquatic ecosystems. *Annual Review of Ecology and Systematics* 29:405-434
- Ginsburg RN (1956) Environmental relationships of grain size and constituent particles in some south Florida carbonate sediments. *American Association of Petroleum Geologists Bulletin* 40:2384-2387
- Glynn PW (1993) Coral reef bleaching: ecological perspectives. *Coral Reefs* 12:1-17
- Glynn PW (1996) Coral reef bleaching: facts, hypotheses and implications. *Global Change Biology* 2:495-509
- Glynn PW, Mate JL, Baker AC, Calderon MO (2001) Coral bleaching and mortality in Panama and Ecuador during the 1997-1998 El Niño-Southern Oscillation event: spatial/temporal patterns and comparisons with the 1982-1983 event. *Bulletin of Marine Science* 69:79-109
- González-Dávila M, Santana-Casiano JM, Rueda MJ, Llinás O (2010) The water column distribution of carbonate system variables at the ESTOC site from 1995 to 2004. *Biogeosciences* 7:3067-3081
- Gratwicke B, Speight MR (2005a) Effects of habitat complexity on Caribbean marine fish assemblages. *Marine Ecology Progress Series* 292:301-310
- Gratwicke B, Speight MR (2005b) The relationship between fish species richness, abundance and habitat complexity in a range of shallow tropical marine habitats. *Journal of Fish Biology* 66:650-667
- Green DH, Edmunds PJ, Carpenter RC (2008) Increasing relative abundance of *Porites astreoides* on Caribbean reefs mediated by an overall decline in coral cover. *Marine Ecology-Progress Series* 359:1-10
- Grottoli AG (2000) Stable carbon isotopes ($\delta^{13}\text{C}$) in coral skeletons. *Oceanography* 13:93
- Grottoli AG, Rodrigues LJ, Palardy JE (2006) Heterotrophic plasticity and resilience in bleached corals. *Nature* 440:1186-1189
- Gunderson LH (2001) Managing surprising ecosystems in southern Florida. *Ecological Economics* 37:371-378
- Guzman HM, Tudhope AW (1998) Seasonal variation in skeletal extension rate and stable isotopic (C-13/C-12 and O-18/O-16) composition in response to several environmental variables in the Caribbean reef coral *Siderastrea siderea*. *Marine Ecology Progress Series* 166:109-118

- Hall-Spencer JM, Rodolfo-Metalpa R, Martin S, Ransome E, Fine M, Turner SM, Rowley SJ, Tedesco D, Buia MC (2008) Volcanic carbon dioxide vents show ecosystem effects of ocean acidification. *Nature* 454:96-99
- Hanor JS, Chan LH (1977) Non-conservative behavior of barium during mixing of Mississippi River and Gulf of Mexico waters. *Earth and Planetary Science Letters* 37:242-250
- Hart SR, Cohen AL (1996) An ion probe study of annual cycles of Sr/Ca and other trace elements in corals. *Geochimica et Cosmochimica Acta* 60:3075-3084
- Healy GF (1996) A decadal-scale perspective of South Florida water quality and climate using stable carbon and oxygen isotopes of two Florida corals. University of Miami, p84
- Helmle KP, Dodge RE, Swart PK, Gledhill DK, Eakin CM (2011) Growth rates of Florida corals from 1937 to 1996 and their response to climate change. *Nature Communications* 2
- Hendriks IE, Duarte CM, Alvarez M (2010) Vulnerability of marine biodiversity to ocean acidification: a meta-analysis. *Estuarine Coastal and Shelf Science* 86:157-164
- Hixon MA, Beets JP (1993) Predation, prey refuges, and the structure of coral-reef fish assemblages. *Ecological Monographs* 63:77-101
- Hoegh-Guldberg O (1999) Climate change, coral bleaching and the future of the world's coral reefs. *Marine and Freshwater Research* 50:839-866
- Hoegh-Guldberg O (2005) Low coral cover in a high-CO₂ world. *Journal of Geophysical Research* 110:1-11
- Hoegh-Guldberg O, Mumby PJ, Hooten AJ, Steneck RS, Greenfield P, Gomez E, Harvell CD, Sale PF, Edwards AJ, Caldeira K, Knowlton N, Eakin CM, Iglesias-Prieto R, Muthiga N, Bradbury RH, Dubi A, Hatziolos ME (2007) Coral reefs under rapid climate change and ocean acidification. *Science* 318:1737-1742
- Hofmann GE, Smith JE, Johnson KS, Send U, Levin LA, Micheli F, Paytan A, Price NN, Peterson B, Takeshita Y, Matson PG, Crook ED, Kroeker KJ, Gambi MC, Rivest EB, Frieder CA, Yu PC, Martz TR (2011) High-frequency dynamics of ocean pH: a multi-ecosystem comparison. *PLoS One* 6
- Hönisch B, Ridgwell A, Schmidt DN, Thomas E, Gibbs SJ, Sluijs A, Zeebe R, Kump L, Martindale RC, Greene SE, Kiessling W, Ries J, Zachos JC, Royer DL, Barker S, Marchitto TM, Moyer R, Pelejero C, Ziveri P, Foster GL, Williams B (2012) The geological record of ocean acidification. *Science* 335:1058-1063
- Houck JE, Buddemeier RW, Smith SV, Jokiel PL (1977) The response of coral growth rate and skeletal strontium content to light intensity and water temperature. *Proceedings Int Coral Reef Symp* 3:425-431
- Houlbrèque F, Tambutté E, Ferrier-Pagès C (2003) Effect of zooplankton availability on the rates of photosynthesis, and tissue and skeletal growth in the scleractinian coral *Stylophora pistillata*. *Journal of Experimental Marine Biology and Ecology* 296:145-166
- Hudson HJ, Powell GN, Robblee MB, Smith Iii TJ (1989) A 107-year-old coral from Florida Bay: barometer of natural and man-induced catastrophes? *Bulletin of Marine Science* 44:283-291

- Hughes TP, Tanner JE (2000) Recruitment failure, life histories, and long-term decline of Caribbean corals. *Ecology* 81:2250-2263
- Hughes TP, Baird AH, Bellwood DR, Card M, Connolly SR, Folke C, Grosberg R, Hoegh-Guldberg O, Jackson JBC, Kleypas J, Lough JM, Marshall P, Nystrom M, Palumbi SR, Pandolfi JM, Rosen B, Roughgarden J (2003) Climate change, human impacts, and the resilience of coral reefs. *Science* 301:929-933
- Iglesias-Prieto R, Matta JL, Robins WA, Trench RK (1992) Photosynthetic Response to Elevated-Temperature in the Symbiotic Dinoflagellate *Symbiodinium-Microadriaticum* in Culture. *Proceedings of the National Academy of Sciences of the United States of America* 89:10302-10305
- IPCC (2007) *Climate Change 2007: the physical science basis. Contribution of Working Group I to the Fourth Assessment Report of the Intergovernmental Panel on Climate Change.* In: Solomon S, Qin D, Manning M, Chen Z, Marquis M, Averyt KB, Tignor M, Miller HL (eds). Intergovernmental Panel on Climate Change, Cambridge, United Kingdom and New York, NY, USA
- Jackson JBC, Kirby MX, Berger WH, Bjorndal KA, Botsford LW, Bourque BJ, Bradbury RH, Cooke R, Erlandson J, Estes JA, Hughes TP, Kidwell S, Lange CB, Lenihan HS, Pandolfi JM, Peterson CH, Steneck RS, Tegner MJ, Warner RR (2001) Historical overfishing and the recent collapse of coastal ecosystems. *Science* 293:629-637
- Jacques TG, Pilson MEQ (1980) Experimental ecology of the temperate scleractinian coral *Astrangia danae* I. Partition of respiration, photosynthesis and calcification between host and symbionts. *Marine Biology* 60:167-178
- Jokiel PL, Coles SL (1977) Effects of temperature on mortality and growth of Hawaiian reef corals. *Marine Biology* 43:201-208
- Jones A, Berkelmans R (2010) Potential costs of acclimatization to a warmer climate: growth of a reef coral with heat tolerant vs. sensitive symbiont types. *PLoS One* 5:e10437
- Jones RJ, Hoegh-Guldberg O, Larkum AWD, Schreiber U (1998) Temperature-induced bleaching of corals begins with impairment of the CO₂ fixation mechanism in zooxanthellae. *Plant Cell and Environment* 21:1219-1230
- Jury CP, Whitehead RF, Szmant AM (2010) Effects of variations in carbonate chemistry on the calcification rates of *Madracis auretenra* (= *Madracis mirabilis sensu* Wells, 1973): bicarbonate concentrations best predict calcification rates. *Global Change Biology* 16:1632-1644
- Keith ML, Weber JN (1965) Systematic relationships between carbon and oxygen isotopes in carbonates deposited by modern corals and algae. *Science* 150:498-501
- Kerr SD (1972) Patterns of coastal sedimentation- carbonate muds of Florida Bay. *American Association of Petroleum Geologists Bulletin* 56:632
- Kinsey DW (1983) Standards of performance in coral reef primary production and carbon turnover. In: Barnes DJ (ed) *Perspectives on Coral Reefs*. Australian Institute of Marine Science, Townsville, pp209-220
- Kinsey DW, Davies PJ (1979) Effects of elevated nitrogen and phosphorus on coral reef growth. *Limnology and Oceanography* 24:935-940

- Kleypas J, Langdon C (2006) Chapter 5 Coral reefs and changing seawater chemistry. In: Phinney J, Hoegh-Guldberg O, Kleypas O, Skirving W, Strong A (eds) *Coral Reefs and Climate Change: Science and Management*. American Geophysical Union, Washington DC, pp73-110
- Kleypas JA, McManus JW, Menez LAB (1999a) Environmental limits to coral reef development: where do we draw the line? *American Zoologist* 39:146-159
- Kleypas JA, Buddemeier RW, Archer D, Gattuso J-P, Langdon C, Opdyke BN (1999b) Geochemical consequences of increased atmospheric carbon dioxide on coral reefs. *Science* 284:118-120
- Knutson DW, Buddemeier RW, Smith SV (1972) Coral chronometers: seasonal growth bands in reef corals. *Science* 177:270-272
- Koch MS, Schopmeyer SA, Nielsen OI, Kyhn-Hansen C, Madden CJ (2007) Conceptual model of seagrass die-off in Florida Bay: links to biogeochemical processes. *Journal of Experimental Marine Biology and Ecology* 350:73-88
- Kohler KE (2002) CoralXDS+. Nova Southeastern University Oceanographic Center / National Coral Reef Institute
- Kroeker KJ, Kordas RL, Crim RN, Singh GG (2010) Meta-analysis reveals negative yet variable effects of ocean acidification on marine organisms. *Ecology Letters* 13:1419-1434
- Kurihara H (2008) Effects of CO₂-driven ocean acidification on the early developmental stages of invertebrates. *Marine Ecology Progress Series* 373:275-284
- Land LS, Lang JC, Barnes DJ (1975) Extension rate- primary control on isotopic composition of West-Indian (Jamaican) scleractinian reef coral skeletons. *Marine Biology* 33:221-233
- Langdon C (2010) Determination of dissolved oxygen in seawater by Winkler titration using the amperometric technique. In: Hood EM, Sabine CL, Sloyan BM (eds) *The GO-SHIP Repeat Hydrography Manual: A Collection of Expert Reports and Guidelines*
- Langdon C, Atkinson MJ (2005) Effect of elevated pCO₂ on photosynthesis and calcification of corals and interactions with seasonal change in temperature/irradiance and nutrient enrichment. *Journal of Geophysical Research* 110:C09S07
- Langdon C, Takahashi T, Sweeney C, Chipman D, Goddard J, Marubini F, Aceves H, Barnett H, Atkinson MJ (2000) Effect of calcium carbonate saturation state on the calcification rate of an experimental coral reef. *Global Biogeochemical Cycles* 14:639-654
- Langdon C, Broecker WS, Hammond DE, Glenn E, Fitzsimmons K, Nelson SG, Peng TH, Hajdas I, Bonani G (2003) Effect of elevated CO₂ on the community metabolism of an experimental coral reef. *Global Biogeochemical Cycles* 17:1-14
- Lea D, Boyle E (1989) Barium content of benthic foraminifera controlled by bottom-water composition. *Nature* 338:751-753
- Leclercq N, Gattuso J-P, Jaubert J (2000) CO₂ partial pressure controls the calcification rate of a coral community. *Global Change Biology* 6:329-334
- Leclercq N, Gattuso J-P, Jaubert J (2002) Primary production, respiration, and calcification of a coral reef mesocosm under increased CO₂ partial pressure. *Limnology and Oceanography* 47:558-564

- Leder JJ, Swart PK, Szmant AM, Dodge RE (1996) The origin of variations in the isotopic record of scleractinian corals. 1. Oxygen. *Geochimica et Cosmochimica Acta* 60:2857-2870
- Leggat W, Badger MR, Yellowlees D (1999) Evidence for an inorganic carbon-concentrating mechanism in the symbiotic dinoflagellate *Symbiodinium* sp. *Plant Physiology* 121:1247-1255
- Lewis E, Wallace DWR (1998) Program developed for CO₂ system calculations. ORNL/CDIAC-105. Carbon Dioxide Information Analysis Center, Oak Ridge National Laboratory, U.S. Department of Energy, Oak Ridge, Tennessee
- Lewis JB (1989) Spherical growth in the Caribbean coral *Siderastrea radians* (Pallas) and its survival in disturbed habitats. *Coral Reefs* 7:161-167
- Linn LJ, Delaney ML, Druffel ERM (1990) Trace metals in contemporary and seventeenth-century Galapagos coral: records of seasonal and annual variations. *Geochimica et Cosmochimica Acta* 54:387-394
- Lirman D, Manzello D (2009) Patterns of resistance and resilience of the stress-tolerant coral *Siderastrea radians* (Pallas) to sub-optimal salinity and sediment burial. *Journal of Experimental Marine Biology and Ecology* 369:72-77
- Lirman D, Manzello D, Macia S (2002) Back from the dead: the resilience of *Siderastrea radians* to severe stress. *Coral Reefs* 21:291-292
- Lirman D, Orlando B, Macia S, Manzello D, Kaufman L, Biber P, Jones T (2003) Coral communities of Biscayne Bay, Florida and adjacent offshore areas: diversity abundance, distribution, and environmental correlates. *Aquatic Conservation: Marine and Freshwater Ecosystems* 13:121-135
- Lirman D, Schopmeyer S, Manzello D, Gramer LJ, Precht WF, Muller-Karger F, Banks K, Barnes B, Bartels E, Bourque A, Byrne J, Donahue S, Duquesnel J, Fisher L, Gilliam D, Hendee J, Johnson M, Maxwell K, McDevitt E, Monty J, Rueda D, Ruzicka R, Thanner S (2011) Severe 2010 cold-water event caused unprecedented mortality to corals of the Florida Reef Tract and reversed previous survivorship patterns. *PLoS One* 6:e23047
- Little AF, van Oppen MJH, Willis BL (2004) Flexibility in algal endosymbioses shapes growth in reef corals. *Science* 304:1492-1494
- Lloyd RM (1964) Variations in the oxygen and carbon isotope ratios of Florida Bay mollusks and their environmental significance. *Journal of Geology* 72:84-111
- Lowenstam HA, Epstein S (1957) On the origin of sedimentary aragonite needles of the Great Bahama Bank. *Journal of Geology* 65:364-375
- Macintyre IG (2003) A classic marginal coral environment: tropical coral patches off North Carolina, USA. *Coral Reefs* 22:474-474
- Macintyre IG, Pilkey OH (1969) Tropical reef corals: tolerance of low temperatures on the North Carolina continental shelf. *Science* 166:374-375
- Manzello DP (2010) Coral growth with thermal stress and ocean acidification: lessons from the eastern tropical Pacific. *Coral Reefs* 29:749-758
- Manzello DP, Berkelmans R, Hendee JC (2007) Coral bleaching indices and thresholds for the Florida reef tract, Bahamas, and St. Croix, US Virgin Islands. *Marine Pollution Bulletin* 54:1923-1931

- Manzello DP, Enochs IC, Melo N, Gledhill DK, Johns EM (2012) Ocean acidification refugia of the Florida reef tract. *PLoS One* 7:e41715-e41715
- Marshall AT, Clode P (2004) Calcification rate and the effect of temperature in a zooxanthellate and an azooxanthellate scleractinian reef coral. *Coral Reefs* 23:218-224
- Marshall JF, McCulloch MT (2002) An assessment of the Sr/Ca ratio in shallow water hermatypic corals as a proxy for sea surface temperature. *Geochimica et Cosmochimica Acta* 66:3263-3280
- Marubini F, Ferrier-Pagès C, Cuif JP (2003) Suppression of skeletal growth in scleractinian corals by decreasing ambient carbonate-ion concentration: a cross-family comparison. *Proceedings of the Royal Society of London Series B-Biological Sciences* 270:179-184
- Marubini F, Barnett H, Langdon C, Atkinson MJ (2001) Dependence of calcification on light and carbonate ion concentration for the hermatypic coral *Porites compressa*. *Marine Ecology Progress Series* 220:153-162
- Marubini F, Ferrier-Pagès C, Furla P, Allemand D (2008) Coral calcification responds to seawater acidification: a working hypothesis towards a physiological mechanism. *Coral Reefs* 27:491-499
- McConnaughey T (1989) ^{13}C and ^{18}O isotopic disequilibrium in biological carbonates: I. Patterns. *Geochimica et Cosmochimica Acta* 53:151-162
- McConnaughey TA (2003) Sub-equilibrium oxygen-18 and carbon-13 levels in biological carbonates: carbonate and kinetic models. *Coral Reefs* 22:316-327
- McConnaughey TA, Adey WH, Small AM (2000) Community and environmental influences on reef coral calcification. *Limnology and Oceanography* 45:1667-1671
- McCulloch M, Falter J, Trotter J, Montagna P (2012) Coral resilience to ocean acidification and global warming through pH up-regulation. *Nature Clim Change* 2:623-627
- McCulloch M, Fallon S, Wyndham T, Hendy E, Lough J, Barnes D (2003) Coral record of increased sediment flux to the inner Great Barrier Reef since European settlement. *Nature* 421:727-730
- Meesters EH, Noordeloos M, Bak RPM (1994) Damage and regeneration: links to growth in the reef-building coral *Montastrea annularis*. *Marine Ecology Progress Series* 112:119-128
- Mehrbach C, Culberson CH, Hawley JE, Pytkowicz RM (1973) Measurement of the apparent dissociation constants of carbonic acid in seawater at atmospheric pressure. *Limnology and Oceanography* 18:897-907
- Millero FJ, Hiscock WT, Huang F, Roche M, Zhang JZ (2001) Seasonal variation of the carbonate system in Florida Bay. *Bulletin of Marine Science* 68:101-123
- Mitsuguchi T, Matsumoto E, Uchida T (2003) Mg/Ca and Sr/Ca ratios of *Porites* coral skeleton: evaluation of the effect of skeletal growth rate. *Coral Reefs* 22:381-388
- Mitsuguchi T, Matsumoto E, Abe O, Uchida T, Isdale PJ (1996) Mg/Ca thermometry in coral skeletons. *Science* 274:961-963
- Montaggioni LF, Le Cornec F, Corregge T, Cabioch G (2006) Coral barium/calcium record of mid-Holocene upwelling activity in New Caledonia, South-West Pacific. *Palaeogeography Palaeoclimatology Palaeoecology* 237:436-455

- Montague CL, Ley JA (1993) A possible effect of salinity fluctuation on abundance of benthic vegetation and associated fauna in northeastern Florida Bay. *Estuaries* 16:703-717
- Morita M, Suwa R, Iguchi A, Nakamura M, Shimada K, Sakai K, Suzuki A (2010) Ocean acidification reduces sperm flagellar motility in broadcast spawning reef invertebrates. *Zygote* 18:103-107
- Mumby PJ, Steneck RS (2008) Coral reef management and conservation in light of rapidly evolving ecological paradigms. *Trends in Ecology & Evolution* 23:555-563
- Nemzer BV, Dickson AG (2005) The stability and reproducibility of Tris buffers in synthetic seawater. *Marine Chemistry* 96:237-242
- Nothdurft LD, Webb GE, Buster NA, Holmes CW, Sorauf JE (2005) Brucite microbialites in living coral skeletons: indicators of extreme microenvironments in shallow-marine settings. *Geology* 33:169-172
- Ohde S, van Woesik R (1999) Carbon dioxide flux and metabolic processes of a coral reef, Okinawa. *Bulletin of Marine Science* 65:559-576
- Ohde S, Hossain MMM (2004) Effect of CaCO₃ (aragonite) saturation state of seawater on calcification of *Porites* coral. *Geochemical Journal* 38:613-621
- Oren R, Ellsworth DS, Johnsen KH, Phillips N, Ewers BE, Maier C, Schafer KVR, McCarthy H, Hendrey G, McNulty SG, Katul GG (2001) Soil fertility limits carbon sequestration by forest ecosystems in a CO₂-enriched atmosphere. *Nature* 411:469-472
- Orr JC, Fabry VJ, Aumont O, Bopp L, Doney SC, Feely RA, Gnanadesikan A, Gruber N, Ishida A, Joos F, Key RM, Lindsay K, Maier-Reimer E, Matear R, Monfray P, Mouchet A, Najjar RG, Plattner G-K, Rodgers KB, Sabine CL, Sarmiento JL, Schlitzer R, Slater RD, Totterdell IJ, Weirig M-F, Yamanaka Y, Yool A (2005) Anthropogenic ocean acidification over the twenty-first century and its impact on calcifying organisms. *Nature* 437:681-686
- Paddock MJ, Reynolds JD, Aguilar C, Appeldoorn RS, Beets J, Burkett EW, Chittaro PM, Clarke K, Esteves R, Fonseca AC, Forrester GE, Friedlander AM, Garcia-Sais J, Gonzalez-Sanson G, Jordan LKB, McClellan DB, Miller MW, Molloy PP, Mumby PJ, Nagelkerken I, Nemeth M, Navas-Camacho R, Pitt J, Polunin NVC, Reyes-Nivia MC, Robertson DR, Rodriguez-Ramirez A, Salas E, Smith SR, Spieler RE, Steele MA, Williams ID, Wormald CL, Watkinson AR, Cote IM (2009) Recent region-wide declines in Caribbean reef fish abundance. *Current Biology* 19:590-595
- Pandolfi JM, Bradbury RH, Sala E, Hughes TP, Bjorndal KA, Cooke RG, McArdle D, McClenachan L, Newman MJH, Paredes G, Warner RR, Jackson JBC (2003) Global trajectories of the long-term decline of coral reef ecosystems. *Science* 301:955-958
- Pierrot D, Lewis E, Wallace DWR (2006) MS Excel program developed for CO₂ system calculations. ORNL/CDIAC-105a. Carbon Dioxide Information Analysis Center, Oak Ridge National Laboratory, U.S. Department of Energy, Oak Ridge, Tennessee
- Porter JW, Lewis SK, Porter KG (1999) The effect of multiple stressors on the Florida Keys coral reef ecosystem: a landscape hypothesis and a physiological test. *Limnology and Oceanography* 44:941-949
- Prouty NG, Hughen KA, Carilli J (2008) Geochemical signature of land-based activities in Caribbean coral surface samples. *Coral Reefs* 27:727-742

- Quinn TM, Sampson DE (2002) A multiproxy approach to reconstructing sea surface conditions using coral skeleton geochemistry. *Paleoceanography* 17
- R Core Development Team (2011) R: a language and environment for statistical computing. R Foundation for Statistical Computing, Vienna, Austria
- Raupach MR, Marland G, Ciais P, Le Quéré C, Canadell JG, Klepper G, Field CB (2007) Global and regional drivers of accelerating CO₂ emissions. *Proceedings of the National Academy of Sciences* 104:10288-10293
- Reaka-Kudla ML (1997) The global biodiversity of coral reefs: a comparison with rain forests. In: Reaka-Kudla ML, Wilson DE, Wilson EO (eds) *Biodiversity 2: understanding and protecting our biological resources*, pp83-108
- Reynaud S, Leclercq N, Romaine-Lioud S, Ferrier-Pagès C, Jaubert J, Gattuso JP (2003) Interacting effects of CO₂ partial pressure and temperature on photosynthesis and calcification in a scleractinian coral. *Global Change Biology* 9:1660-1668
- Reynaud S, Ferrier-Pagès C, Meibom A, Mostefaoui S, Mortlock R, Fairbanks R, Allemand D (2007) Light and temperature effects on Sr/Ca and Mg/Ca ratios in the scleractinian coral *Acropora* sp. *Geochimica et Cosmochimica Acta* 71:354-362
- Riahi K, Rao S, Krey V, Cho C, Chirkov V, Fischer G, Kindermann G, Nakicenovic N, Rafaj P (2011) RCP 8.5—A scenario of comparatively high greenhouse gas emissions. *Climatic Change* 109:33-57
- Rice SA, Hunter CL (1992) Effects of suspended sediment and burial on scleractinian corals from west central Florida patch reefs. *Bulletin of Marine Science* 51:429-442
- Ridgwell A, Schmidt DN (2010) Past constraints on the vulnerability of marine calcifiers to massive carbon dioxide release. *Nature Geoscience* 3:196-200
- Ries JB (2011a) A physicochemical framework for interpreting the biological calcification response to CO₂-induced ocean acidification. *Geochimica et Cosmochimica Acta* 75:4053-4064
- Ries JB (2011b) Biodiversity and ecosystems: acid ocean cover up. *Nature Clim Change* 1:294-295
- Ries JB, Cohen AL, McCorkle DC (2009) Marine calcifiers exhibit mixed responses to CO₂-induced ocean acidification. *Geology* 37:1131-1134
- Robblee MB, Barber TR, Carlson PR, Durako MJ, Fourqurean JW, Muehlstein LK, Porter D, Yarbro LA, Zieman RT, Zieman JC (1991) Mass mortality of the tropical seagrass *Thalassia testudinum* in Florida Bay (USA). *Marine Ecology Progress Series* 71:297-299
- Roberts CM, McClean CJ, Veron JEN, Hawkins JP, Allen GR, McAllister DE, Mittermeier CG, Schueler FW, Spalding M, Wells F, Vynne C, Werner TB (2002) Marine biodiversity hotspots and conservation priorities for tropical reefs. *Science* 295:1280-1284
- Roberts HH, Rouse LJ, Walker ND, Hudson JH (1982) Cold-water stress in Florida Bay and northern Bahamas: a product of winter cold-air outbreaks. *Journal of Sedimentary Research* 52:145-155
- Rodolfo-Metalpa R, Houlbreque F, Tambutte E, Boisson F, Baggini C, Patti FP, Jeffree R, Fine M, Foggo A, Gattuso JP, Hall-Spencer JM (2011) Coral and mollusc resistance to ocean acidification adversely affected by warming. *Nature Clim Change* 1:308-312

- Rosenberg AD (2011) Insight from the depths of the Straits of Florida: assessing the utility of Atlantic deep-water coral geochemical proxy techniques. University of Miami, p159
- Sabine CL, Feely RA, Gruber N, Key RM, Lee K, Bullister JL, Wanninkhof R, Wong CS, Wallace DWR, Tilbrook B, Millero FJ, Peng TH, Kozyr A, Ono T, Rios AF (2004) The oceanic sink for anthropogenic CO₂. *Science* 305:367-371
- Schneider K, Erez J (2006) The effect of carbonate chemistry on calcification and photosynthesis in the hermatypic coral *Acropora eurystoma*. *Limnology and Oceanography* 51:1284-1293
- Seibel BA, Maas AE, Dierssen HM (2012) Energetic plasticity underlies a variable response to ocean acidification in the pteropod, *Limacina helicina antarctica*. *PLoS One* 7:e30464
- Shen GT, Boyle EA (1988) Determination of lead, cadmium and other trace-metals in annually-banded corals. *Chem Geol* 67:47-62
- Sheppard C, Rioja-Nieto R (2005) Sea surface temperature 1871-2009 in 38 cells in the Caribbean region. *Marine Environmental Research* 60:389-396
- Silverman J, Lazar B, Cao L, Caldeira K, Erez J (2009) Coral reefs may start dissolving when atmospheric CO₂ doubles. *Geophysical Research Letters* 36
- Sinclair DJ, McCulloch MT (2004) Corals record low mobile barium concentrations in the Burdekin River during the 1974 flood: evidence for limited Ba supply to rivers? *Palaeogeography Palaeoclimatology Palaeoecology* 214:155-174
- Smith SV, Buddemeier RW, Redalje RC, Houck JE (1979) Strontium-calcium thermometry in coral skeletons. *Science* 204:404-407
- Sorauf JE, Harries PJ (2009) Rotatory colonies of the corals *Siderastrea radians* and *Solenastrea* ssp (Cnidaria, Scleractinia), from the Pleistocene Bermont Formation, South Florida, USA. *Paleontology* 52:111-126
- Soto I, Muller Karger F, Hallock P, Hu C (2011) Sea surface temperature variability in the Florida Keys and its relationship to coral cover. *Journal of Marine Biology* 2011
- Spalding MD, Grenfell AM (1997) New estimates of global and regional coral reef areas. *Coral Reefs* 16:225-230
- Swart PK (1983) Carbon and oxygen isotope fractionation in scleractinian corals: a review. *Earth-Science Reviews* 19:51-80
- Swart PK, Coleman ML (1980) Isotopic data for scleractinian corals explain their palaeotemperature uncertainties. *Nature* 283:557-559
- Swart PK, Price K (2002) Origin of salinity variations in Florida Bay. *Limnology and Oceanography* 47:1234-1241
- Swart PK, Burns SJ, Leder JJ (1991) Fractionation of the stable isotopes of oxygen and carbon in carbon-dioxide during the reaction of calcite with phosphoric-acid as a function of temperature and technique. *Chem Geol* 86:89-96
- Swart PK, Elderfield H, Greaves MJ (2002) A high-resolution calibration of Sr/Ca thermometry using the Caribbean coral *Montastraea annularis*. *Geochem Geophys Geosyst* 3:8402

- Swart PK, Leder JJ, Szmant AM, Dodge RE (1996a) The origin of variations in the isotopic record of scleractinian corals. 2. Carbon. *Geochimica et Cosmochimica Acta* 60:2871-2885
- Swart PK, Healy GF, Dodge RE, Kramer P, Hudson JH, Halley RB, Robblee MB (1996b) The stable oxygen and carbon isotopic record from a coral growing in Florida Bay: a 160 year record of climatic and anthropogenic influence. *Palaeogeography Palaeoclimatology Palaeoecology* 123:219-237
- Swart PK, Healy G, Greer L, Lutz M, Saied A, Anderegg D, Dodge RE, Rudnick D (1999) The use of proxy chemical records in coral skeletons to ascertain past environmental conditions in Florida Bay. *Estuaries* 22:384-397
- Swart PK, Greer L, Rosenheim BE, Moses CS, Waite AJ, Winter A, Dodge RE, Helmle K (2010) The C-13 Suess effect in scleractinian corals mirror changes in the anthropogenic CO₂ inventory of the surface oceans. *Geophysical Research Letters* 37
- Tambutté E, Allemand D, Mueller E, Jaubert J (1996) A compartmental approach to the mechanism of calcification in hermatypic corals. *Journal of Experimental Biology* 199:1029-1041
- Tanzil J, Brown B, Tudhope A, Dunne R (2009) Decline in skeletal growth of the coral *Porites lutea* from the Andaman Sea, South Thailand between 1984 and 2005. *Coral Reefs* 28:519-528
- Taylor KE, Stouffer RJ, Meehl GA (2012) An overview of CMIP5 and the experiment design. *Bulletin of the American Meteorological Society* 93:485-498
- van Oppen MJH, Gates RD (2006) Conservation genetics and the resilience of reef-building corals. *Molecular Ecology* 15:3863-3883
- van Vuuren D, Edmonds J, Kainuma M, Riahi K, Thomson A, Hibbard K, Hurtt G, Kram T, Krey V, Lamarque J-F, Masui T, Meinshausen M, Nakicenovic N, Smith S, Rose S (2011) The representative concentration pathways: an overview. *Climatic Change* 109:5-31
- van Woesik R, Jordan-Garza AG (2011) Coral populations in a rapidly changing environment. *Journal of Experimental Marine Biology and Ecology* 408:11-20
- Vaughan TW (1913) Studies of the geology and of the Madreporaria of the Bahamas and of southern Florida. *Carnegie Institution of Washington Year Book* 11:153-162
- Vecsei A (2004) A new estimate of global reefal carbonate production including the fore-reefs. *Global and Planetary Change* 43:1-18
- Walters C, Gunderson L, Holling CS (1992) Experimental policies for water management in the Everglades. *Ecological Applications* 2:189-202
- Warner ME, Fitt WK, Schmidt GW (1996) The effects of elevated temperature on the photosynthetic efficiency of zooxanthellae in hospite from four different species of reef coral: a novel approach. *Plant Cell and Environment* 19:291-299
- Watanabe T, Winter A, Oba T (2001) Seasonal changes in sea surface temperature and salinity during the Little Ice Age in the Caribbean Sea deduced from Mg/Ca and ¹⁸O/¹⁶O ratios in corals. *Marine Geology* 173:21-35
- Weber JN (1973) Incorporation of strontium into reef coral skeletal carbonate. *Geochimica et Cosmochimica Acta* 37:2173-2190

- Weber JN (1974) Skeletal chemistry of scleractinian reef corals: uptake of magnesium from seawater
American Journal of Science 274:84-93
- Weber JN, Woodhead PMJ (1970) Carbon and oxygen isotope fractionation in the skeletal carbonate of
reef-building corals. Chem Geol 6:93-117
- Weber JN, Woodhead PMJ (1972) Temperature dependence of oxygen-18 concentration in reef coral
carbonates. J Geophys Res 77:463-473
- Wei GJ, Sun M, Li XH, Nie BF (2000) Mg/Ca, Sr/Ca and U/Ca ratios of a porites coral from Sanya Bay,
Hainan Island, South China Sea and their relationships to sea surface temperature.
Palaeogeography Palaeoclimatology Palaeoecology 162:59-74
- Wilson SK, Graham NAJ, Pratchett MS, Jones GP, Polunin NVC (2006) Multiple disturbances and the
global degradation of coral reefs: are reef fishes at risk or resilient? Global Change Biology
12:2220-2234
- Wood HL, Spicer JJ, Widdicombe S (2008) Ocean acidification may increase calcification rates, but at a
cost. Proceedings of the Royal Society B-Biological Sciences 275:1767-1773
- Wooldridge SA (2008) Mass extinctions past and present: a unifying hypothesis. Biogeosciences Discuss
5:2401-2423
- Wootton JT, Pfister CA, Forester JD (2008) Dynamic patterns and ecological impacts of declining ocean
pH in a high-resolution multi-year dataset. Proceedings of the National Academy of Sciences
105:18848-18853
- Yamano H, Sugihara K, Nomura K (2011) Rapid poleward range expansion of tropical reef corals in
response to rising sea surface temperatures. Geophysical Research Letters 38
- Yates KK, Halley RB (2006) Diurnal variation in rates of calcification and carbonate sediment dissolution
in Florida Bay. Estuaries and Coasts 29:24-39
- Yates KK, Dufore C, Smiley N, Jackson C, Halley RB (2007) Diurnal variation of oxygen and carbonate
system parameters in Tampa Bay and Florida Bay. Marine Chemistry 104:110-124
- Yonge CM (1936) Studies on the biology of Tortugas Corals. II. Variation in the genus *Siderastrea*. Papers
from the Tortugas Laboratory of the Carnegie Institution of Washington 29:185-198
- Zieman JC, Fourqurean JW, Frankovich TA (1999) Seagrass die-off in Florida Bay: long-term trends in
abundance and growth of turtle grass, *Thalassia testudinum*. Estuaries 22:460-470
- Zlatarski VN, Martínez EN (1982) Les scléactiniaires de Cuba avec des données sur les organismes
associés. Bulgarian Academy of Sciences, Sofia